Development and characterisation of monoclonal antibodies to tumour endothelial marker 'Melanoma Cell Adhesion Molecule' (MCAM) and approaches to targeting MCAM on tumour vessels

By

Marta Čorić

UNIVERSITY OF BIRMINGHAM

A thesis submitted to the University of Birmingham for the degree of

DOCTOR OF PHILOSOPHY

Institute of Cardiovascular Sciences

College of Medical and Dental Sciences

University of Birmingham

August 2018

Abstract

Renal cell carcinoma (RCC) patients are routinely treated with cytokines and VEGF targeted anti-angiogenics. Resistance to therapy due to the by-passing of VEGF pathway and severe systemic side effects induced by cytokines and VEGF targeting pose major drawbacks. Melanoma cell adhesion molecule (MCAM) is a marker of RCC blood vessels, with low or no expression on healthy vasculature. This thesis aimed to generate mouse MCAM targeted antibodies and recombinant human MCAM extracellular domain (hMCAMecd) receptor trap to investigate MCAM as a potential therapeutic target. Around 50 anti-mouse MCAM hybridoma clones were generated from immunized rats, with two of them sub-cloned to stable antibody expressing hybridomas (mMCAM10 and mMCAM66). The two antibodies recognize mMCAM by flow cytometry, immunohistochemistry, Western blot and immunoprecipitation. The mMCAM10, but not the mMCAM66, localises to tumour vessels within one hour of intravenous injection into the tumour bearing mice. This indicates MCAM's potential as a target for tumour vascular disruption. The variable region of the mMCAM10 was sequenced for future antibody engineering. The hMCAMecd fused to an Fc tag caused significant reduction in endothelial cell migration, tube formation and transmigration, and had no effect on proliferation or cell cycle, highlighting MCAM's potential for anti-angiogenic therapy.

I dedicate this work to my mum and dad.

Acknowledgments

I would like to thank my supervisors Roy Bicknell and Victoria Heath for their support, guidance and kind encouragements throughout my PhD. I would also like to thank them for sharing their knowledge and advice and the opportunity to work in their lab.

I would like to thank all the people in the medical school that have helped me with new techniques and especially Margaret Goodall for her kindness and invaluable help and advice with the hybridoma production.

I also thank Aleksandra, Marco and Jagoda for sharing the VAMPIRE project ups and downs throughout the 4 years that we have been working together. I would like to thank them for their help in the lab, constructive discussions, and psychological support during disappointing times. You have been a big part of this PhD journey and I cannot thank you enough for all the moments we shared and for your true friendship. I also thank all the other members of the Bicknell/Heath group for their friendship and help.

I would like to thank my family for supporting me and always believing in me. A special thanks to my best friend Iris for being there always, through good and bad. And a big thank you to all of my friends, old and new. I couldn't have done it without all of you.

Lastly, I would like to thank my husband Sergio, for waiting for me in the evenings with amazing dinners and prepared lunches for the next day, for making me laugh and for being so positive and supportive. Thank you for being 'here' and singing all the time.

I also thank the EU for funding this project and making it possible to develop my scientific skills.

Table of Contents

List of illustrations:

List of tables:

Abbreviations:

× g	Centrifugal Force
°C	Degree Celsius
ADC	Antibody-Drug Conjugate
ANOVA	Analysis of Variance
APS	Ammonium Persulfate
bEND	Mouse Brain Endothelial Cells
bFGF	Basic Fibroblast Growth Factor
bp	Base Pair
BSA	Bovine Serum Albumin
C-terminus	Carboxyl-Terminus of Protein
CAM	Chicken Chorioallantoic Membrane
CAR-T	Chimeric Antigen Receptor T Cell
cDNA	Complementary DNA
CLEC14A	C-Type Lectin Domain Family 14 Member A
CRF	Chronic Renal Failure
CTLA-4	Cytotoxic T-Lymphocyte-Associated Protein 4
ctrl	Control
DAPI	4',6-Diamidino-2-Phenylindole
dCTP	Deoxycytidine Triphosphate
DMEM	Dulbecco's Modified Eagle's Medium
DMSO	Dimethyl Sulfoxide
DNA	Deoxyribonucleic Acid
dH_2O	Deionised Water
dNTP	Deoxyribonucleotide
DPBS	Dulbecco's Phosphate-Buffered Saline
EBM	Endothelial Basal Medium
EC	Endothelial Cell
ECL	Enhanced Chemiluminescent Detection
EDTA	Ethylenediaminetetraacetic Acid
EGFR	Epidermal Growth Factor Receptor
ELISA	Enzyme-Linked Immunosorbent Assay
EPC	Endothelial Progenitor Cell
ERM	Ezrin/Radixin/Moesin Family
FACS	Fluorescence-Activated Cell Sorting
FAK	Focal Adhesion Kinase
Fc	Fragment Crystallisable Region of Human Immunoglobulin
FCA	Freund's Complete Adjuvant
FCS	Foetal Calf Serum
FDA	Food and Drug Administration
FIA	Freund's Incomplete Adjuvant
GFP	Green Fluorescent Protein
h	Hour/s
HAT	Hypoxanthine, Aminopterin, Thymidine
HDF	Human Dermal Fibroblasts
HEK	Human Endothelial Kidney
HER2	Human Epidermal Growth Factor Receptor 2
HIF	Hypoxia-inducible factor
His	Histidine

HRP	Horseradish Peroxidase
hMCAMecd	Human MCAM Extracellular Domain
HMVEC	Human Microvascular Endothelial Cell
HT	Hypoxanthine, Thymidine
HUVEC	Human Umbilical Vein Endothelial Cell
Ig	Immunoglobulin
IF	Immunofluorescence
IFN-α	Interferon Alpha
IHC	Immunohistochemistry
IL	Interleukin
IP	Immunoprecipitation
IRES	Internal Ribosome Entry Site
kb	Kilo Base
LAMA4	Laminin Subunit Alpha-4
LB medium	Luria-Bertani Medium
LSGS	Low Serum Growth Supplement
M106/M199	Medium 106/199
mAb	Monoclonal Antibody
MCAM	Melanoma Cell Adhesion Molecule
MEM	Minimum Essential Medium
min	Minute/s
mMCAMecd	Mouse MCAM Extracellular Domain
mMCAMfl	Mouse MCAM Full Lenght
MMP	Matrix Metalloproteinases
mRNA	Messenger Ribonucleic Acid
mTOR	Mammalian Target of Rapamycin
N-terminus	Amino-Terminus of Protein
Ni-NTA	Nickel-Nitrilotriacetic Acid
NP-40	Nonidet P-40, Octylphenoxypolyethoxyethanol
NS0	Mouse Myeloma Cell Line
NSCLC	Non-Small-Cell Lung Carcinoma
OCT	Optimum Cutting Temperature
OD	Optical Density
ORR	Overall Response Rate
OS	Overall Survival
PAGE	Polyacrylamide Gel Electrophoresis
PBS	Phosphate-Buffered Saline
PBS-T	Phosphate-Buffered Saline Tween
PCR	Polymerase Chain Reaction
PD-1/PD-L1	Programmed Death 1/Programmed Death-Ligand 1
PEG	Polyethylene Glycol
PEI	Polyethylenimine
PFA	Paraformaldehyde
PFS	Progression-Free Survival
pH	Measure of The Activity of The (Solvated) Hydrogen Ion
PKC	Protein Kinase C
PMSF	Phenylmethylsulfonyl Fluoride
PVDF	Polyvinylidene Fluoride
qRT-PCR	Quantitative Reverse Transcription Polymerase Chain Reaction
RACE	Rapid Amplification Of cDNA Ends

RCC	Renal Cell Carcinoma
RENCA	Murine Renal Adenocarcinoma Cell Line of Balb/C Origin
RNA	Ribonucleic Acid
rpm	Revolutions Per Minute
RPMI	Roswell Park Memorial Institute Medium
sec	Seconds
sEND	Mouse Skin Endothelial Cells
SDS	Sodium Dodecylsulfate
siRNA	Small Interfering RNA
Sp2/0Ag14	Mouse Myeloma Cell Line
TAE	Buffer Solution Containing A Mixture of Tris Base, Acetic Acid and EDTA
Tc	Cytotoxic T Cell
TEMED	Tetramethylethylenediamine
Th	T Helper Cell
TKI	Tyrosine Kinase Inhibitor
Tm	Melting Temperature
TMB	Tetramethylbenzidine
Tris	Tris(Hydroxymethyl)Aminomethane
VEGF	Vascular Endothelial Growth Factor
VEGFR	Vascular Endothelial Growth Factor Receptor
VHL	Von Hippel–Lindau
WB	Western Blot

1 INTRODUCTION

1.1 General introduction

Cancer treatment has become much advanced with the development of targeted therapy in the course of last two decades. By taking advantage of biological features of cancer cells and their changed environment, the much-needed reduction in systemic negative effects on the healthy tissue was accomplished. Specific targeting of tumour related molecules posed great advantage over traditional chemotherapy and radiotherapy and improved survival and disease stabilisation of many cancer patients. Data generated from large numbers of clinical trials using targeted therapies accomplished exponential success and is continuing to improve both clinical output in the sense of patient benefit as well as enhancing the knowledge of cancer biology. However, better understanding of several aspects such as cancer progression mechanisms, development of resistance to therapy and patient stratification is still much needed in order to further improve cancer treatment. Therefore, every new approach is a step closer to finding cure for this diverse and complex disease.

This thesis will focus on generation and characterisation of targeted therapy for renal cell carcinoma, by targeting Melanoma Cell Adhesion Molecule (MCAM), which is highly expressed on tumour blood vessels and correlates with poor patient prognosis. It will explore the potential of MCAM as a target for tumour vessel disruption using monoclonal antibodies to MCAM, as well as potential of soluble recombinant MCAM extracellular domain fused to human Fc for angiogenesis inhibition.

1.2 Monoclonal antibodies and their use in research and clinic

Antibodies are widely used and valuable tools in life science, however they can be problematic with a number of characteristics that have to be verified such as cross-reactivity, the strength of affinity and stability in experimental conditions, in order for their proper use [1]. Well-characterised antibodies, both polyclonal and monoclonal, provide valuable resources in research. Furthermore, monoclonal antibodies are increasingly being introduced into clinical setting as treatment tools for various conditions including cancer [2–4].

Antibodies are formed of two heavy and two light chains connected by disulphide bonds. Both heavy and light chains contain a constant region and a variable region with antigen binding specificity. The constant region of heavy chain is involved in the immune effector function by binding to and activating immune system components via Fc receptors. The variable regions are formed by gene rearrangements creating three complementarity-determining regions on both the heavy and light chain, which then together form an antigen-binding site. Gene rearrangements in B-cells are capable of generating around 200 million different antigen binding regions, but each B-cell contains only one. Once the specific antigen is present in the body, B-cell with affinity to that antigen will be activated and start producing antibodies. Cells with reactivity to self-protein are deleted in early development in the B-cell maturation sites, where cells die upon binding the self-antigen [5,6].

1.2.1. Antibodies in cancer targeted therapies and mechanisms of action

Antibodies are unique because of their high specificity and several mechanisms of action based on the targeted antigen and immune effector functions. When binding the antigen antibodies can induce an antibody-dependent cellular cytotoxicity or antibody-

dependent phagocytosis by binding and activating receptors on immune cells, or initiate complement dependent cytotoxicity by recruiting proteins of the complement system. Antibodies can also block the receptor function, abrogate signalling, induce internalisation and receptor down-regulation or directly induce cell apoptosis [7,8]. The host antibody immune response in cancer is dependent on the presentation of neo-antigens that arise from mutations in tumour proteins or in some cases expression of foetal antigens that are silenced in the adult, and to which B-cells have not been deleted [9]. This ability of immune system has been shown to protect against cancer development if the cancer can be recognised as foreign. However, tumours often evolve to express regulatory proteins which inhibit effective immune response [10]. Thus, much research has been focused on how to promote immune system in the fight against cancer by activating its components or blocking the immune checkpoint proteins expressed by the tumour. Major breakthrough was the development of monoclonal antibody (mAb) hybridoma technology in 1975 that allowed generation of clonal antibodies targeting almost any known biological substance [11]. Initially antibodies were produced in laboratory animals and so they could not be used in humans due to immunogenicity of immunoglobulins. The innovation in a form of grafting complementarity-determining regions of monoclonal antibodies to human immunoglobulin backbone [12] enabled the use of antibodies in clinical setting without inducing a patient's immune response. Ever since, a plethora of antibody-targeted therapies have been generated and are in clinical trials, with more than a dozen being approved by the US food and drug administration (FDA) to date.

Furthermore, antibody engineering led to development of antibodies with modified constant regions in order to enhance or decrease activation of immune cells or complement system. Another form in which an antibody can be used is antibody drug conjugates (ADC),

specific therapy that uses antibodies to specifically deliver a toxic drug to the antigen presenting tissue. The antigen binding regions of antibodies can be cloned into chimeric antigen receptor in T cells (CAR-T), which can then be introduced into a patient.

A major breakthrough in haematological malignancy treatment was introduction of the first monoclonal antibody approved for cancer treatment, Rituximab (mAb to CD20), in 1997. The binding of rituximab to CD20 expressed on all B-cells induces cell apoptosis, having a cytotoxic effect both on cancer and healthy cells. Furthermore, antibodies targeting antigens HER2 and EGFR on solid tumours also showed a remarkable success in several tumour types. Trastuzumab (an antibody to HER2) in combination with another anti-HER2 antibody (pertuzumab) against a different epitope showed synergistic improvement in patients' response and overall survival with 50% of patients experiencing complete response in HER2 positive non-metastatic breast cancer [13]. Besides targeting tumour cells, antibodies have been developed against the stroma components. One of the most used antibodies against stroma is Bevacizumab, an antibody specific for soluble vascular endothelial growth factor - A (VEGF-A)[14]. Bevacizumab acts by binding and sequestering VEGF, reducing tumour angiogenesis and in some cases normalising tumour blood vessels. The effect of Bevacizumab on vessel normalisation induces a therapeutic window in which chemotherapy can be effectively delivered to the tumour, having more potent effect than chemotherapy alone. The latest success in harnessing immune system to treat cancer is development of antibodies against immune checkpoint proteins CTLA-4, PD-1 and PD-L1 [3,15]. These proteins down-regulate immune responses and are often expressed by tumour and immune cells infiltrating the tumour as a way of tumour's escape from the immune response.

Despite the proven success and potential of antibodies in cancer treatment, several drawbacks leave room for much further improvement. One of the most important aspects of antibody targeting is the selection of a good target. Antibodies to CD20 or CD52 target lineage proteins expressed in equal amounts on healthy and cancer cells, eradicating all immune cells and causing the lack of functional immune system as well as cytokine release related toxicities. Furthermore, these antigens are not crucial for cancer progression, and so the tumours can evolve to down-regulate the expression of this antigen causing resistance to therapy. Antibodies targeting VEGF, HER2 or EGFR have toxic effects on healthy tissue due to involvement of these proteins in vital homeostatic processes [16–18]. Much effort is thus invested in finding tumour markers with specific expression on the tumour cells or stroma. Lastly, targeting immune system regulating proteins causes increase in autoimmune toxicities, and is only effective if the immune cells with specificity against cancer antigens are present in the tumour environment [10].

1.3 Targeting tumour vessels: anti-angiogenics and vascular disrupting agents

Once a tumour grows beyond 1 mm^3 the cells are no longer able to access oxygen and dispose of metabolic by-products and the environment becomes hypoxic. Hypoxia triggers many signalling pathways in cancer cells, resulting in, amongst others, secretion of pro-angiogenic factors. New vessels then invade from the existing vasculature causing the 'angiogenic switch' [19,20], a critical step for cancer progression.

In normoxia (1-4% O_2), the VHL protein acts as a negative regulator of HIF-1 transcription factor. When oxygen is present, prolyl hydroxylases (PHD1–3, prolyl hydroxylase domain 1–3) hydroxylate two prolines on HIF-1α protein (Pro402 and Pro564). VHL then recognises and binds these residues, marking HIF-1α for degradation. This process is highly dependent on the level of molecular oxygen in cells [21,22]. In poorly perfused tissues oxygen levels are low, prolines are not hydroxylated and proteasomal destruction of HIF-1α does not occur. HIF-1α levels increase and can now bind to HIF-1β, located in the nucleus [23] (Figure 1.1 – schematic representation of HIF pathway in normoxic and hypoxic conditions). The HIF-1 heterodimer then mediates expression of vast amount of genes involved in angiogenesis, survival, cellular metabolism and cell migration [24–26]. Amongst other significant genes, HIF-1 induces overexpression of VEGF-A [27]. VEGF-A plays a significant role in angiogenesis by stimulating sprouting of new blood vessels from the existing ones. In tumours the expression of VEGF-A as well as other growth factors is abnormally high due the fast growth of tumours, which induces hypoxic conditions. Thus, constant exposure to high pro-angiogenic signalling and lack of homeostatic feedback regulation causes abnormal formation of new blood vessels. This and other pathological conditions occurring in tumours (low shear stress, low pH,

hypoglycaemia) hugely affect tumour vasculature causing lack of hierarchical arrangements, poor mural cell coverage, vessel enlargement and leakage, and poor perfusion. These conditions result in low oxygenation, a feature that often causes failure of administered chemotherapy and radiotherapy [28]. However, these differences cause expression of proteins on tumour vessels that might not be expressed on healthy vessels, making them useful targets for cancer treatment.

Blocking tumour angiogenesis or destroying tumour blood vessels is considered a promising approach for cancer therapy due to a number of advantages over targeting tumour cells: the molecules on tumour vessels are easily accessible to intravenously administered agents; endothelial cells are not genetically unstable like cancer cells, so are less likely to develop resistance via mutation; and disturbance of blood vessel can cause damage to many tumour cells. So far, the major approach has been inhibition of angiogenesis through targeting the VEGF pathway either by tyrosine kinase inhibitors or antibodies.

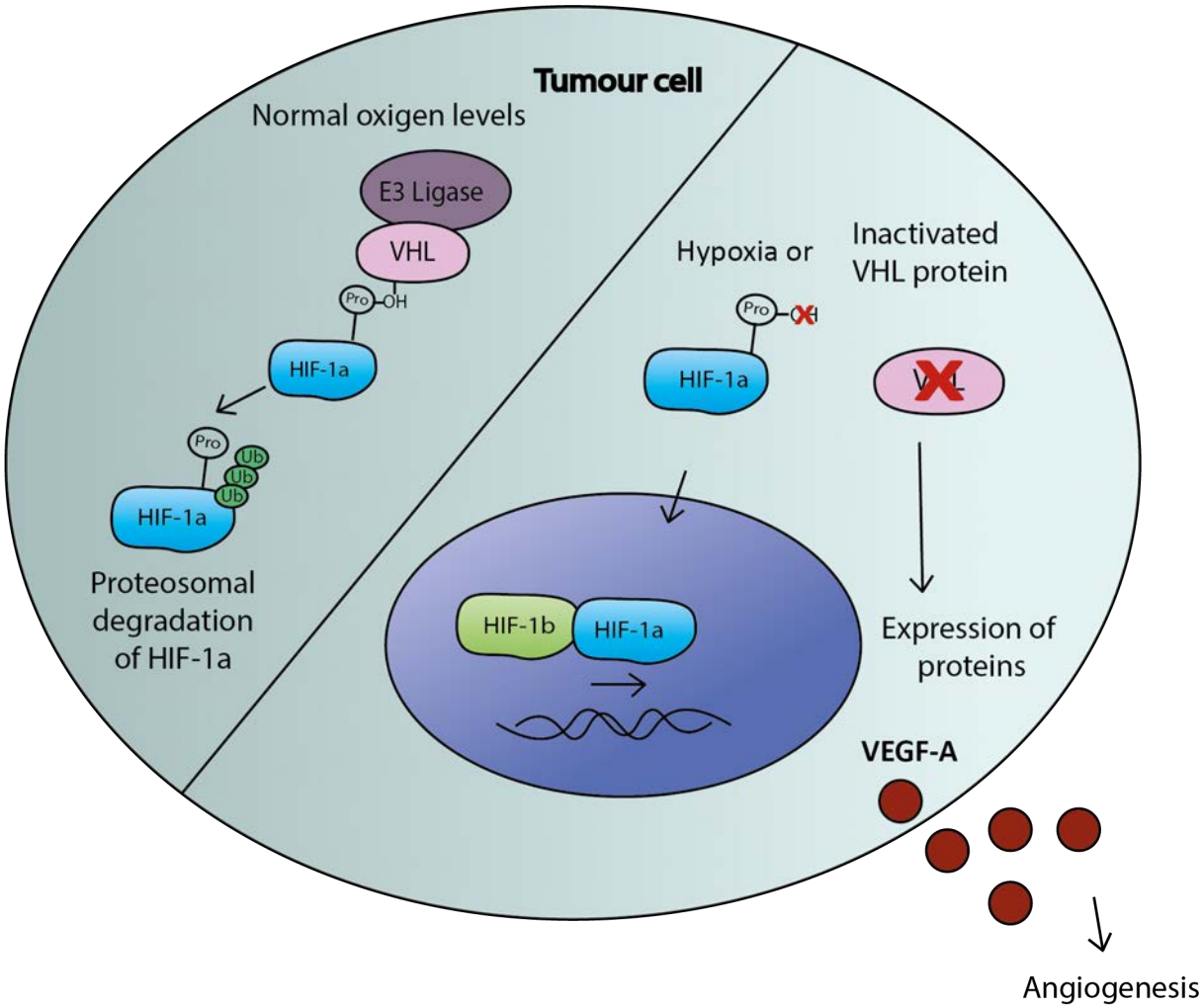

Figure 1.1 VHL regulation during normal oxygen levels and in hypoxia. During normal oxygen levels in the tissue VHL protein recognises hydroxylated prolines on HIF-1a transcription factor and marks it for protein degradation, while during hypoxic conditions or in case of inactivated VHL protein HIF-1a remains stable and binds HIF-1b in the nucleus. The HIF-1 dimer affects expression of numerous genes including VEGF-A, which then activates formation of new blood vessels from the neighbouring vessels.

Renal cell carcinoma

Renal cell carcinoma (RCC) is the most frequent form of kidney cancer, comprising around 85% of all cases. The remaining 15% of kidney cancers are urothelial carcinoma, sarcoma, Wilms tumour and lymphoma. Statistically, kidney cancer is the 12th most common cancer in the world, but 9th most common cancer in the more developed countries (North America, Europe, Australia and New Zealand) [29]. This is due to higher rates of smoking and 'fast-food' diets high in unhealthy fat, both of which increase the risk of renal cancer [30]. The diseases mostly develops in older people with an average age of diagnosis of 64, and is more frequent in men than women [31]. Moreover, the occurrence of kidney cancer increases yearly [32], for example a 41% increase from 2003 to 2014 has been reported in the UK [33], and a further increase of 26% is expected in the next 12 years.

Renal cell carcinoma predominantly presents with clear cell histology (ccRCC), which is in 90% of cases connected to the loss of function of the VHL gene [34]. In around 50% of RCC sporadic mutations or deletions of the VHL gene are observed in both alleles, and other cases fail to express the VHL protein due to epigenetic hypermethylation of the VHL gene [35]. Hereditary mutation of the VHL gene is called the VHL syndrome and patients with this syndrome have a tendency to develop RCC, and other highly vascular tumours at a much younger age [36]. VHL syndrome is an autosomal dominant genetic disorder due to mutation in one allele of the VHL gene when there is a subsequent loss or mutation in the remaining VHL allele [37,38]. VHL inactivation in RCC creates an environment in which angiogenesis is continuously activated via production of VEGF-A without the need for hypoxic conditions, resulting in increased vascularisation of this cancer.

1.3.1. Treatment of RCC

Renal cell carcinoma often presents with minimal or generic symptoms such as slight abdominal or lower back pain and is thus, often detected at a late stage. The current standard of care for localised RCC is surgical resection and subsequent monitoring for progression [39,40]. Early stage RCC patients have a 74% chance of 5-year survival. However, progressed disease is often hard to treat with the approved treatments, and complete response is seen in a disappointingly small number of patients, around 1-3% [41]. Moreover, around 30% of patients with localised disease will experience recurrence during their lifetime [42] and the 5 year survival rate drops drastically for patients with advanced or metastatic disease to only 8% [31].

Traditional forms of therapy (chemotherapy and radiotherapy) have proven inefficient in the treatment of RCC. However, based on several observations of spontaneous remission in cases with progressed RCC, it was postulated that the host immune system could be activated to target and eradicate the cancer [43]. Subsequently, cytokine based therapies IFN-α and IL-2 demonstrated an effect on survival in some patients with progressive metastatic disease [44]. However, no significant benefit on survival was observed for patients with locally advanced RCC with high risk of recurrence after nephrectomy [45]. These therapies are significantly more effective in higher doses, but unfortunately induce severe immune system related side effects [46], which can cause serious damage and have proved fatal in some cases [47]. Therefore, their use is often restricted to younger patients with good performance status. Furthermore, complete response is observed in only 7% of patients receiving high doses of IL-2 [48].

In 2005 the first targeted therapy was approved for the treatment of RCC. Using targeting therapies finally showed improved patient survival with fewer side effects compared

to previous systemic therapies and led to approval of several anti-angiogenic drugs, mTOR inhibitors and targeted immunotherapy. However, targeting angiogenesis is the preferred first line option for advanced and metastatic RCC, specifically in cases with clear cell histology. Once the patient progresses on anti-angiogenics, the second line treatment includes other type of anti-angiogenic drug, mTOR inhibitor or targeted immunotherapy depending on the patient's status and pathology of the tumour [49].

1.3.2. Anti-angiogenic therapy in RCC

Sunitinib, a tyrosine kinase inhibitor (TKI), was the first anti-angiogenic drug approved for first line treatment of metastatic RCC due to a significant improvement in progression free survival when compared to cytokine therapy in untreated patients [50]. Pazopanib, another TKI, was also approved for the first line treatment in advanced RCC, after showing a 5-month improvement in progression free survival when compared with placebo in patients that were untreated as well as in those progressed after cytokine therapy [51]. Sorafenib, axitinib, cabozantinib, and lenvatinib are other approved TKIs for RCC treatment. Bevacizumab, an antibody that sequesters VEGF protein, is approved in combination with IFN-α for first line setting [52], however is rarely used in UK due to its high cost. Yearly improvement in targeted therapies can be seen in the latest successful trial testing cabozantinib with sunitinib, showing a further increase in progression free survival in patients presented with poor prognosis RCC in a first line treatment setting [53]. Due to this cabozantinib was approved in December 2017 for first line treatment for intermediate or poor risk advanced RCC patients by the FDA and in Europe.

1.3.3. Combinational therapeutic approaches

Combining different strategies to improve the outcome of patients has proven beneficial in some cases. Targeting different aspects such as the VEGF pathway together with activation of immune system with cytokines by using Bevacizumab together with cytokine IFN-α had improved PFS when compared with the cytokine therapy alone (10.2 and 5.4 months, respectively) [52].

Combination of lenvatinib with an mTOR inhibitor everolimus presented superior overall response rate (ORR) than the everolimus therapy alone (43% versus 6%, respectively) [54]. The PFS and OS were significantly increased as well, and it was approved in 2016 as a combination therapy for patients that progressed after anti-VEGF treatment. However, another trial that investigated combinations of temsirolimus (mTOR inhibitor) and Bevacizumab, in comparison to single agent therapies showed no significant difference in PFS and OS, but the grade 3-4 side effects were significantly more frequent in the combination group. Many on-going clinical trials are focusing on optimizing combinations and sequencing of different agents in order to establish the maximum benefit approach in treating advanced and metastatic RCC.

1.3.4. Future directions based on present knowledge

Finding appropriate targets and marker molecules in order to develop tools for treatment and prediction of disease progression remains a great challenge.

Notwithstanding all of the recent advances in therapies, there are still numerous unanswered questions regarding markers for optimal treatment selection and prediction of disease progression. There is an unmet need for improved treatments with fewer and less severe side effects to be developed in order to improve patients' survival and quality of life.

Further research on predictive biomarkers will help in the effort to treat each patient's tumour with individualized therapy [55].

Screening for molecules expressed by tumour or stromal cells are providing a platform of novel molecules that can be used as targets on RCC. Specifically, interesting proteins would be ones that are differentially expressed on the pathological tissue and absent or lowly expressed on the healthy tissue. Furthermore, proteins that are not relevant for healthy tissue homeostasis are preferred, as targeting those molecules would cause less damage to healthy organs. VEGF and receptor tyrosine kinases are present in most tissues and are important for homeostasis, and thus targeted therapies against those molecules affect the healthy tissue and cause systemic side effects.

Wragg et al.[56] screened for differences between tumour vessels of RCC and healthy blood vessels in order to identify specific tumour endothelial markers. They isolated endothelial cells from matched healthy and tumour tissue taken during nephrectomy of patients that had received no therapy prior to surgery. RNA from cells was analysed using whole human genome expression microarrays. Besides finding of 'expected' upregulated genes in tumour angiogenesis they found MCAM (melanoma cell adhesion molecule) and its ligand LAMA4 (laminin alpha 4) to be highly expressed in RCC blood vessels, but absent from the healthy vessels taken from the same patients. LAMA4 is an extracellular matrix protein, which is a component of basal lamina and MCAM is a cell adhesion molecule involved in tumour angiogenesis and metastasis in several tumours (described in detail below).

Wragg et al. confirmed these findings by qRT-PCR and immunostaining, where they showed strong MCAM staining of the tumour vessels, whereas no staining was observed in healthy tissue. Furthermore, they compared the staining of tumour tissue and matched

healthy tissue of 18 different tumours. MCAM expression was specific for vasculature, except in melanoma, where MCAM was expressed on tumour cells. MCAM had strong expression in 90% of RCC and some of the other cancers while it was absent from the healthy tissue whereas, LAMA4 showed mixed expression in healthy and tumour tissue (Figure 1.2).

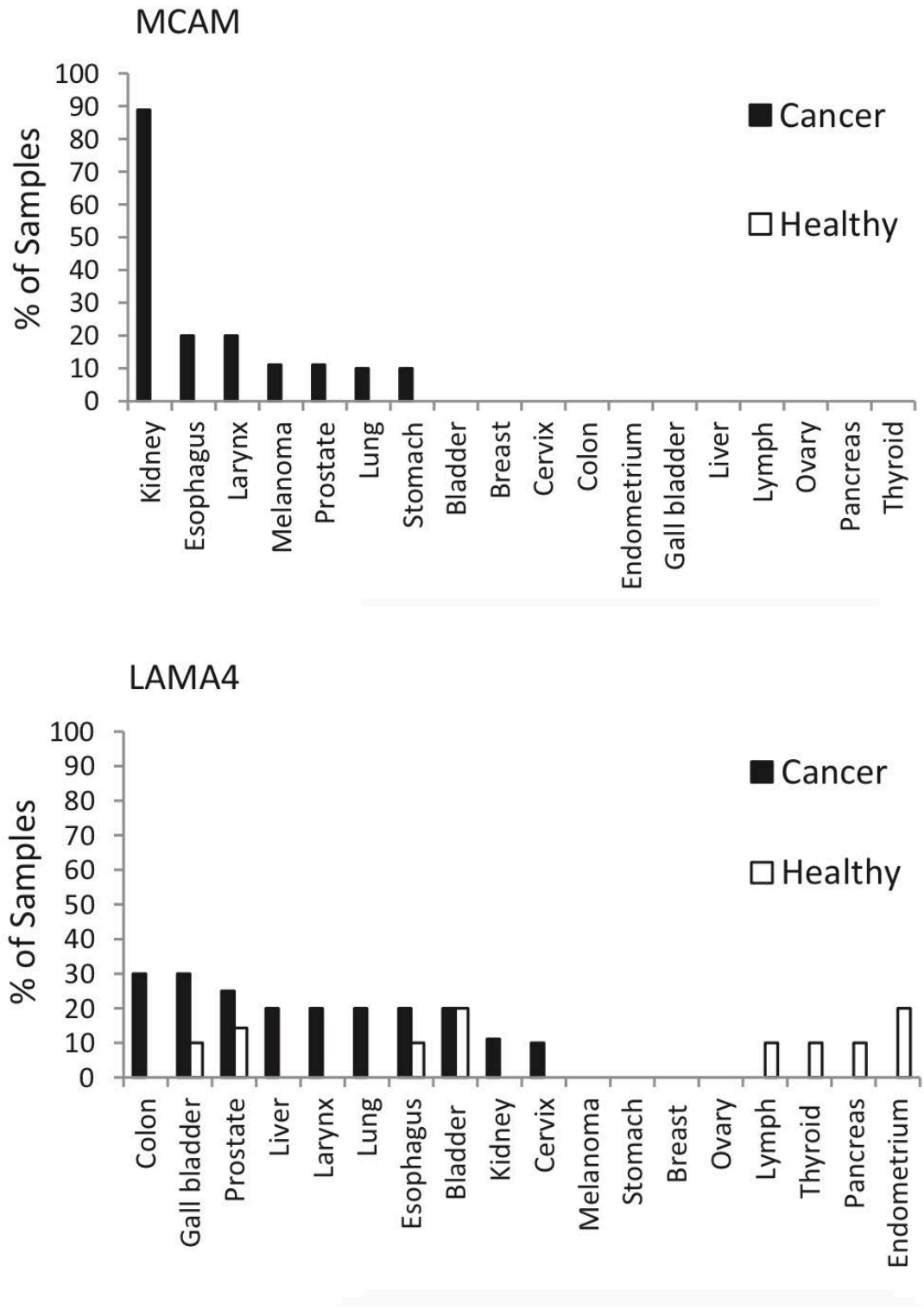

Figure 1.2 Strong staining of MCAM and LAMA4 on blood vessels of matched tumour and healthy tissue. [56]

1.4 Melanoma cell adhesion molecule – MCAM

1.4.1. MCAM gene and protein description

MCAM (also known as CD146, MUC18, S-Endo1, A32 antigen) is a multifunctional protein expressed on the cell surface of several cell types including cancer and tumour endothelial cells. The 113 kDa-protein has a single transmembrane domain, short cytoplasmic tail and an extracellular domain that consist of characteristic immunoglobulin-like V–V–C2–C2–C2 domains [57,58]. Each of the immunoglobulin domains contains a single intra-chain disulphide bond, and the extracellular domain undergoes post-translational glycosylation [59,60]. Orthologous of MCAM have been identified in other mammalian species (mouse, rat, canine) [58,61], in avian species also known as HEMCAM or gicerin [62,63], and in fish [64]. The human MCAM gene has a single copy on chromosome 11 and to date only one mRNA of around 3.3 kb has been identified [59,65,66]. However, three different mRNA isoforms have been described in chicken: MCAM long, MCAM short and soluble MCAM [67]. The longer isoform of MCAM (lgMCAM) is present in all the species and consists of the extracellular domain, transmembrane domain and a cytoplasmic domain which contains two protein kinase C (PKC) recognition sites and an ERM (ezrin/radixin/moesin) binding site. The shorter MCAM isoform (shMCAM) has a deletion in the cytoplasmic region, causing a reading frame shift that results in loss of one of the PKC binding regions. The third MCAM isoform is a soluble extracellular domain (sMCAM), which, in chicken, is produced by mRNA splicing [67]. Soluble MCAM has been found in human plasma and in HUVECs supernatants [68], however there is no evidence that this protein is a product of RNA splicing. Rather, evidence shows that this is due to the enzymatic cleavage of the membrane form of MCAM with metalloproteinases [69].

1.4.2. MCAM expression in healthy tissue

MCAM has been found expressed in numerous tissues during embryonic development, such as kidney, retina and the nervous system [63,70,71]. However, its expression hugely diminishes in adult tissue. Immunohistochemistry with MUC18 antibody showed limited expression of MCAM, detected only on smooth muscle cells of vessels, on hair follicles [65] and in a small percentage of capillaries, but absent from larger vessels [72]. Another antibody to MCAM, A32, confirmed this expression pattern [60]. In contrast, S-Endo-1 anti-MCAM monoclonal antibody, developed against human endothelium, detected MCAM expression on all vessels in human tissue regardless of the vessel size or location [73].

MCAM was further found to be expressed on a subset of nonhaematopoietic bone marrow mesenchymal stem cells [74,75], on a small population of T and B lymphocytes and NK cells with an effector memory cell phenotype [76], and on CD4+ Th17 and CD8+ Tc17 lymphocytes with higher affinity for endothelium [77,78]. MCAM is also expressed on intermediate trophoblast [79,80]. In mice, ME-9F1 antibody to mouse protein identified MCAM expression on endothelial cells and on a subset of mature NK cells with reduced cytotoxicity [81,82].

1.4.3. MCAM expression in cancer and other pathological conditions

The first discovery of MCAM was with MUC18 antibody in 1987, showing upregulated expression on malignant melanoma and in metastasis when compared to healthy melanocytes and benign melanoma lesions [65]. Much further research on MCAM involvement in melanoma confirmed that MCAM is an excellent predictor of melanoma progression with higher confidence rate than tumour grade or lymph node [83,84]. Besides melanoma, MCAM expression correlates with tumour progression and metastasis in several other tumours such as prostate

[85,86], epithelial ovarian cancer [87,88], gastric cancer [89], breast cancer [90,91], kidney cancers [56] and non-small-cell lung cancer (NSCLC) [92]. However, it does not correlate with tumour progression and metastasis in all cases. For example studies in breast cancer are mixed, with several studies showing the opposite effect of MCAM on progression and metastatic potential of tumour cells, showing more compact and tightly bound cells [93,94]. Similarly MCAM is considered a tumour suppressor in naso-pharyngeal carcinoma [95].

MCAM is often expressed in endothelial-derived tumours such as haemangioma, angiosarcoma and Kaposi's sarcoma [96]. Finally, MCAM is expressed in a subset of leukemic cell lines and in some haematopoietic malignancies [97].

The exact mechanism of MCAM overexpression in tumours is not yet known, however, it was shown that its expression is not due to mutations of the MCAM gene or chromosome translocations in melanoma [57]. In prostate cancer, the MCAM promoter was found significantly hypermethylated when compared to the healthy prostate, and the amount of methylation correlated with the progression of the tumour [98]. The possibility that MCAM is expressed due to environmental factors was further endorsed by the discovery that certain growth factors such as VEGF, as well as inflammatory cytokines (IFN-α) can promote MCAM expression [56,99].

1.4.4. MCAM function

There is much research into the function of MCAM protein showing its involvement in a broad range of cellular signalling pathways. Initially, it was thought that MCAM played a role as a cell adhesion molecule in malignant melanoma and was connected to melanoma progression and metastasis [65]. However, a function for MCAM has since been described in

tumour angiogenesis, cellular communication, cell-matrix interactions, transendothelial migration and immune responses [66].

MCAM is involved in embryonic vessel development

The involvement of MCAM in angiogenesis has been shown in early development. MCAM knock out impedes embryonic development of blood vessels in zebrafish [64], and blood vessels of kidney and retina in chicken [63,71]. The mouse MCAM knock out develops normal blood vessels however, it has a negative effect on tumour angiogenesis in adult mice [100]. Moreover, an antibody that inhibits angiogenic properties of MCAM diminished early vessel branching in the chicken chorioallantoic membrane (CAM) assay [101].

MCAM in angiogenesis

MCAM plays a role in many cell processes that are involved in angiogenesis, for example matrix degradation, loosening of cell junctions, proliferation, chemotaxis, migration and cell adhesion. *In vitro* assays on human endothelial cells showed that knock-down of MCAM by siRNA caused arrest in HUVEC proliferation, adhesion and migration [102]. Antibodies against MCAM also inhibited HUVEC tube formation *in vitro* [101,103].

Loosening of endothelial junctions and interaction with extracellular matrix

The first step in angiogenesis is degradation of basal membrane and extracellular matrix protein complexes in order for endothelial cells to invade into the tissue [104]. MCAM affects expression of several matrix metalloproteinases (MMP-2, MMP-9) [105,106], and targeting MCAM with an antibody AA98 inhibits tumour growth in xenograft mouse models due to impaired matrix degradation and invasion of blood vessels into the tumours [101]. Furthermore, the endothelial cells in formed blood vessels need to loosen their connection, in order to start migrating and proliferating. It was found that in the presence of VEGF, MCAM induces

loosening of endothelial cell junctions and increases paracellular permeability as a co-receptor for VEGFR-2 [100,107,108]. MCAM antibody called P1H12 increased paracellular permeability of cultured human microvascular endothelial cells (HMVECs) [105]. Increased permeability could also be caused by MCAM shedding form the cell membrane in response to selected environmental signalling, including VEGF and cellular calcium increase [69,99]. Soluble MCAM further promotes endothelial cell proliferation.

MCAM was found to increase cell migration on laminins. It was found that MCAM binds laminin 421 and 411 and facilitates cell migration *in vitro* [109]. MCAM and laminin alpha 4 are highly expressed in several types of cancers possibly involved in tumour angiogenesis and tumour cell migration [110].

Cell migration

It has been shown that the neuronal guidance molecule netrin-1 has an effect on angiogenesis through its interactions with MCAM. Netrin-1 in low concentrations promotes angiogenic properties of HUVECs, such as proliferation, migration and network formation. It does so by binding MCAM and inducing dimerization, which then activates VEGFR-2, ERK1/2 and p38 protein phosphorylation. However, this process is dependant on the amount of netrin-1 in the tissue, and a higher concentration (2000 ng/ml) activates UNC5B signalling and inhibits angiogenesis [111]. MCAM can also activate migration by binding and initiating phosphorylation of ERM protein, which then activates RhoA-induced cytoskeleton reorganisation [112]. Furthermore, MCAM knock down decreases the activity of RhoA [88].

MCAM is also involved in regulation of cell polarity and migration by activating non-canonical Wnt signalling. MCAM acts as a receptor for Wnt5a, activating downstream signalling by Dishevelled (Dvl) and JNK (c-jun amino- terminal kinase), as well as blocking Wnt

canonical signalling by promoting β-catenin degradation [113]. Furthermore, MCAM causes cytoskeletal rearrangements by recruiting myosin and F-actin which cause cell membrane retraction in the direction of cell movement [114].

Cell adhesion

Cells expressing MCAM have increased self-adhesion [62] and MCAM is found expressed in the cellular junctions in cell-cell contacts of confluent cultured endothelial cells [107]. MCAM crosslinking with S-Endo-1 promotes a signalling cascade by recruiting Fyn kinase (a Src family kinase) which then phosphorylates FAK and paxilin [115], proteins involved in forming focal adhesion plaques. Furthermore, MCAM expression increases as cells reach confluence [60], and it was reported that the phosphorylation of FAK and paxilin increases with cell density [116]. MCAM is thus possibly involved in the connection between cells during formation of established blood vessels. Additionally, it was shown that balanced levels of VEGF are involved in maintenance of vessel integrity [16,117] and MCAM knock out impaired FAK phosphorylation in response to VEGF signalling [100].

Soluble MCAM and tumour angiogenesis

Soluble MCAM (sMCAM) has been found both in cultured HUVEC supernatants and in the blood of healthy individuals [68]. However many reports indicate that sMCAM is increased in the plasma of cancer patients as well as in other conditions that involve endothelial disruption and inflammation [80,118–121]. sMCAM binds Angiomotin isoform p80 (Amot p80) and induces pro-angiogenic effects on cultured endothelial cells as well as inducing angiogenesis *in vivo* in matrigel plug model and in mouse xenograft tumours [106]. It is involved in promoting tumour progression by increasing expression of MMP-9, Ang-2, IL-8 as well as VEGF [106].

1.4.5. MCAM function in the immune system

T-cells positive for MCAM expression secrete significantly more IL-17A, IL-6, and IL-8 than MCAM negative cells [76,77]. These cells show an effector memory phenotype and have a tendency to bind endothelium in order to extravasate into various tissues including crossing the blood brain barrier in certain neurodegenerative conditions [109,122]. It is believed that MCAM facilitates this attachment to the blood vessels and facilitates extravasation by binding to either itself or another protein on endothelial cells. Certain immune modulating factors such as TNFα increase expression of MCAM on endothelial cells, as well as increase MCAM shedding by metalloproteinase [99]. Shedding of MCAM from endothelial cells influences transmigration of immune cells by loosening endothelial cell junctions and inducing chemotaxis [99]. This action can be blocked by antibodies against MCAM or by MCAM silencing via siRNA [99].

Besides immune cells it was shown that MCAM knock out in mouse endothelial cells (isolated from MCAM knock out mice) significantly reduced transmigration of melanoma cells in response to VEGF signals, further confirming MCAM involvement in the endothelial barrier [100].

1.4.6. MCAM expression and function in renal cell carcinoma

In healthy kidneys, MCAM is present in arteriolar endothelial cells (EC), mesangial cells and arteriolar smooth muscle cells [120]. In chicken, MCAM is involved in kidney development and its expression is reduced in the adult tissue [63]. However, MCAM is significantly upregulated in Wilms tumour (a form of kidney cancer) in adult chicken [71].

The first paper indicating involvement of MCAM in human metastatic renal cell carcinoma showed that 769-P cells (primary renal cancer cell line) transfected with IGFBP- 4

(insulin-like growth factor binding protein 4) had a 74-fold increase in MCAM mRNA, and an increase in MCAM protein level [123]. They found that IGFBP-4 expression correlated with progression of RCC and activated Wnt signalling, which plays a role in progression of several cancers [124]. IGFBP-4 affected proliferation, migration and invasion of transfected cells *in vitro* and increased cancer growth in a mouse model. They concluded that IGFBP-4 activates expression of MCAM in renal cell carcinoma and that both proteins could serve as potential prognostic markers for this cancer. Another group confirmed significant increase in MCAM expression in patients with progressed and metastatic RCC when compared to patients with localised disease [125]. Additionally, they showed that MCAM expression correlated with higher risk of recurrence after partial or complete nephrectomy in patients that had no treatment prior to surgery. They showed this by analysing MCAM mRNA levels from the whole tumour tissue taken during the nephrectomy. Our group later identified MCAM expression in vessels of renal cell carcinoma, rather than in cancer cells, by immunohistochemistry [56]. Here as well MCAM expression was connected to the poor patient prognosis. In the same study a monoclonal antibody towards mouse MCAM showed *in vivo* localisation to vessels in mouse RENCA tumour (a murine model of renal cell carcinoma), showing that targeting MCAM with monoclonal antibodies could be a possible new approach to treat advanced stages of RCC.

Soluble MCAM is present in plasma of healthy donors, but is significantly increased in patients with chronic renal failure (CRF) [120]. The same is true for MCAM expression in renal biopsies of CRF. MCAM is expressed on the cell junctions and CRF has been associated with endothelial cell junction changes [107]. MCAM is possibly overexpressed and cleaved form the cell surface influencing the connectivity between neighbouring cells.

A study this year (2018) showed that soluble MCAM is increased in clear cell RCC in patients with higher risk of recurrence after initial sunitinib treatment [126]. MCAM is a co-receptor for VEGFR-2, a target of sunitinib, it is possible that an increase in MCAM expression and shedding could have an impact on bypassing anti-VEGF-targeted therapy. Thus, there may be benefit in dual targeting MCAM together with VEGF pathway to synergistically improve responses of clear cell RCC patients.

1.4.7. Antibodies to MCAM protein

Numerous antibodies against human MCAM have been developed over the years, with fairly diverse properties. For example, different antibodies pull down MCAM of different weight: 113 kDa (MUC18, A32) [60,65], 118 kDa protein (S-Endo-1)[73] or 110 kDa (mAb 541-30B2, 541-1082 and 541-2E5) [127]. Different immunohistochemistry staining patterns have been reported for different MCAM antibodies as well. MUC18 antibody stains only endothelial cells of capillaries and smooth muscle cells surrounding the vessels, while S-Endo-1 stains all the endothelial cells no matter the vessel size [65,73]. Two monoclonal antibodies to MCAM (541-1082 and 541-2E5) react with activated T cells, while no reaction to these cells was observed with MUC18 and A32 [127]. Antibody AA98 recognises MCAM expressed only on the tumour endothelium but does not recognise healthy vessels [101]. In contrast, another antibody recently described against MCAM (TsCD146 mAb) stains only the tumour cells, without staining the blood vessels, while S-Endo-1 stains both the tumour cells and the blood vessels in the same tissue sample [128]. It is assumed that this is due to the different glycosylation patterns, or available epitopes within different cells based on MCAM functions and environment in those cells [73,129]. Lastly, antibody M2J-1 recognises only the soluble protein but not membrane bound MCAM [106].

The effects of antibodies on cell signalling and different MCAM pathways is also diverse. For example anti-human MCAM antibody ABX-MA1 blocks xenograft tumour growth and angiogenesis in mice [130], possible by decreasing expression of MMP-2 [103], which is important in matrix degradation for blood vessel infiltration into the tumour tissue. Similarly it was found that antibody AA98 suppressed NF-kB activation and expression of MMP-9 and ICAM-1 and thus inhibits tumour angiogenesis [131]. Furthermore, AA98 blocks *in vitro* HUVECs proliferation, while ABX-MA1 does not [101,103]. In contrast, both antibodies inhibit capillary tube formation in a HUVECs angiogenesis assay. TsCD146 antibody which is specific to only tumour cells but not endothelial MCAM induces cell apoptosis [128].

1.5 Aims and objectives

We hypothesised that MCAM is a possible therapeutic target for vascular disruption and/or anti-angiogenic treatment in renal cell carcinoma. Therefore, we aimed to investigate MCAM as a possible therapeutic target in renal carcinoma mouse models (RENCA) by generating monoclonal antibodies targeting mMCAM.

Next, we aimed to characterise the properties of anti-mMCAM antibodies for technical use as well as possible therapeutic utilisation.

Lastly, in order to confirm whether MCAM has anti-angiogenic properties, we aimed to investigate soluble human MCAM extracellular domain as a receptor trap in various angiogenesis assays.

2 MATERIALS AND METHODS

2.1 Materials

Commonly used chemicals and reagents were purchased from Sigma Aldrich (Gillingham, UK), unless otherwise stated.

Table 2.1 Buffers and solutions

Buffer:	Contents:
PBS	Commercially available PBS tablets
PBS-T	PBS, 0.1% (v/v) Tween 20
Ampicilin LB	100 µg/ml in LB agar or LB broth
Kanamicin LB	50 µg/ml in LB agar or LB broth
SDS-PAGE running buffer	25 mM Tris base, 250 mM glycine, 0.5% (v/v) SDS
SDS-PAGE transfer buffer	25 mM Tris, 192 mM glycine, 20% (v/v) methanol
Membrane blocking buffer	PBS-T, 5% (w/v) dried skimmed milk (Marvel)
ELISA blocking buffer	PBS, 2% (w/v) dried skimmed milk
Tris-acetate-EDTA (TAE) buffer	40 mM Tris, 20 mM acetic acid, 1 mM EDTA
Flow cytometry buffer	PBS, 0.2% (w/v) BSA, 0.02% (v/v) sodium azide
Papain cleavage buffer	150 mM NaCl, 0.67 mM EDTA, 5 mM L-cysteine, 10 mM NaH2PO4
Oligo annealing buffer	10 mM Tris pH 7.5, 50 mM NaCl, 1 mM EDTA
Beads wash buffer	PBS, 287 mM NaCl, 0.1% (v/v) NP-40
Non-reducing protein loading buffer	50 mM Tris HCl pH 6.8, 10% (v/v) glycerol, 2% (v/v) SDS, 0.001% (w/v) bromophenol blue
Reducing protein loading buffer	Non-reducing protein loading buffer, 1.25% (v/v) β-mercaptoethanol
NP-40 lysis buffer	50 mM Tris pH 7, 1% (v/v) NP-40, 150 mM NaCl, 1 mM EDTA, protease inhibitors, Pierce

Table 2.2 List of antibodies and dilutions used for given applications: WB – Western blot, FC – flow cytometry, IF – immunofluorescence, IHC – immunohistochemistry, ELISA – enzyme-linked immunosorbent assay, IP – immunoprecipitation

Specificity	Species	Application dilution	Reference number	Source
Human MCAM	Rabbit	WB 1:1000 ELISA 1 µg/ml	HPA008848	Sigma
Mouse MCAM	Sheep	WB 1:500 ELISA 1 µg/ml	AF6106	R&D (Minneapolis, US)
Mouse MCAM	Rat monoclonal	WB 1:500 FC 10 µg/ml IP 2 µg/ml	MAB7718 (0.5mg/ml)	R&D
His tag	Mouse monoclonal	WB 1:1000 ELISA 1 µg/ml	MAB050	R&D
FLAG tag	Mouse monoclonal	WB 1:1000	ab49763 (M2)	Abcam (Cambridge, UK)
Human Tubulin	Rabbit	WB 1:1000	2144S	Cell Signalling Technology (Danvers, USA)
Human CD31	Mouse monoclonal	IF 1:200	550389 (WM59)	BD Biosciences (Oxford, UK)
Human IgG-HRP	Goat	WB 1:1000 ELISA 1 µg/ml	A0170	Sigma
Rabbit IgG-HRP	Goat	WB 1:5000 ELISA 1:2000	7074S	Cell signalling
Sheep IgG-HRP	Donkey	WB 1:5000 ELISA 1:2000	HAF016	R&D
Rat IgG-HRP	Rabbit	WB 1:5000 IHC 1:100 ELISA 1:2000	P0450	DAKO (Cambridge, UK)
Mouse IgG-HRP	Goat	WB 1:5000 ELISA 1:2000	P0447	DAKO
AlexaFluor® 546 anti-rat IgG	Goat	IF 1:200 FC 1:100	A11081	Invitrogen (Paisley, UK)
AlexaFluor® 647 anti-rat IgG	Gaot	IF 1:200	A21247	Invitrogen
AlexaFluor® 488 anti-rat IgG	Goat	IF (ab localisation) 1:200	A11006	Invitrogen

Table 2.3 List of control species IgG

Control IgG	Concentration	Application dilution	Reference number	Source
Rat IgG	2mg/ml	IHC 10/15 µg/ml IF 10 µg/ml FC 10 µg/ml IP 2 µg/ml	6-001-A	R&D

2.2 Molecular cloning

Table 2.4 List of gene DNA templates

Reference number	cDNA	Source
MHS 6278-202760082	Human MCAM	Provided by Victoria Heath
MMM 1013-202770023	Mouse MCAM	Provided by Victoria Heath

Table 2.5 List of oligonucleotides

Oligo lable	Name	Sequence 5’ – 3’
VH517	mMCAM EcoRI forward	TAGTAGGAATTCGGAAGCATGGGGCTGCCCAAAC
VH518	mMCAM NotI reverse	CTACTAGCGGCCGCCACCTTTGCTCTCTGGCTGTGG
VH519	hMCAM EcoRI forward	TAGTAGGAATCCGGAAGCATGGGGCTTCCCAGG
VH520	hMCAM NotI reverse	CTACTAGCGGCCGCCGCCCCGGCTCTCCGGCTCCGG
MC08	His NotI forward	GGCCGCCATCATCACCATCACCACTAGT
MC09	His XbaI reverse	CTAGACTAGTGGTGATGGTGATGATGGC
MC12	hMCAMseq701 forward	GGAACCACATGAAGGAGTCC
MC13	hMCAMseq1295 forward	CCCCTTGGATGGCATTCAAG
MC14	mMCAMseq654 forward	GGAAGACAAAGATGCCCAGT
MC15	mMCAMseq1254 forward	TCCTGGCTTGAATCGTACCC
MC24	mMCAM FL-FLAG reverse1	CTACTTGTCATCGTCATCCTTGTAATCACTCGATGAAG AATGCCTCAGATCGATG
MC25	mMCAM FL-FLAG forward	CGAGACTAGCCTCGAGGTTTAAACGGAAGCATGGGG CTGCCC
MC26	mMCAM FL-FLAG reverse2	ATTCCTGCAGCCCGTAGTTTAAACCTACTTGTCATCGT CATCCTTGTAATCACTC
MC30	mMCAMdel1 NotI reverse	TAGTAGGCGGCCGCCTGCCATCCATGGGGACCC
MC31	mMCAMdel2 NotI reverse	TAGTAGGCGGCCGCCCAGCAGCTCCAGGGGGTC
MC32	mMCAMdel3 NotI reverse	TAGTAGGCGGCCGCCTGCAGGGTAGAAAACAG
CMV fwd	CMV promotor forward	CGCAAATGGGCGGTAGGCGTG
EF-1a fwd	EF-1a promotor forward	TCAAGCCTCAGACAGTGGTTC
IRES rev	5' end of IRES reverse	CCTCACATTGCCAAAAGACG
EGFP-N rev	5' end of EGFP reverse	CGTCGCCGTCCAGCTCGACCAG

DNA oligonucleotides were ordered from Eurogentec S.A. (Seraing, Belgium).

Table 2.6 List of cloned DNA plasmid constructs

Construct	Vector	Restriction site	PCR primers	Ligation
mMCAMecd-Fc	pcDNA3.Fc	F: EcoRI R: NotI	F: VH517 R: VH518	T4
hMCAMecd-Fc	pcDNA3.Fc	F: EcoRI R: NotI	F: VH519 R: VH520	T4
mMCAMecd-His	pcDNA3.Fc	F: EcoRI R: NotI	F: MC08 R: MC09	T4
hMCAMecd-His	pcDNA3.Fc	F: EcoRI R: NotI	F: MC08 R: MC09	T4
mMCAMfl-FLAG	pWPI	F: PmeI R: PmeI	F: MC25 R1: MC24 R2: MC26	GA
mMCAMecd-D1-Fc	pcDNA3.Fc	F: EcoRI R: NotI	F: VH517 R: MC30	T4
mMCAMecd-D2-Fc	pcDNA3.Fc	F: EcoRI R: NotI	F: VH517 R: MC31	T4
mMCAMecd-D3-Fc	pcDNA3.Fc	F: EcoRI R: NotI	F: VH517 R: MC32	T4

F – forward primer, R – reverse primer, T4 – T4 DNA ligase reaction, GA – Gibson Assembly reaction

2.2.1. Agarose gel electrophoresis and DNA visualization

Agarose gel electrophoresis was used for the separation, size estimation and visualization of DNA. Agarose gels were prepared from 0.7% - 2% (w/v) agarose powder in Tris-acetate-EDTA (TAE) buffer (40 mM Tris, 20 mM acetic acid, 1 mM EDTA), with addition of SYBR™ Safe DNA Gel Stain (Invitrogen, Paisley, UK). DNA was mixed with 6x DNA loading buffer (Thermo Scientific, Walmington, UK) and loaded to gels immersed in TAE buffer. Electrophoresis was carried out in electrophoresis tanks at 100 - 120 V for 20 - 40 minutes (min), depending on the size of the DNA and percentage of agarose gels. DNA size markers were used to distinguish the DNA base pare (bp) length: GeneRuler 1 kb DNA Ladder, GeneRuler 100 bp DNA Ladder (both Thermo Scientific). DNA was visualised and analysed using a Gene Genius Bio Imaging System and GeneSnap software (Syngene, Cambridge, UK).

2.2.2. DNA isolation and purification

DNA was purified from polymerase chain reaction (PCR) mix using a QIAquick PCR Purification Kit (Qiagen, Manchester, UK) following manufacturer's instructions. DNA was extracted and purified from agarose gels using a QIAquick Gel Extraction Kit (Qiagen). Plasmid DNA was isolated from bacterial lysates using a QIAprep Spin Miniprep Kit (Qiagen) or a NucleoBond® Xtra Midi (Fisher Scientific, Loughborough, UK) plasmid DNA purification kit. For all isolations, DNA was eluted in the elution buffer provided by the manufacturer and the DNA concentration was determined by a NanoDrop™1000 spectrophotometer (Thermo Scientific).

2.2.3. DNA amplification

2.2.3.1 Polymerase chain reaction (PCR)

DNA fragments were amplified by PCR with specific primers (listed in Table 2.5 and Table 2.6) using Q5® High-Fidelity DNA Polymerase (New England Biolabs, Herts, UK) following the manufacturer's instructions and summarised in Table 2.7 and

Table 2.8. The initial denaturation step was prolonged to 5 min when the DNA was amplified from bacterial cells. The annealing temperature was adjusted based on the Tm (melting temperature) of primers and the elongation time was adjusted to the length of the DNA construct.

Table 2.7 PCR reaction reagents

Reagent	Concentration
5X Q5 Reaction Buffer	1X
10 mM dNTPs	200 µM
10 µM Forward Primer	0.5 µM
10 µM Reverse Primer	0.5 µM
Template DNA	< 1,000 ng
Q5 High-Fidelity DNA Polymerase	0.02 U/µl
5X Q5 High GC Enhancer	1X
Nuclease-Free Water	To the final volume

Table 2.8 PCR reaction conditions

Step	Temp	Time	Cycles
Initial Denaturation	98°C	30 seconds/5min	1
Denaturation Annealing Elongation	98°C 50–72°C 72°C	5–10 sec 10–30 sec 20–90 sec	25–40 Cycles
Final Extension	72°C	7min	1
Hold	4°C	∞	1

2.2.3.2 Plasmid DNA amplification

Plasmid DNA was amplified in bacteria. A single colony was taken from a selective LB (Luria Bertani) agar plate and incubated overnight in 5 ml (miniprep) or 250 ml (midiprep) of fresh LB broth medium with the appropriate antibiotic selection, at 37 °C in a shaking incubator at 200 rpm. The overnight bacterial culture was pelleted and used for plasmid DNA purification in mini- or midipreps as described in 2.2.2.

2.2.4. Restriction digests

Restriction digests were carried out in 20 - 50 µl volumes, using 1 - 5 µg of DNA following manufacturer's recommendations for each enzyme. When possible, double digestion using two enzymes, was carried out in the most suitable buffer. Restriction enzymes EcoRI, NotI, XbaI and PmeI were from New England Biolabs (NEB). The cut DNA fragments were separated by agarose gel electrophoresis and purified as per section 2.2.2.

2.2.5. T4 DNA ligase reaction

Plasmid vectors and PCR products, cut with complementary restriction enzymes, were ligated together in a 1:3 ratio with T4 DNA ligase (NEB) in the provided T4 DNA ligase buffer,

as recommended by the manufacturer. The reaction was carried out at room temperature for 5 h or overnight. The reaction was directly transformed into bacterial cells.

2.2.6. Annealing of His tag oligonucleotides and cloning of His-tagged MCAM proteins

The sense and antisense 6xHis tag oligonucleotides (oligos) (MC08 and MC09) were annealed to form the 6xHis tag DNA insert. Briefly, 2 µg of each oligo was mixed together in 50 µl of annealing buffer (10 mM Tris pH 7.5, 50 mM NaCl, 1 mM EDTA). This was incubated at 92.5 °C for 5 min. The reaction was then slowly cooled to room temperature for 1 h. Annealed oligos were diluted 10 times in nuclease free water, and the concentration was checked by a NanoDrop™. This tag was used in construction of the m/hMCAMecd-His constructs. The human Fc sequence was excised from the m/hMCAMecd-Fc plasmids using NotI and XbaI restriction enzymes and the 6xHis tag was cloned in to replace the Fc tag in a ligation reaction with T4 DNA ligase, generating m/hMCAMecd-His constructs.

2.2.7. Gibson assembly and cloning of FLAG-tagged full length mouse MCAM

Primers for Gibson cloning were designed using the online NEB builder tool (http://nebuilder.neb.com). Constructs were designed to conserve the restriction sites flanking the inserted DNA. The FLAG tag was added at the C-terminus of the mouse MCAM full length in a PCR reaction using primers MC24 and MC25. This PCR product was then used as a template for the second PCR reaction using Gibson Assembly designed primers (MC25 and MC26). pWPI plasmid was cut with PmeI restriction enzyme, as described in 2.2.4. The second PCR product and the cut plasmid were mixed in a 3:1 ratio with 2X Gibson Assembly Master Mix (NEB) according to the manufacturer's instructions and incubated for 30 min at 50 °C. The reaction was then placed on ice and used to transform bacterial cells.

2.2.8. Transformation of chemically competent *E. coli*

Plasmid DNA solution (2 µl of a ligation or Gibson Assembly) was added to chemically competent *E. coli* (α-Select Gold Efficiency, Bioline, London, UK) and mixed gently. Cells were incubated on ice for 20 min, heat-shocked at 42 °C for 90 seconds (sec) and immediately transferred to ice. Room temperature LB broth medium without antibiotics was added to the bacterial cells before shaking horizontally (200 rpm) at 37 °C for 1 h. After shaking, bacterial cells were spread on the pre-warmed LB agar plates containing appropriate antibiotic and incubated overnight at 37 °C. Five to ten colonies were picked the following day and analysed for transformation efficiency using direct PCR from bacteria (colony PCR). Positive colonies were cultured overnight in 5 ml of LB broth medium with antibiotics, the plasmids purified and digested with restriction enzymes flanking the insert. Finally, plasmids with the predicted digestion pattern were sequenced.

2.2.9. DNA sequence analysis

Plasmid DNA was purified as described in section 2.2.2 and the concentration was determined by a NanoDrop™. Approximately 500 ng of DNA was mixed with 1 µl of 3 µM sequencing primer in a reaction volume of 10 µl. The samples were processed by University of Birmingham DNA sequencing services and run on the capillary sequencer ABI 3730 for sanger sequencing. The correct nucleotide sequence and amino acid reading frame of constructs were checked manually using ChromasPro software (Technelysium Pty Ltd, South Brisbane, Australia).

2.3 Cell culture

Table 2.9 Cell culture media and solutions

Cell type	Medium name and supplements	Concentration of supplements
HUVEC (isolated in the lab)	**Complete M199 (Sigma Aldrich)**	
	FCS (Thermo Scientific)	10% (v/v)
	L-glutamine (Gibco, Paisley, UK)	2 mM
	Penicillin (Gibco)	100 U/ml
	Streptomycin (Gibco)	100 µg/ml
	Heparin (LKT Laboratories, Ontario, Canada)	45 µg/ml
	Bovine brain extract [132]	0.1% (v/v)
	Low passage M199	
	FCS	10% (v/v)
	L-glutamine	2 mM
	Penicillin	100 U/ml
	Streptomycin	100 µg/ml
	Gentamicin (Gibco)	10 µg/ml
	Amphotericin B (Gibco)	0.25 µg/ml
	Heparin	45 µg/ml
	Bovine brain extract	0.1% (v/v)
	Serum free M199	
	L-glutamine	2 mM
	Penicilin	100 U/ml
	Streptomicin	100 µg/ml
	Heparin	45 mg/ml
Commercial HUVEC	**Complete EBM2 (Lonza clonetics)**	
	EBM®-2 Bulletkit (Lonza clonetics)	1X
HEK293T/bEND/sEND	**Complete DMEM (Sigma Aldrich)**	
	FCS	10% (v/v)
	L-glutamine	2 mM
	Penicillin	100 U/ml
	Streptomycin	100 µg/ml
HEK293T	**Serum free Opti-MEM (Gibco)**	
	L-glutamine	2 mM
	Penicillin	100 U/ml
	Streptomycin	100 µg/ml
Mouse hybridoma cells	**Hybridoma RPMI (Gibco)**	
	FCS	15% (v/v)
	Penicillin	100 U/ml
	Streptomycin	100 µg/ml
	β-mercaptoethanol (Gibco)	50 µM
	HT-supplement (Gibco)	1X
Rat hybridoma cells	**Hybridoma DMEM**	
	FCS	15% (v/v)
	L-glutamine	2 mM
	Stable L-glutamine (Biochrom GmbH)	2 mM

	β-mercaptoethanol	50 µM
	Non-essential amino acids (Gibco)	1X
	HT-supplement	1X
	Hybridoma Opti-MEM	
	L-glutamine	2 mM
	Stable L-glutamine	2 mM
	β-mercaptoethanol	50 µM
	Non-essential amino acids	1X
	HT-supplement	1X
RENCA	**Complete RPMI**	
	FCS	10% (v/v)
	Penicillin	100 U/ml
	Streptomycin	100 µg/ml
HDF	**Complete M106 (Gibco)**	
	LSGS (Life Tech)	1X

2.3.1. General cell culture and passaging

All procedures were carried out in sterile conditions in a Class II, Type A2 biological safety cabinet (Holten Laminar Air). Cell culture plates for Human Umbilical Vein Endothelial Cells (HUVECs), Human Dermal Fibroblast (HDF) cells and Mouse Brain Endothelial (bEND) cells were coated with 0.1% (w/v) gelatin (Fluka BioChemika) in PBS before cell seeding. Different mammalian cell types were grown in cell culture media (listed in Table 2.9) as stated in the different methods sections. Cells were cultured in a humidified cell culture incubator (Sanyo CO_2 incubator, Osaka, Japan) at 37 °C and 5% CO_2.

Cells were grown until 80 - 90% confluent, washed 2 times with sterile PBS and detached from plates using vigorous pipetting (HEK, RENCA, hybridomas), 0.1% (v/v) Trypsin-EDTA (Gibco) in PBS (HUVEC, bEND, sEND, HDF), or non-enzymatic cell dissociation solution (Sigma) (when used for flow cytometry). Cells were washed from dissociation solutions with complete medium (specific for each cell type, Table 2.9), spun down at 196 x g for 5 min and resuspended in complete medium and reseeded. HUVECs and rat hybridoma cells were split

in a ratio of 1:3; bEND, sEND and HDF cells were split in a ratio of 1:5; HEK293T and RENCA cells were split in a ration of 1:10.

2.3.2. Human umbilical vein endothelial cells preparation

Umbilical cords were obtained from the Birmingham Women's Hospital, with mothers' consent by members of the Birmingham Biorepository. Cords were cannulated, and the vein washed 2 times with PBS to remove blood. The vein was filled with collagenase type 1A (1 mg/ml) in M199 medium and incubated at 37 °C for 20 min to dissociate the endothelial cells from the cord. Cells were flushed through the cord with PBS into a 50 ml centrifuge tube, washed 2 times with PBS to remove the collagenase and seeded onto gelatin coated tissue culture flasks in low passage M199 medium (Table 2.9). The medium was changed 4 hours (h) later, and the cells cultured until confluent. HUVECs were used from passage 2 to 6.

2.3.3. Mammalian cell storage

Cells were washed with PBS and detached from plates as described in 2.3.1. Spun-down cells were resuspended in freezing medium [10% (v/v) DMSO in FCS] and stored in Mr. Frosty™ freezing container at -80 °C overnight. Cells were then transferred to liquid nitrogen for long-term storage. For reseeding, frozen cells were rapidly thawed in a 37 °C water bath, washed with their respective medium, spun down at 196 x g for 5 min, and plated in the complete medium.

2.3.4. Mammalian cell lysis

Cells in the culture dishes were washed 2 times with non-sterile PBS on ice. NP-40 lysis buffer [50 mM Tris pH7, 1% (v/v) NP-40, 150 mM NaCl, 1 mM EDTA, protease inhibitors, Pierce] was added to the cells on each plate (100 µl on a 6-well plate, 500 µl on a 10 cm plate).

Cells were scraped and collected into a microcentrifuge tube, vortexed for 20 sec and incubated on ice for 15 min. Cell debris was pelleted by centrifugation at 16602 x g for 15 min at 4 °C, and the supernatants collected.

2.4 Mammalian cell DNA transfection and transduction

2.4.1. HEK293T cell transient DNA transfection using PEI

Table 2.10 shows the conditions for cell transfections related to the size of the culture plates. HEK293T cells were seeded at an appropriate density in complete DMEM (10% FCS). On the following day, the plasmid DNA was mixed with 1 mg/ml polyethylenimine (PEI) as indicated in Table 2.10 in Opti-MEM, gently vortexed and incubated for 10 min at room temperature. The DNA-PEI mix was added drop-wise to the cells. Transfected cells, or cultured medium, were analysed two or more days after transfection.

Table 2.10 PEI transfection reagents for different sizes of cell cultures

Plate size	Medium volume	Cells seeded	Opti-MEM	DNA	PEI
6-well	2 ml	$3x10^5$	100 µl	1 µg	4 µl
6 cm	3 ml	$1x10^6$	300 µl	3 µg	12 µl
10 cm	10 ml	$3x10^6$	1 ml	9 µg	36 µl
15 cm	20 ml	$6x10^6$	2 ml	18 µg	72 µl

2.4.2. Production of lentivirus in the cell culture medium of HEK293T cells

HEK293T cells were seeded in complete DMEM the day before PEI transfection; $3x10^6$ cells per 10 cm cell culture plate. The cells were transfected with 36 µl of PEI and a mix of plasmids:

1) 4.4 µg of lentivirus vector

2) 3.3 µg of packaging vector (PsPAX2)

3) 1.3 µg of envelope vector (PMD2G),

as described in section 2.4.1. The cells were left to generate and secrete the virus into the supernatant. Cell supernatant containing lentivirus was collected after 48 h and filtered with a 0.45 µm syringe filter.

2.4.3. Lentiviral transduction of HEK293T cells

Sterile polybrene was added to lentivirus medium to a final concentration of 8 µg/ml. Media was then added to the HEK293T cells seeded ($3x10^6$) a day previously in a 10 cm plate. Cells were cultured in lentivirus medium for 24 h before the medium was replaced with complete DMEM. Cells were analysed for transduction efficiency two days later using fluorescence imaging (EVOS® fl, Thermo Fisher) by checking the expression of green fluorescent protein (GFP) expressed from the pWPI vector.

2.4.4. Lentiviral transduction of HUVECs for angiogenesis assays

HEK293T cells were PEI transfected, as described previously (2.4.2), with GFP expressing plasmid and a mix of plasmids encoding lentiviral proteins. Lentivirus-containing medium was collected after two days, filtered through a 0.45 µm syringe filter and stored at -80 °C. HUVECs were seeded the day before transduction ($2.5x10^5$) in a T25 tissue culture flask. Polybrene was added to the lentivirus medium to a final concentration of 8 µg/ml. This medium was added to the HUVECs for transduction. After 24 h, the medium was replaced with complete M199 or complete EBM-2 medium and the cells were used in *in vitro* assays.

2.5 Protein expression in mammalian cells and affinity purification

2.5.1. Small scale protein production and affinity pull-down

HEK293T cells were transiently transfected with plasmids containing recombinant protein expression construct (as described in 2.4.1) and cultured for 48 h in complete DMEM, after which the medium was changed to serum free OptiMEM. The Opti-MEM was sampled (1 ml) after two days, sterilised through a 0.22 µm syringe filter and incubated with 20 µl of protein A (Sigma) or Ni-NTA sepharose bead slurry (Sigma) overnight at 4 °C with rotation. Beads were washed 3 times with 1 ml of beads wash buffer followed by boiling at 95 °C for 5 min in reducing protein loading buffer. Binding of proteins to the beads was visualised using SDS-PAGE and Coomassie blue staining of the gels.

2.5.2. Large scale protein production

HEK293T cells were transiently transfected with plasmids containing recombinant protein construct and expanded to 10 x 15 cm tissue culture plates in complete DMEM. After reaching confluence, the medium was replaced by serum free Opti-MEM. The Opti-MEM containing recombinant protein was then collected twice a week for two weeks and sterile filtered through a 0.22 µm filter with addition of 0.5 mM EDTA and a small amount of PMSF crystals (for protease inhibition). In His-tagged protein containing medium only PMSF crystals were added. Collected medium was stored at 4 °C until use.

2.5.3. Purification of Fc-tagged proteins on a Protein A column

All buffers and media were sterile filtered through a 0.22 µm filter prior to use. HiTrap™ Protein A HP column (GE healthcare, Amersham, UK) was assembled on a pump system (Miniplus 2, GILSON) at 4 °C. The column was then washed with five column volumes of dH_2O, followed by five volumes of 20 mM sodium phosphate buffer (pH 7) to equilibrate the column. Medium containing mMCAMecd-Fc/hMCAMecd-Fc protein was run through the column at a speed of less than 1 ml per minute. The column was then washed with five volumes of 20 mM sodium phosphate (pH 7) and proteins eluted with 100 mM Sodium Citrate (pH 3) in around 20 fractions of 0.5 ml to complete protein elution. The pH of eluted fractions was adjusted to pH 7 by addition of 1 M Tris (pH 9). Fractions with the highest concentration of protein (measured on a NanoDrop™) were pooled together and dialysed against PBS, sterile filtered through a 0.22 µm filter and stored at 4 °C.

After elution, the column was washed with five volumes of 20 mM sodium phosphate buffer (pH 7), followed by five volumes of dH_2O and then five volumes of 20% (v/v) ethanol, in which the column was stored.

2.5.4. Purification of His-tagged proteins on a Ni-NTA column

A HisTrap™ Excel column (GE healthcare) was assembled on a pump system at 4 °C, washed with five column volumes of dH_2O, followed by five volumes of PBS, and then five volumes of PBS, 0.5 M NaCl. After that, the medium containing mMCAMecd-His/hMCAMecd-His protein was run through the column at a speed of less than 1 ml per minute. The column was washed with five volumes of PBS, 0.5 M NaCl and the proteins were eluted in elution buffer (PBS, 0.5 M NaCl, 250 mM imidazole) in 0.5 ml fractions. The elution buffer was left to stand in the column for 30 min, to allow the protein to detach from the beads, and then eluted.

This step was repeated until no protein could be detected in the elution fractions. Protein concentration was checked by a NanoDrop™. Collected elution fractions were pooled together and dialysed against PBS, sterile filtered through a 0.22 µm filter and stored at 4 °C. The column was washed with five volumes of PBS, 0.5 M NaCl, followed by five volumes of PBS and five volumes of dH_2O. Finally, the column was flushed with 20% (v/v) ethanol and stored for later use.

2.5.5. Papain cleavage and depletion of the Fc tag

2.5.5.1 Optimization of enzyme digest

30 µg of Fc-tagged protein was incubated at 37 °C in 100 µl of papain cleavage buffer (150 mM NaCl, 0.67 mM EDTA, 5 mM L-cysteine, 10 mM NaH_2PO_4). Before the addition of 0.8 µl of 0.2 mg/ml of papain, 10 µl of this reaction was sampled. After the addition of papain, an additional 10 µl of reaction was taken at 5, 10, 20, 30, 40, 50 and 60 min and the reaction was stopped by addition of reducing protein loading buffer and boiling at 95 °C for 5 min. The proteins were separated by SDS-PAGE and analysed by Coomassie blue staining.

2.5.5.2 Large scale papain digest

Larger amounts of protein were papain cleaved in 1 ml of papain cleavage buffer containing 1.6 µg/ml papain. The reaction was carried out for 30 min at 37 °C and was stopped by the addition of 6.5 mM (final concentration) iodoacetic acid (pH 6.8) for 30 min at room temperature. The cleaved Fc fragment was depleted from the solution using Protein A beads. Before use, the protein A beads were washed 3 times with beads wash buffer and 50 µl of beads were added to the protein solution. The solution was incubated with beads for 2 h at 4 °C with rotation. The beads were spun down; the supernatant collected and incubated with

fresh beads twice more. Absence of the Fc tag in the depleted solution was confirmed using Western blot and Coomassie blue staining of the SDS polyacrylamide gel (described in section 2.6).

2.6 SDS-PAGE and Western blot

Table 2.11 SDS-PAGE gel contents

Buffer:	Contents:
10% resolving gel	375 mM Tris pH 8.8 0.1% (v/v) SDS 10% (w/v) Acrylamide; 0.26% (w/v) Bis-Acryl-amide 0.1% (w/v) ammonium persulphate (APS) 0.1% (v/v) TEMED
Stacking SDS gel	125 mM Tris pH 6.8 0.1% (v/v) SDS 5% (w/v) Acrylamide; 0.13% (w/v) Bis-Acryl-amide 0.1% (w/v) APS 0.1% (v/v) TEMED

Sodium dodecyl sulphate – polyacrylamide gel electrophoresis (SDS-PAGE) was used to separate and visualise proteins. Gels consisted of a 10% resolving gel at the bottom and a stacking gel at the top (Table 2.11). Proteins were loaded in protein loading buffer (reducing or non-reducing) to the stacking gel. Electrophoresis was carried out in SDS running buffer at 80 V while proteins went through the stacking gel, and 120 V through the resolving gel; in a gel electrophoresis tank XCell SureLock™ Electrophoresis (Invitrogen). Proteins were subsequently stained in the gel with InstantBlue™ protein gel staining solution (Expedeon) as recommended by the manufacturer (referred to as Coomassie blue later in text) or transferred to Immobilon®-P PVDF membrane (Merck-Millipore, Darmstadt, Germany).

Prior to transfer, the membrane was activated with methanol and rinsed with water and then transfer buffer. The membrane and gel were assembled as a sandwich between blotting paper and sponges immersed in the transfer buffer in an XCell II™ Blot Module (Invitrogen). The transfer was carried out at 4 °C, 30 V and 400 mA for 2 h. The membrane was then incubated in blocking buffer [5% (w/v) dried skimmed milk, PBS-T] at room temperature for 1 h. Proteins on the membrane were blotted with antigen-specific antibodies in 3% (w/v)

BSA, PBS-T (concentrations specified in Table 2.2 for each antibody) for 1 h at room temperature or overnight at 4 °C. Membranes were washed 4 times for 5 min with PBS-T, and probed with species specific secondary antibody conjugated to HRP (1:5000) in blocking buffer. Membranes were then washed 4 times for 5 min with PBS-T. The membranes were incubated with Amersham™ ECL™ Western Blotting Detection Reagents and placed in a developing cassette (Hypercassette™, Amersham Biosciences) together with the film (Amersham Hyperfilm™). Film was developed in the X-ray film developer (ECOMAX X-Ray Film Processor, Protec).

2.7 The enzyme-linked immunosorbent assay (ELISA)

C96 MaxiSorp Nunc-Immuno Plates (Thermo Scientific) were coated overnight with an appropriate amount of protein (20-500 ng/well) with agitation at 4 °C. Wells were then washed 3 times with 200 µl PBS, before blocking with 300 µl of PBS, 2% (w/v) milk powder (Marvel) for 2 h at room temperature. Wells were then washed again 3 times with 200 µl of PBS. Proteins were then probed with antigen-specific antibodies (100 µl, concentration of 1 µg/ml), diluted animal serum (100 µl), undiluted cell supernatants (100 µl) or PBS without antibody for 1 h at room temperature. Unbound antibody solutions were washed 3 times with PBS-T and 3 times with PBS before probing with 100 µl of species-specific secondary antibody conjugated to HRP (1:2000 dilution in PBS) for 1 h at room temperature. Wells were again washed 3 times with PBS-T and 3 times with PBS. Reaction was initiated by addition of 50 µl of HRP substrate solution BM Blue POD Substrate (Roche) and incubation for 10-30 min before stopping the reaction with 30 µl of 3 M HCl. Absorbance was recorded on VersaMax™ ELISA Microplate Reader (Molecular Devices).

2.8 Antibody generation

2.8.1. Mouse immunisations

2.8.1.1 Mouse immunisation carried out by Eurogentec S.A.

Eurogentec S.A. carried out mice immunisation and splenocyte fusion. Six mice were immunised with mMCAMecd-Fc (50 µg) 4 times with two weeks between immunisations. The first immunisation was with Freund's complete adjuvant (FCA) while the rest were with Freund's incomplete adjuvant (FIA). Bleeds were taken from mice prior to the first immunisation and one week after the last one and tested on ELISA. A positive mouse was culled for fusion. Mouse splenocytes were fused with mouse myeloma cell line (Sp2/OAg 14) to generate the hybridoma cells. Pools of hybridoma cells were cultured and the supernatants of different pools tested on ELISA for reactive antibodies.

2.8.1.2 Mouse immunisation carried out at University of Birmingham

This work was carried out under the home office license number 70/8704. Three 6-week-old male Balb/c mice were first immunized the first time with a mix of antigen (50 µg) and Freund's complete adjuvant subcutaneously. Subsequently, mice were injected subcutaneously every two weeks with 50 µg of antigen and Freund's incomplete adjuvant. Bleeds from saphenous veins were taken prior to the first immunisation and 13 days after each immunisation to assess the antibody titre in the serum. After four immunisations, the mice with the highest titre were boosted with a final injection of 10 µg of antigen in PBS intraperitoneally and culled 3 days later. The spleen was taken for the immediate isolation of splenocytes and fusion with mouse myeloma cells (described in section 2.8.3).

2.8.2. Rat immunisations carried out by Biogenes GmbH

Three Dark Agouti rats (female, 8 weeks old) were immunised intraperitoneally 4 times over a period of 39 days. Rats were immunised with water-in-oil emulsion that was prepared by emulsifying the 50 µg of antigen in equal volumes of Freund's complete adjuvant (first immunisation) and Freund's incomplete adjuvant (subsequent boosts). Bleeds were taken one week after the 3rd immunisation and tested on ELISA with m/hMCAMecd-His protein. Two rats were boosted 20 days after the last immunisation and culled for fusions 3 days later. Spleens were pooled and homogenized and the cells fused to mouse myeloma Sp2/0-Ag14 cells. The hybridoma cells were plated on the pre-coated peritoneal exudate cells as feeder cells in complete cell growth medium supplemented with 20 % FCS, antibiotic/antimycotic (final concentrations: 100 U/ml Penicillin G, 250 ng/ml Amphotericin B, and 100 µg/ml Streptomycin) and HAT supplement (100 µM hypoxanthine, 400 nM aminopterin and 16 µM thymidine). The supernatants of individual hybridoma clones were tested on ELISA. The third rat was immunised again after around four months of waiting period. This rat was then culled 3 days later. The spleens were taken immediately and splenocytes fused as described for the other two rats.

Positive hybridoma cells were then sub-cloned by limiting dilution. Wells with single cell colonies were regarded as monoclonal cell lines and tested for mMCAMecd-His recognition. These cells were then again sub-cloned in the same way, and only wells containing a single clone were selected for further processing. Cells from positive wells were passaged several times to identify the best clones with regard to cell growth and antigen specificity as assayed by ELISA signal.

2.8.3. Hybridoma cell fusion carried out within University of Birmingham

The isolated spleen was punctured with a syringe to create small holes through which the cells were flushed with RPMI medium into the petri dish. Cells and spleen were then gently pushed through a 40 µm Blue filter (BD) to create a single cell suspension. Cells were washed 3 times with RPMI without serum and counted. Myeloma cells (NSO) were collected from plates, washed and counted. Myeloma cells and spleen cells were mixed together (in a ratio of 1:5) in a tube with a spherical bottom. Cells were spun down and the medium aspirated leaving the pellet as dry as possible. 1 ml of PEG (50% v/v) was added slowly, over 1 minute, to the cells with a plastic Pasteur while stirring the cells gently with the Pasteur. After this, 20 ml of warm RPMI was added in the same manner as the PEG, 1 ml per minute gently while stirring the cells. Cells were left in this solution for 5 min without disturbance. Another 30 ml of RPMI was then added in the same way but a bit faster. Cells were then spun down at 468 x g for 7 min and the supernatant removed. Cells were resuspended in 50 ml of RPMI containing 20 % (v/v) FCS. Cells were counted and the amount of 96 well plates needed for seeding 1 cell per well was calculated. Cells were diluted in 15 % (v/v) FCS RPMI and seeded in 96 well plates at 150 µl/well. On the following day, 150 µl/well of RPMI containing 15 % (v/v) FCS and 2X HAT was added to the cells in addition to the antecedent medium. 10 days later the plates were screened for growing colonies in each well. The media from wells with colonies were collected and screened on ELISA.

2.8.4. Isotype determination

The monoclonal antibody isotype was determined with Ig Isotyping Rat Uncoated ELISA Kit (Invitrogen). The antibodies were tested for IgG1, IgG2a, IgG2b, IgG2c, Kappa and Lambda chains. Capturing antibodies were diluted in coating buffer (PBS) and used to coat the

wells of an ELISA plate overnight. This was aspirated, and the wells washed 2 times with wash buffer [PBS, 0.05% (v/v) Tween 20] and blocked with 250 µl of blocking buffer [PBS, 0.1% (v/v) Tween 20, 1% (w/v) BSA] for 3 h at room temperature. The hybridoma supernatants were diluted 2 times in PBS and 50 µl of diluted supernatants were mixed with 50 µl of assay buffer [PBS, 0.05% (v/v) Tween 20, 0.05% (w/v) BSA]. Blocking buffer was washed from the wells and the wells incubated with supernatants and controls for 2 h at room temperature. This was washed 4 times with wash buffer, then 100 µl of detection antibody diluted in the assay buffer was added and incubated for 1 h at room temperature. This was again washed 4 times and the substrate solution, Tetramethylbenzidine, TMB, added and incubated for 15 min at room temperature. Finally, the stop solution (3 M HCl) was added and the absorbance at 450 nm read with a plate reader.

2.8.5. Antibody purification

Small scale rat monoclonal antibody purification from hybridoma supernatants was performed by incubation of 10 ml of supernatants with 300 µl of protein A beads overnight at 4 °C with agitation. Beads were washed 3 times with 5 ml of beads wash buffer. Antibodies were eluted with 100 mM Sodium Citrate (pH 3), and pH set to neutral (pH7) with 1 M Tris (pH 9). The concentration was checked by a NanoDrop™. Margaret Goodall, University of Birmingham, purified monoclonal antibodies on a large scale using a protein G column.

2.8.6. Antibody labelling

Purified rat monoclonal antibody mMCAM10 against mMCAMecd was fluorescently labelled with Alexa Fluor™ 488 [MAN0009630 (Life Technologies)] following the manufacturer's instructions.

2.9 Flow cytometry

2.9.1. Flow cytometry for antibody validation

HEK293 and bEND cells were detached from plates using non-enzymatic cell dissociation solution (Sigma), collected into cell culture medium (specific for each cell type listed in Table 2.9) and centrifuged at 196 x g for 5 min (same speed and time used in all the centrifugation steps in this protocol). The cells were then resuspended in flow cytometry buffer [PBS, 0.5% (v/v) FCS, 2 mM EDTA] and separated into Eppendorf tubes in equal amounts for the different samples (at least 100,000 cells per sample). Cells were centrifuged and resuspended in 50 µl of antibody solution, isotype control, hybridoma supernatants or empty flow cytometry buffer and incubated for 1 h on ice. The primary antibody and a species-matched non-specific IgG were diluted in flow cytometry buffer to a final concentration of 10 µg/ml. Undiluted tissue culture supernatants from rat hybridoma clones were used. Following incubation, cells were washed with 300 µl of flow cytometry buffer and spun down. Cells were resuspended in the buffer with fluorescently labelled species-specific secondary antibody (1:100) and incubated in the dark for 1 h on ice. 300 µl of buffer was added to the cells before analysis by a CyAn ADP flow cytometer (Beckman Coulter), using Summit software. Gates were set with the control cells incubated with flow cytometry buffer only for single cells (singlets), and cells incubated with control IgG and secondary were used to set the gates for specific channels. Flow cytometry data was analysed using FlowJo software.

2.9.2. Antibody competition assay

bEND cells were prepared as in 2.9.1 then incubated with 50 µl of blocking antibody at a concentration of 100 µg/ml in flow cytometry buffer for 2 h at 4 °C with agitation. Cells were then washed with flow cytometry buffer two times and incubated with 50 µl of fluorescently labelled mMCAM10 antibody (100 µg/ml) targeted at the same protein, for 1 h at 4 °C with agitation. Binding of the second antibody was analysed as in 2.9.1.

2.9.3. Flow cytometry for propidium iodide staining

Cells were detached using Trypsin-EDTA and washed with PBS. Cells were again pelleted and fixed by the drop-wise addition of ice cold 100% ethanol while slowly vortexing. Cells were fixed in ethanol at -20 °C for 1 h. Cells were then centrifuged for 5 min to remove the ethanol and washed twice with PBS. Cells were then resuspended in 0.25% (v/v) Triton X-100 in PBS and incubated at 4 °C for 15 min with agitation. Cells were spun down and washed with PBS. Finally, 470 µl of PBS was added to the cell pellet and the cells transferred to a flow cytometry tube. 5 µl of 0.1 mg/ml of RNAse A and 25 µl of 50 µg/ml of propidium iodide was added and the cells incubated in the dark for 30 min. Cells were then analysed on a CyAn ADP flow cytometer.

2.10 Immunostaining of cells and tissues

2.10.1. Immunofluorescence staining of paraformaldehyde fixed cells on coverslips

Cells were seeded in complete medium on round (13 mm) coverslips coated with 0.1% (w/v) gelatin, in 6-well plates. After attaching for 24-48 h, cells were washed 3 times with PBS (washing step) and fixed with 4% (w/v) paraformaldehyde (PFA) in PBS for 10 min at room temperature. This was followed by a washing step, and then with incubation with 50 mM NH_4Cl in PBS for 10 min at room temperature and another washing step. Cells were then blocked with blocking buffer [PBS, 3% (w/v) BSA, 10% (v/v) FCS, 0.1% (v/v) Tween 20] for 1 h at room temperature. Cells were then incubated for 1 h at room temperature with 50 µl of primary antibody or the same species nonspecific IgG diluted in blocking buffer (final concentration 10 µg/ml). Antibody solution was washed, and the coverslips were incubated with fluorescently labelled appropriate secondary antibody (diluted 1:200 in blocking buffer) in the dark for 1 h at room temperature. Coverslips were washed 3 times with PBS and then with dH_2O and mounted onto DAPI Prolong gold mounting medium (Invitrogen) on glass slides. Images were taken with a Leica DM6000 and analysed using ImageJ software.

2.10.2. Embedding of cells into agarose blocks

Cells were collected from plates using non-enzymatic cell dissociation solution and spun down at 196 x g for 5 min. The supernatant was removed, and the cells were resuspended in 300 µl of preheated 1% (w/v) low melting point agarose in PBS at 50 °C. The tubes with cells were placed on ice until the agarose solidified.

2.10.3. Tissue and cell preparation for immunostaining

Mouse tissue and agarose embedded cells for immunohistochemistry were fixed in formalin for 24 h and further processed, embedded in paraffin and sectioned by the Birmingham tissue bank. The slides were stored at room temperature until used.

The tissue and agarose embedded cells used for frozen tissue immunofluorescence were immersed in OCT freezing medium and snap frozen. Tissue was then processed and sectioned by the Birmingham tissue bank, and slides stored at -80 °C until used.

2.10.4. Immunofluorescence staining of frozen sections

Frozen agarose embedded cells and frozen mouse tissue were used for immunofluorescence staining. Sections were thawed at room temperature for 10 min, followed by fixing in acetone at -20 °C for another 10 min. Slides were then washed 3 times for 5 min with PBS. Shandon coverplates (Thermo Fisher) were placed on top of the tissue slides and placed into a Sequenza slide rack (Thermo Fisher). Tissue was blocked with 100 µl of 2.5% (v/v) horse serum (Vector laboratories, Orton, UK) at room temperature for 30 min. Species nonspecific IgG (10 µg/ml in PBS), or undiluted supernatants were added in 100 µl to the slides and incubated at room temperature for 1 h. Slides were then washed 3 times with 2 ml of PBS and the secondary antibody conjugated to a fluorophore (diluted 1:200 in PBS) was added. This was incubated for 1 h at room temperature in the dark and the slides washed as previously. Slides were additionally washed with 1 ml of dH_2O, mounted with DAPI prolong gold mounting media (Invitrogen) and then coversliped. Sections were imaged using a Leica DM6000. In the case of the antibody localisation experiment, the incubation with primary antibody was omitted and only secondary antibody incubation was carried out.

2.10.5. Immunohistochemistry staining of formalin-fixed paraffin-embedded cells and tissues

Formalin-fixed agarose embedded cells and formalin-fixed mouse tissues were used for immunohistochemical staining. Cells and tissues were fixed in formalin for 24 h, and then processed, embedded in paraffin and sectioned by the Birmingham tissue bank. Slides were heated at 60 °C for 30 min, and deparaffinised by immersion in xylene (Acros Organics) 3 times for 2 min. Slides were then hydrated by incubation in 100%, 95% and 75% (v/v) ethanol for 2 min each, followed by incubation 2 times in dH_2O for 2 min. After this, slides were incubated in 3% (v/v) hydrogen peroxide in methanol for 5 min. Slides were then washed 3 times with PBS-T and subjected to antigen unmasking with either Sodium Citrate based (pH 6), or Tris based (pH 9) unmasking solution (Vector laboratories), by boiling in the microwave at 900 W for 15 min. The slides were cooled under running tap water for 30 min. Next, the slides were blocked with 2.5% (v/v) horse serum (Vector laboratories) for 1 h at room temperature and probed with monoclonal antibodies mMCAM10, mMCAM66 or control rat IgG at a concentration of 15 µg/ml for 1h at room temperature. The slides were then washed with PBS and incubated with HRP conjugated anti-rat secondary antibody diluted (1:100) in 2.5% horse serum for 45 min at room temperature. The reaction was developed using peroxidase substrate kit (ImmPACT™ NovaRED™, Vector laboratories) for approximately 5 min and immediately immersed in dH_2O for 5 min. Slides were then immersed in haematoxylin solution (Pfm Medical) for 2 min and washed with dH_2O for 1 min. Slides were incubated under running tap water for 5 min, and with dH_2O for 5 min. Finally, slides were dehydrated in 70%, 95% and 100% ethanol for 2 min each, and immersed in xylene 3 times for 2 min. Slides were mounted with DPX mounting medium (Cellpath, Newtown, UK).

2.11 Immunoprecipitation

bEND cells were lysed in NP-40 lysis buffer by the protocol described in 2.3.4. The cell lysate supernatant (1 ml) was pre-cleared by first incubating with 50 µl of protein G beads with 1 µg/ml of rat IgG control for 1 h at 4 °C on a wheel. Beads were centrifuged, and the supernatant collected and then incubated with 2 µg/ml of individual rat monoclonal antibodies or rat IgG control overnight at 4 °C with agitation. The following day 20 µl of protein G beads were added to the lysates with antibodies/IgG and incubated for 1 h at 4 °C. The beads were centrifuged, washed 4 times with beads wash buffer and boiled at 95 °C in reducing protein loading buffer. Samples were subjected to SDS-PAGE and Western blotting.

2.12 Mouse tumour implantation and antibody injection

RENCA cells were cultured for 1 week before the experiment. The cells were collected from the plates by pipetting and centrifuged at 196 x g for 5 min. Cells were diluted in basal DMEM at $1x10^6$ cells per 100 µl and kept on ice. 8-week-old male Balb/c mice were injected with $1x10^6$ RENCA cells subcutaneously on the side of the body. Tumours were measured twice a week until they reached 1 cm^3. The purified monoclonal antibodies in PBS (20 µg in total) were injected into the tail vain. Mice were monitored for 1 hour and then culled. The tumour and organs were taken and snap-frozen in OCT freezing medium.

2.13 Sequencing the variable regions of monoclonal antibodies

2.13.1. mRNA extraction and reverse transcription

Rat hybridoma cells were collected from plates and spun down in an amount of up to $5x10^6$ cells. RNeasy RNA Purification kit (Qiagen) was used to isolate the mRNA as recommended by the manufacturer. Cells were lysed in 350 µl of RTL buffer, containing β-mercaptoethanol. The lysate was disrupted by centrifugation through Qiagen qiashredder column (Qiagen) at a maximum speed (16602 x g) for 2 min. 350 µl of 70% (v/v) ethanol was added to the lysate and mixed by pipetting. This was transferred to the RNeasy spin column and centrifuged for 15 sec at 7379 x g, and the flow-through discarded. 700 µl of RPE buffer was added to the column, centrifuged for 15 sec at 7379 x g, and the flow-through discarded. 500 µl RPE buffer was added to the column, centrifuged for 2 min at 7379 x g, and the flow-through discarded. The column was placed in a clean collection tube, 30 µl of nuclease free water was added directly to the membrane and centrifuged for 1 min at 7379 x g. The concentration of mRNA was checked by a NanoDrop™. The RNA was stored at -80 °C. Reverse transcription to generate cDNA was carried out using QuantiTect® Reverse Transcription kit (Qiagen), following manufacturer's instructions. First, the genomic DNA was removed using gDNA Wipeout buffer (Table 2.12) by incubating the reaction at 42 °C for 2 min. This RNA was then used with reverse-transcription master mix (Table 2.13) and incubated at 42 °C for 1 h, and then at 95 °C for 3 min to inactivate the reverse transcriptase. The RT primer mix provided in the kit was a mix of oligo-dT and random primers in order to generate high yields of cDNA with the correct sequence reaching all the way to the 5' region. The cDNA was stored at - 20 °C.

Table 2.12 Genomic DNA removal reaction

Component	Volume/reaction
gDNA Wipeout Buffer, 7x	2 µl
Template RNA	1 µg of RNA
RNase-free water	Up to 14 µl
Total volume	14 µl

Table 2.13 Reverse transcription reaction

Component	Volume/reaction
Quantiscript Reverse Transcriptase	1 µl
Quantiscript RT Buffer, 5x	4 µl
RT Primer Mix	1 µl
Template RNA	14 µl of previous reaction
Total volume	20 µl

2.13.2. Addition of the Poly-C tail to the cDNA

Addition of poly C chain to the cDNA 3' end was carried out with a terminal transferase kit (NEB). The DNA was heated to 95 °C for 1 minute and immediately chilled on ice. The terminal transferase reaction was assembled (Table 2.14) and incubated at 37 °C for 30 min, and then at 75 °C for 30 min. 500 µl of nuclease free H_2O was added, and the solution was concentrated down in an Amicon ultra-0.5 centrifuge filter column (Millipore) to approximately 5 µl.

Table 2.14 Terminal transferase reactions

Component	Volume/reaction
Molecular biology H_2O	6 µl
Terminal transferase buffer (10X)	2 µl
dCTP 20 mM	1 µl
Terminal transferase	1 µl
Template cDNA	10 µl
Total volume	20 µl

2.13.3. Rapid amplification of cDNA ends (RACE) PCR

Dr Steve Lee, University of Birmingham, kindly provided primers for the RACE PCR reactions (Table 2.15).

Table 2.15 Primer list for RACE PCR; W: A or T; I: Inosine

Primer Name (S.L.*)	Primer description	Sequence
pGI-TdT	Poly G-anchor primer	ACG GTG CAA ACC TTC CTC CAA ATC GGG IIG GGI IGG GII
rtIGHG1/2A	Rat IgG1 heavy chain constant region specific outer primer	TCC CAG GGT CAC CAT GGA GTT AC
rtIGKC	Rat kappa light chain constant region specific outer primer	GAT ACA CGA CTG WGG CAC CTC CAG T
pGI-TdT anchor	Anchor primer	ACG GTG CAA ACC TTC CTC CAA ATC GGG
rtIGHG1/2A nest	Rat IgG1 heavy chain constant region specific inner primer	GTC ACC ATG GAG TTA CTT TTG AGA GCA GT
rtIGKC nest	Rat kappa light chain constant region specific inner primer	GGA AGA TRG ATA CAG TTG GTG CAG CAT C

***provided by Dr Steve Lee, University of Birmingham**

First PCR

The DNA from previous terminal transferase reaction was used as a template for the first PCR in the RACE PCR protocol (C-tailed cDNA). The forward primer used was specific for the poly-C tail added to the cDNA and contained an anchor sequence at the end (pGI-TdT) that was used as a recognition sequence for the second PCR (pGI-TdT). The reverse primer used was the specific outer primer for the rat IgG1 or rat kappa constant region (rtIGHG1/2A and rtIGKC, respectively). The Platinum PCR supermix (Thermo Fisher) was used to amplify the DNA following manufacturers recommendations (Table 2.16 and Table 2.17).

Second PCR

DNA from first PCR was used as a template for the second RACE PCR reaction (PCR1 product). The Platinum PCR supermix (Thermo Fisher) was used to amplify the DNA following manufacturers recommendations (Table 2.16 and Table 2.17) using forward anchor primer (pGI-TdT anchor) and reverse specific inner primer for the constant region of the rat IgG1 or rat kappa (rtIGHG1/2A nest and rtIGKC nest, respectively). The polymerase enzyme from the Platinum PCR supermix adds 3´-adenine overhangs to the PCR product.

Table 2.16 PCR reaction mix reagents

Component	Volume/reaction
Platinum mastermix	47 µl
C-tailed cDNA/PCR1 product	1 µl
Primer Forward 25 µM	1 µl
Primer Reverse 25 µM	1 µl
Total volume	50 µl

Table 2.17 PCR reaction conditions

temp	time	cycles
94 °C	2 min	
94 °C	30 sec	
56 °C	30 sec	26 x
72 °C	90 sec	
72 °C	10 min	
4°C	∞	

2.13.4. Cloning of variable regions into TOPO vector

TOPO® TA Cloning® was used for the direct insertion of the amplified variable regions from the RACE PCR protocol with single 3´-adenine (A) overhangs into a TOPO vector [linearised with single 3´-thymidine (T) overhangs]. Topoisomerase I is covalently bound to the vector so the ligation is performed in 5 min at room temperature. The reaction was carried out according to the manufacturer's recommendations (Table 2.18) and used to directly transform competent bacteria.

Table 2.18 TOPO cloning reaction

Reagent	Volume
PCR product	1 µl
Salt solution	1 µl
Water	3 µl
TOPO® vector	1 µl
Total volume	6 µl

2.14 Angiogenesis assays

2.14.1. Cell proliferation analysis

CellTiter 96® Non-Radioactive Cell Proliferation Assay (Promega, Southampton, UK) was used for cell proliferation analysis. HUVECs were seeded in 0.1% (w/v) gelatin in PBS coated 96-well plates at a density of 5,000 cells/well in a volume of 100 µl and cultured at 37 °C in complete M199 medium. hMCAMecd-Fc protein or control Fc protein were added at a concentration of 1.54 µM. After 24, 48 or 72 h of cell growth, the medium was removed, and cells washed once with PBS. 100 µl of Opti-MEM with 15 µl of Dye Solution was added to the wells and the cells incubated for 4 h at 37 °C, after which the reaction was stopped with 100 µl of Solubilisation solution/Stop mix. The plates with cells were left overnight at 4 °C and the absorbance at 570 nm was recorded using a Versa max microplate reader.

2.14.2. Endothelial cell migration assay

HUVECs were seeded on gelatin coated 96 well plates (IncuCyte 96-Well ImageLock, Essen Bioscience), 5,000 cells/well and left to adhere and form a monolayer over 1-2 days. A wound in the cell monolayer in the middle of the wells was made using an IncuCyte WoundMaker (Essen Bioscience). The detached cells were washed away with 100 µl PBS and fresh complete M199 medium containing recombinant proteins (hMCAMecd-Fc protein or control Fc protein at 1.54 µM concentration) was added. The assay was carried out at 37 °C and 5% CO_2. Cell migration towards the closure of the wound was imaged with an IncuCyte ZOOM Live-Cell analysis system (Essen Bioscience) at 0, 6, 12, 18 and 24 h. Photos of cells were processed using IncuCyte ZOOM software and the percentage of wound closure was analysed using ImageJ software.

2.14.3. Chemotactic transmigration of endothelial cells through a semipermeable membrane

FluoroBlok HTS 24 Well Plate Cell Culture Inserts (Falcon) with 8.0 µm High Density PET Membrane (FloroBlock insert) were used in the HUVEC transmigration assay. 24 well tissue culture plates were used to hold the inserts and the bottom compartment was in all conditions filled with 700 µl of complete M199 medium containing FCS and bovine brain extract. FluoroBlock inserts were coated with 0.1% (w/v) gelatin in PBS for 30 min at 37 °C. HUVECs were incubated ('starved') in serum free M199 (without FCS and bovine brain extract) 1 h prior to seeding. Cells were then detached with Trypsin-EDTA and added to the gelatin coated inserts at $3x10^4$ cells/well in 300 µl serum free M199 containing either hMCAMecd-Fc protein or control Fc protein at a concentration of 1.54 µM. The inserts with cells were placed in wells containing complete medium. Cells were left to migrate through the membrane for 5 h at 37 °C. The inserts with cells were then washed twice with PBS and fixed in 4% (w/v) PFA. The membrane was cut out and mounted on in situ mounting medium with DAPI (Duolink) on the glass slide. Transmigrated cells were imaged using an Olympus 1X2-UCB fluorescent microscope under 10X magnification and nuclei were counted in 9 fields of view per insert using ImageJ software.

2.14.4. Endothelial cell network formation in 2D matrigel assay

Matrigel was taken from -80 °C freezer the day before the assay and left to thaw overnight on ice. On the following day, the wells of a 12 well tissue culture plates were rinsed with sterile PBS, which was immediately aspirated leaving a thin layer of PBS in the well, in order to easily and equally spread the matrigel. 70 µl of matrigel was added to the wells and left to set for 10 min at 37 °C. HUVECs were detached with Trypsin-EDTA and seeded at

140,000 cells per well in 1 ml of complete M199 medium (containing 1.54 µM hMCAMecd-Fc or Fc) on the matrigel coated wells. Cells were incubated at 37 °C, 5% CO_2 and imaged in the IncuCyte ZOOM Live-Cell analysis system. The assay was monitored every 6 h over a period of 24 h. Statistical analysis were carried out on a number of different measures such as tube number, length and branching and number of meshes.

2.14.5. Endothelial cell network formation in a 2D fibroblast co-culture assay

Human dermal fibroblasts were cultured on a 24 well tissue culture plate to confluence. HUVECs were seeded on top of the HDF cells at $1.5x10^4$ cell/well in complete M199 medium containing recombinant proteins (hMCAMecd-Fc and Fc). The experiment was carried out for 6 days with a change of medium every two days. Cells were then fixed with 4% (w/v) PFA for 15 min at room temperature. PFA was washed twice with PBS and the cells incubated with 0.1% (v/v) Triton X-100 in PBS for 4 min at 4 °C. This was washed 3 times with PBS and the cells blocked with 1% (w/v) BSA in PBS for 1 h at room temperature. The cells were stained with anti-CD31 antibody (1:200) in blocking buffer for 1h at room temperature. The primary antibody was washed 3 times with PBS and the cells probed with secondary antibody conjugated to alkaline phosphatase (1:500) for 1 h at 37 °C. Cells were washed 2 times with PBS and once with dH_2O before developing the reaction with the chromogenic substrate BCIP/NBT for 25 min. The reaction was washed with dH_2O and the cells dried before imaging with a Leica 10447157 microscope. The endothelial cell network formation was analysed using ImageJ angiogenesis analyser plug-in.

2.14.6. Endothelial cell network formation in 3D fibroblast co-culture assay

HUVECs were lentiviraly transduced with GFP expressing plasmid two days prior to the experiment (as described in 2.4.4). Fibrinogen was dissolved in DPBS at a 2.5 mg/ml final concentration and filter sterilized. 47.5 µl of sterile aprotinin was added per 1 ml of fibrinogen. HUVECs ($8x10^5$ cells) and HDF cells ($4x10^5$ cells) were mixed together in a 1.5 ml eppendorf tube and spun down. The supernatant was removed, and the cells gently resuspended in 1 ml fibrinogen/aprotinin solution and kept on ice. 1 µl of 5U/ml thrombin was added to the middle of each well of the µ-Plate Angiogenesis 96-well plate (IBIDI), followed by the addition of 9 µl of the cell mix. Plates with cells were incubated for 40 min in the cell culture incubator at 37 °C, after which the cells were overlaid with 70 µl of complete EBM-2 medium containing the different conditions of proteins. The assay was monitored throughout 10 days using the Olympus 1X2-UCB fluorescent microscope and the medium was replaced every other day. After a 10-day period cells were fixed in 4% (w/v) PFA for storage. The network formation was analysed using ImageJ software and angiogenesis analyser plug-in.

2.14.7. Statistical analysis

Statistical analyses were carried out using Graphpad Prism software version 7.0c (La Jolla, CA, USA). Paired student's t test was used for single data comparisons in angiogenesis assays, while two-way ANOVA was used for three or more comparisons. Statistical significance was considered for $p < 0.05$ and indicated in figures by an asterisk (*).

3 GENERATION OF MONOCLONAL ANTIBODIES TO MOUSE MCAM

3.1 Introduction

Renal cell carcinoma (RCC) is often correlated with the loss of function of the von Hippel Lindau factor (VHL). This loss of function promotes strong angiogenic signalling due to elevation of HIF-1 levels and increased VEGF expression, leading to highly vascular tumours [133]. Targeting blood vessels in RCC is well established, however many patients develop severe side effects, resistance to therapy and recurrence of the disease [49,134]. Therefore, a new approach is much needed. MCAM is highly expressed on the tumour vasculature of RCC, correlating with the stage of cancer and poor patient prognosis [56]. Thus, developing a monoclonal antibody towards MCAM could enable the development of new therapies for renal cell carcinoma.

To further investigate MCAM as a target in RCC, we aimed to generate new monoclonal antibodies to MCAM. Our group had previously generated antibodies by immunizing mice with recombinant mouse CLEC14A protein [135]. This yielded five monoclonal antibodies with cross reactivity to mouse and human CLEC14A. The same approach was successfully used in mouse ROBO4 vaccination of mice [136] and extra domain B of fibronectin (ED-B) vaccination of tumour bearing mice [137].

This chapter will describe the production and purification of recombinant mouse and human MCAM (m/hMCAM) proteins, and their use to immunise rodents. The chapter will describe rodent immunisation, assessments of immune responses, fusions of splenocytes with myeloma cells and screening of positive hybridomas. Finally, this chapter will report the generation of stable hybridoma clones expressing rat monoclonal antibodies to mouse MCAM.

3.2 Production and purification of recombinant MCAM proteins

3.2.1. Production of mMCAMecd-Fc recombinant protein

Attempts to immunise mice with self-protein encounters the barrier of immunological tolerance. As a result, generating a high antibody titre sufficient to enable successful fusion is often not achieved. Our group has successfully broken tolerance in mice to several self-proteins by using a human IgG1 Fc fusion tag and a strong adjuvant. Therefore, the Fc fusion tag was added to the C-terminal end of the extracellular domain of mMCAM (mMCAMecd-Fc), depicted in Figure 3.1 A and the protein used in mouse and rat immunisations. The human Fc tag was incorporated by cloning of the extracellular domain of mMCAM protein into the pcDNA-Fc (pIg) vector [138]. This vector contains the human Fc sequence. The cloning was performed by Dr Victoria Heath, University of Birmingham.

HEK293T cells were PEI transfected with mMCAMecd-Fc or with the empty pIg vector. Cells were cultured to confluence in complete DMEM, before the medium was changed to serum free Opti-MEM. The expression of mMCAMecd-Fc protein was confirmed by Western blotting, using anti-human Fc (A0170, Sigma), and anti-mMCAM antibodies (AF6106, R&D). Thus, the mMCAMecd-Fc protein was successfully expressed by cells and secreted into the cell culture medium (Figure 3.1 B).

Small scale protein pull-down from the medium was performed by incubating 1 ml of conditioned Opti-MEM (collected 48h after addition to transfected cells) with a small amount of Protein A beads overnight. The beads were washed, boiled in reducing protein loading buffer and the proteins run on an SDS-polyacrylamide gel that was then stained with Coomassie blue. The mMCAMecd-Fc protein from the conditioned medium efficiently bound

to the beads and was not degraded (Figure 3.1 C). Comparison to BSA standards showed there was around 10 µg of protein per 1 ml of medium.

To obtain at least 10 mg of protein, large-scale production was carried out. HEK293T cells were expanded to ten 15 cm cell culture dishes; transfected with the mMCAMecd-Fc plasmid and after reaching confluence, the medium was replaced by serum free Opti-MEM. Opti-MEM was collected every third day over two weeks. Medium (around 1 litre) containing the protein was filtered, run through a Protein A column and the protein eluted at pH 3. The elution fractions with the highest concentration of protein were loaded on an SDS-polyacrylamide gel and stained with Coomassie blue (Figure 3.1 D). The protein yield was >10 mg/litre of medium. The elution fractions were pooled and dialysed to exchange the elution buffer with PBS. This was sterile filtered and stored at 4 °C before use in immunisation.

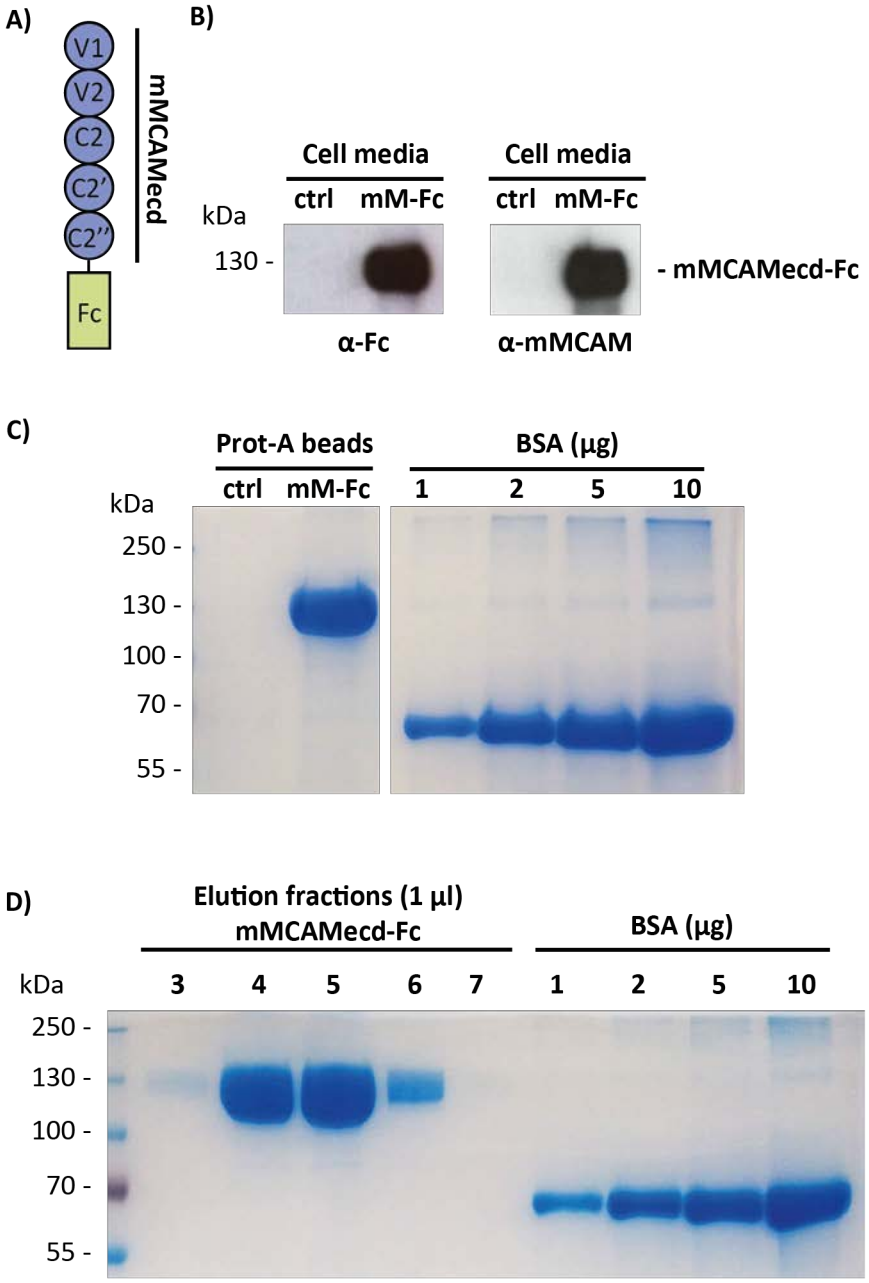

Figure 3.1 Production and purification of mMCAMecd-Fc recombinant protein. A) Schematic image of the extracellular domain of mMCAM fused to the human Fc tag; **B)** Western blot of 10 µl of supernatants from the HEK293T cells taken two days after transfection with empty pIg vector (ctrl) and mMCAMecd-Fc (mM-Fc) blotted with anti-human Fc antibody (α-Fc) and anti-mMCAM antibody (α-mMCAM); **C)** Coomassie blue staining of small scale protein pull down with Protein A beads from the mMCAMecd-Fc and pIg transfected HEK293T cell media (1 ml), 20 µl of beads were loaded on the gel, BSA standard in µg; **D)** Coomassie blue staining of large scale purification of mMCAMecd-Fc on a Protein A column, 1 µl of elution fractions with the highest amount of protein was loaded on the gel, BSA standard in µg.

3.2.2. Production of mMCAMecd-His and hMCAMecd-His recombinant proteins

To probe the antibody reactivity to the mMCAM protein and screen rodent plasma antibody titre, a recombinant mMCAMecd was cloned containing a 6xHis tag (mMCAMecd-His), (Figure 3.2 A). This His-tagged MCAM allowed identifying antibodies that recognise the extracellular domain of MCAM by ELISA, or Western blot. A human version of the MCAM extracellular domain containing a 6xHis tag (hMCAMecd-His) was also produced and used to screen for antibodies that may have dual reactivity, towards mouse and human protein. m/hMCAMecd-Fc plasmids were used in the cloning. The Fc sequence was excised from both plasmids using NotI and XbaI restriction enzymes and the 6xHis sequence was inserted (using T4 ligase) at the C-terminal end of h/mMCAMecd in pIg vector (detailed protocol can be found in material and methods).

HEK293T cells were PEI transfected with mMCAMecd-His/hMCAMecd-His or with the empty pIg vector, and grown in complete DMEM to confluence, when the medium was changed to serum free Opti-MEM. The expression of proteins was confirmed by Western blotting using anti-His antibody (MAB050, R&D), and anti-mMCAM (AF6106, R&D) or anti-hMCAM (HPA008848, Sigma). Both proteins were expressed by cells and secreted into the media (Figure 3.2 B and Figure 3.3 A).

Small scale protein pull-down from the medium was carried out by incubating 1 ml of conditioned Opti-MEM cell medium (collected 48h after addition to cells), with a small amount of Ni-NTA beads overnight. The beads were washed, boiled in reducing protein loading buffer, run on an SDS-polyacrylamide gel, and proteins stained with Coomassie blue. The proteins bound to the beads and did not get degraded (Figure 3.2 C and Figure 3.3 B).

HEK293T cells were expanded to ten 15 cm cell culture dishes; transfected with the mMCAMecd-His/hMCAMecd-His and after reaching confluence, serum free Opti-MEM was used to replace DMEM. Opti-MEM was collected every three days over two weeks. The medium containing the protein was filtered, run through a Ni-NTA column and eluted with 250 mM imidazole in 0.5 ml fractions. The elution fractions with the highest concentration of protein were loaded onto an SDS-polyacrylamide gel and stained with Coomassie blue (Figure 3.2 D). The protein yield for mMCAMecd-His protein was >10 mg/litre of medium.

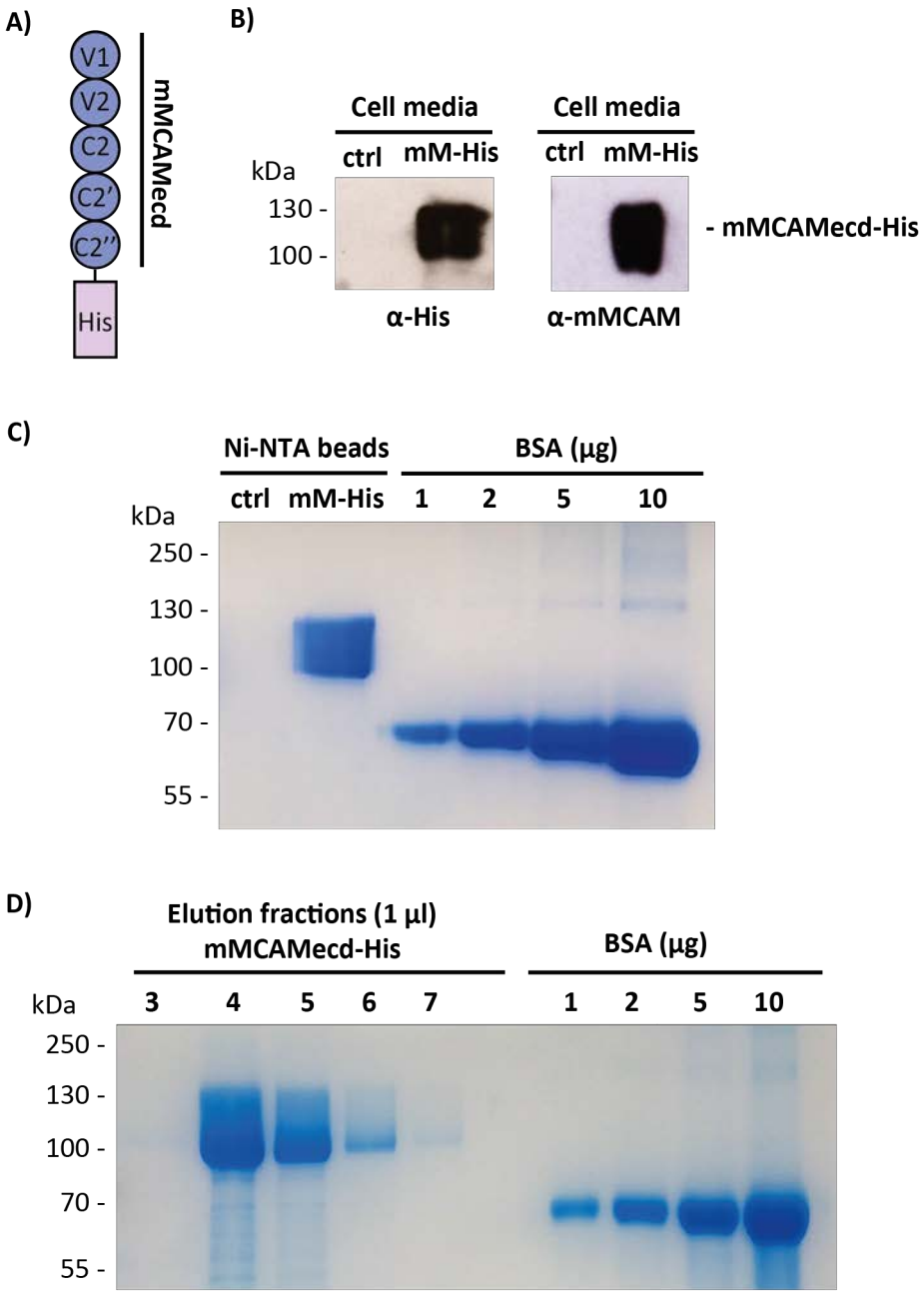

Figure 3.2 Production and purification of mMCAMecd-His recombinant protein. A) Schematic image of the extracellular domain of mMCAM fused to the 6xHis tag; **B)** Western blot of 10 µl of supernatants from the HEK293T cells taken two days after transfection with empty pIg vector (ctrl) and mMCAMecd-His (mM-His) blotted with anti-His antibody (α-His) and anti-mMCAM antibody (α-mMCAM); **C)** Coomassie blue staining of small scale pull down with Ni-NTA beads from the mMCAMecd-His and pIg transfected HEK293T media (1 ml), 20 µl of beads were loaded on the gel, BSA standard in µg; **D)** Coomassie blue staining of large scale purification of mMCAMecd-His on a Ni-NTA column, 1 µl of elution fractions with the highest amount of protein were loaded on the gel, BSA standard in µg.

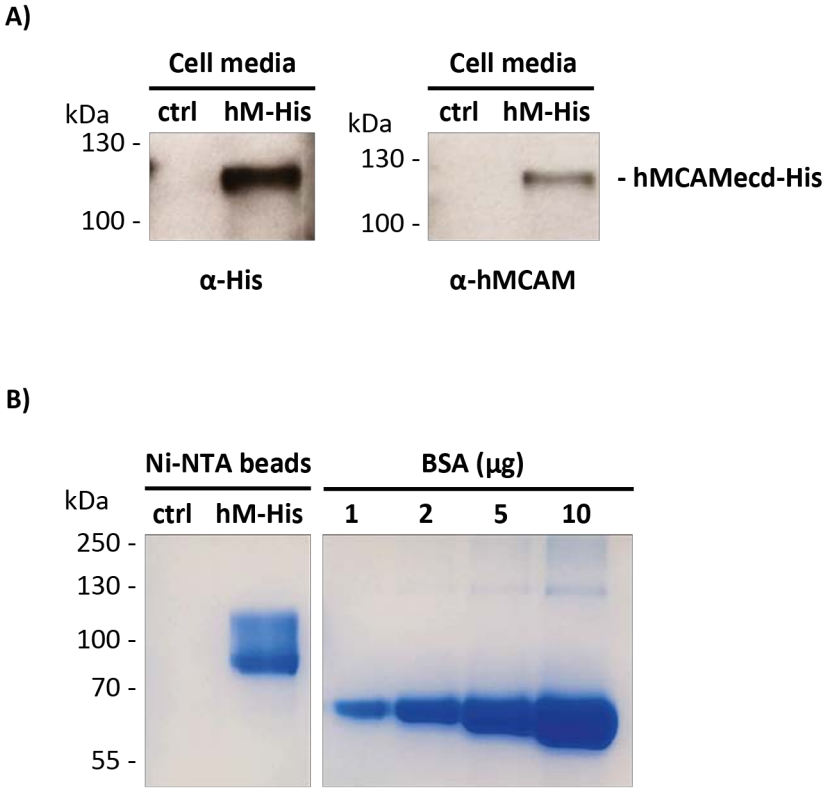

Figure 3.3 Production and purification of hMCAMecd-His recombinant protein. A) Western blot of 10 µl of supernatants from the HEK293T cells taken two days after transfection with empty pIg vector (ctrl) and hMCAMecd-His (hM-His) blotted with anti-His antibody (α-His) and anti-hMCAM antibody (α-hMCAM); **B)** Coomassie blue staining of small scale protein pull down with Ni-NTA beads from the hMCAMecd-His and pIg transfected HEK293T media (1 ml), 20 µl of beads were loaded on the gel, BSA standard in µg.

3.3 Papain cleavage of the Fc tag from mMCAMecd-Fc

Following initial immunisation with mMCAMecd-Fc, the titre in mice showed a strong response to the human Fc tag but not to the mouse MCAM self-antigen. To increase the immune response to mMCAM protein and prevent a stronger response to the human Fc tag, the tag was removed by cleavage with the protease papain (Figure 3.4 A). The cleaved protein was then used to boost mouse and rat immunisation.

Optimisation of papain cleavage

Papain cleaves the Fc tag but at the same time degrades the protein and so it was essential to optimise the time point at which the amount of cleaved mMCAMecd peaked. The mMCAMecd-Fc protein was mixed with the papain cleavage buffer to a final concentration of 0.3 µg/µl to enable protein to be visualized on an SDS-polyacrylamide gel (Coomassie blue readily stains 3 µg of protein on this size of gel). Thus, 10 µl of this reaction was sampled as a starting point before addition of papain. The reaction mixture was then sampled over one hour and analysed by protein separation by SDS-polyacrylamide gel electrophoresis and stained with Coomassie blue. The mMCAMecd-Fc band at the start was much greater than the bands after addition of papain. The reason for this could be that the reaction was not fully quenched by the addition of reducing protein loading buffer and storing the samples on ice before boiling at 95 °C. Thus, when on ice, papain was probably still catalytically active. Over the course of 60 min, almost all the protein was cleaved, however, the greatest amount of cleaved mMCAMecd as shown on the gel was reached at 30 min. After that the cleaved protein was further degraded (Figure 3.4 B).

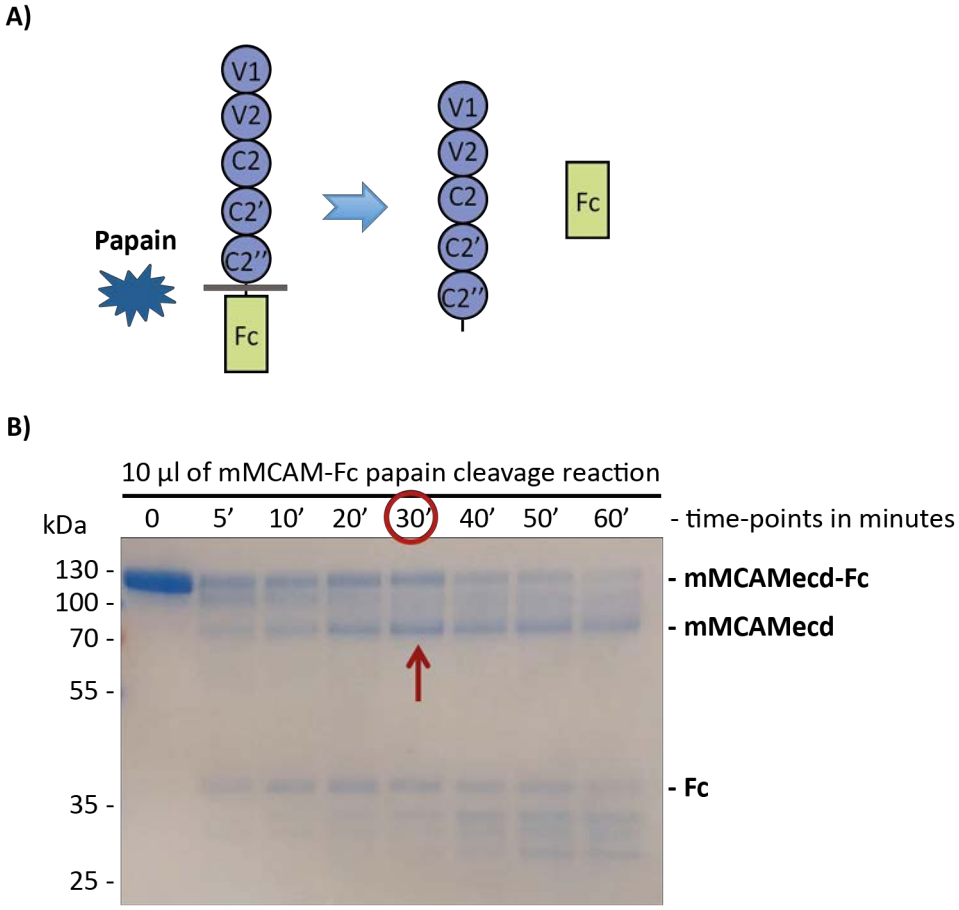

Figure 3.4 Optimisation of papain cleavage of the Fc tag from mMCAMecd-Fc. A) Schematic image of papain cleavage of mMCAMecd-Fc at the connection of MCAM extracellular domain and the Fc tag, Protein A beads capture cleaved Fc tag leaving the purified mMCAMecd; **B)** mMCAMecd-Fc protein was cleaved using protease papain at 37 °C in a 100 µl reaction with 10 µl sample collection at time-points over 1 hour, each sample was mixed with reducing SDS loading buffer and boiled at 95 °C before loading on the gel and visualised with Coomassie blue staining. Arrow showing the time-point at which the amount of cleaved mMCAMecd was the highest.

Large scale papain cleavage and purification of the cleaved mMCAM

A large scale papain cleavage of mMCAMecd-Fc was carried out in 1 ml of reaction mix with 300 µg of protein. After 30 min of cleavage, the reaction was quenched. Protein A beads were used to sequester the Fc tag. The reaction mixture was incubated with Protein A beads for 2 h at 4 °C, the beads were centrifuged, and the supernatant collected. The supernatant was incubated twice more with fresh Protein A beads. The final product was loaded on an SDS-polyacrylamide gel and examined by Western blot analysis with anti-human-Fc (A0170, Sigma) and anti-mMCAM (AF6106, R&D) to ensure that there was no Fc tag left (Figure 3.5 A). Coomassie blue staining of the gel confirmed the purity of the cleaved mMCAMecd (Figure 3.5 B). Purified cleaved mMCAMecd was dialysed against PBS, sterile filtered and subsequently used in mouse and rat immunisation.

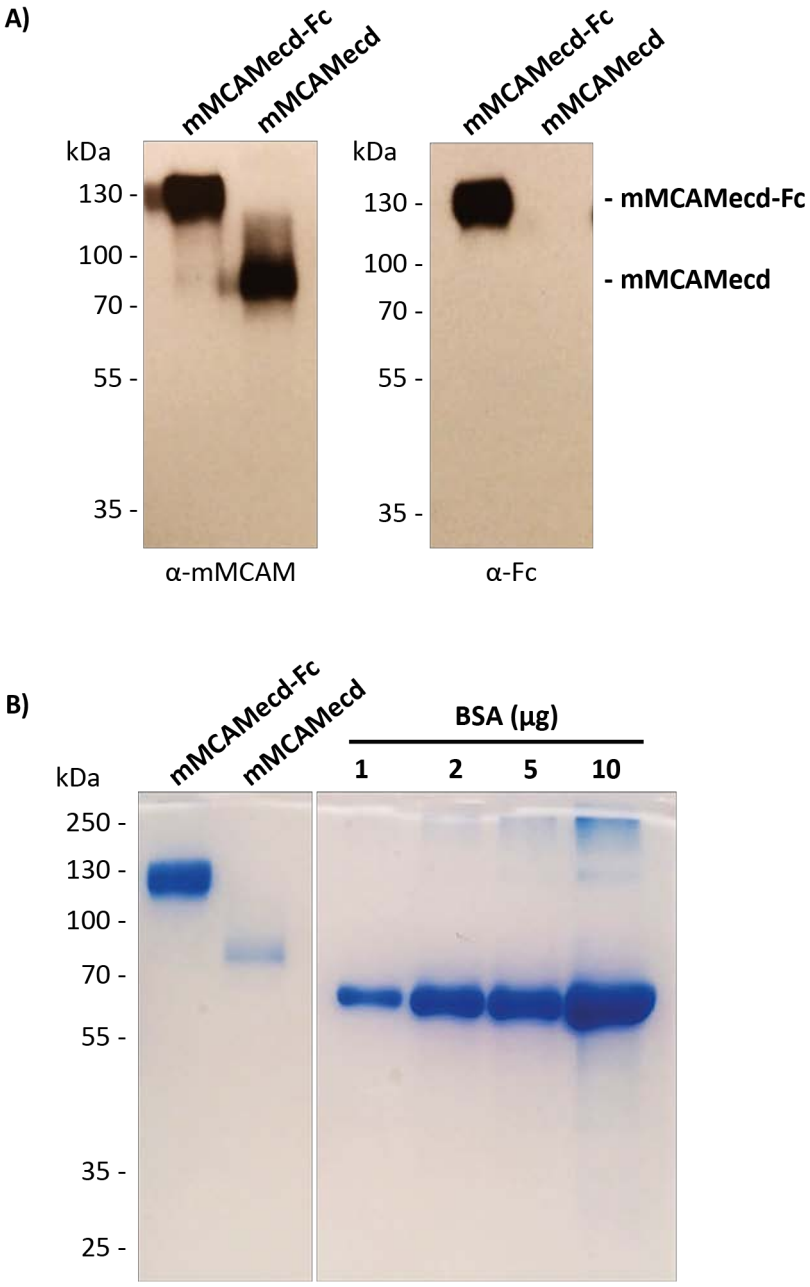

Figure 3.5 Large scale papain cleavage of mMCAMecd-Fc and Fc depletion. Large scale papain cleavage was carried out in 30 min reaction with 1.6 µg/ml papain; the Fc tag was removed by incubation with Protein A beads: **A)** Western blot with anti-mMCAM (α-mMCAM) and anti-human Fc (α-Fc) and **B)** Coomassie blue staining of mMCAMecd-Fc protein before papain cleavage (mMCAMecd-Fc), and after papain cleavage and Fc depletion with Protein A beads (mMCAMecd), BSA standard in µg.

3.4 Generation of monoclonal antibodies that recognise mMCAMecd in mice

The previous successful attempts to generate an immune response to self-protein in mice used human Fc tag as a tool to break tolerance. To generate monoclonal antibodies towards mouse MCAM extracellular domain, purified mMCAMecd-Fc was used to immunise mice. Eurogentec S.A. biotech was employed to perform the immunisation and the purified protein was supplied to the company. The immunisation was as previously described for another self-antigen fused to the human Fc tag (mROBO4-Fc) [136] (section 2.8.1.1). In brief, mice were immunised every two-weeks using 50 µg of mMCAMecd-Fc in Freund's complete adjuvant (FCA) for the first immunisation, and subsequently with Freund's incomplete adjuvant (FIA) (Table 3.1).

Pre-immunisation bleeds were collected as a negative control. Bleeds collected after the fourth immunisation were compared to the pre-immune bleeds by ELISA assay on mMCAMecd-Fc and mMCAMecd-His. 500 ng of protein was used to coat each well of an ELISA plate. The ELISA plates were probed overnight with the 1/500 bleed dilution in PBS. As expected the response (antibody titre) to mMCAMecd-Fc was strong, while a response to mMCAMecd-His was only detected in one mouse (mouse 33354) (Figure 3.6). Serial dilutions of bleeds were tested, however the response in mouse 33354 was seen only in the 1/500 dilution, and so the higher dilutions were not taken into considerations.

Table 3.1 Mouse immunisation protocol - Eurogentec S.A.

Day	Date	Protocol: Standard Programme
0	20/10/15	Preimmune bleed
		Injection with 50 µg mMCAMecd-Fc/Freund's complete adjuvant
14	03/11/15	Injection with 50 µg mMCAMecd-Fc/Freund's incomplete adjuvant
28	17/11/15	Injection with 50 µg mMCAMecd-Fc/Freund's incomplete adjuvant
42	01/12/15	Injection with 50 µg mMCAMecd-Fc/Freund's incomplete adjuvant
48	07/12/15	Test bleed and fusions

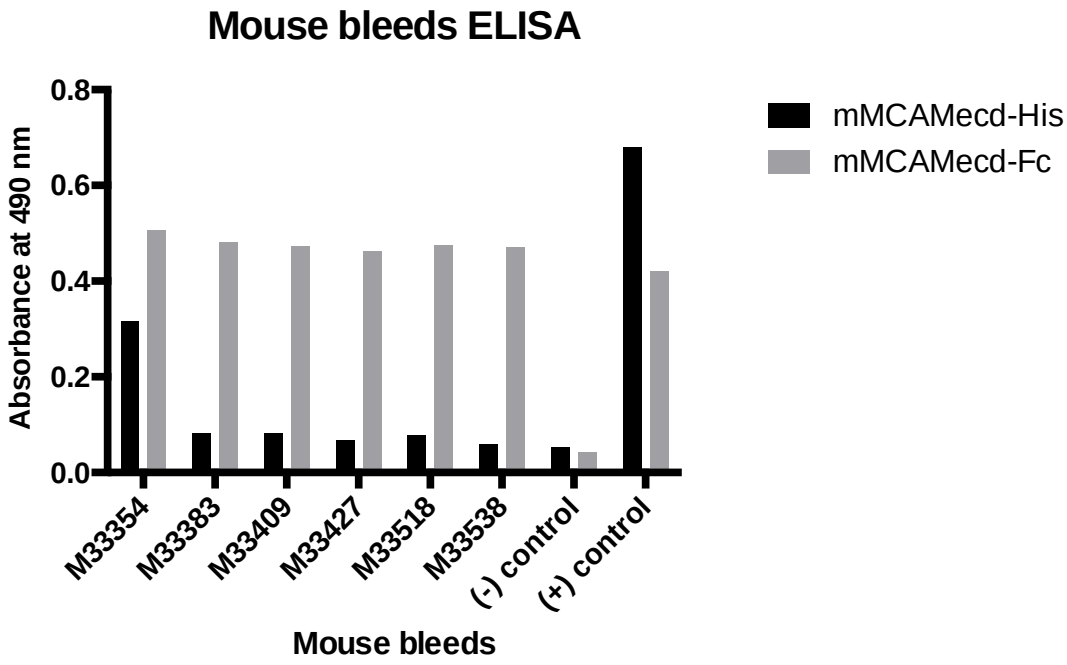

Figure 3.6 Screening mouse bleeds by ELISA. 500 ng per well of mMCAMecd-His and mMCAMecd-Fc was used to coat the ELISA plate; 1:500 dilutions of mouse bleeds were used to probe the ELISA and the absorbance was recorded at 490 nm. Unimmunised mouse bleed was used as a negative control, and 1 µg/µl of anti-His (MAB050, R&D) and anti-Fc (A0170, Sigma) antibodies was used as a positive control.

Splenocytes from the single positive mouse (M33354) were isolated and fused with mouse myeloma cells to generate antibody-producing hybridomas. Single sample of undiluted supernatants from pools of hybridoma cells were screened for reactivity towards the original immunogen mMCAMecd-Fc and the mMCAMecd-His protein to assess specificity of supernatants. The reactivity of supernatants was high to mMCAMecd-Fc but negative to mMCAMecd-His indicating that none of the antibodies recognised the mMCAMecd protein (Figure 3.7). Due to the small volume of the supernatants one repeat per hybridoma was tested by ELISA.

Two further fusions were carried out with different immunisation protocols with mouse MCAM recombinant proteins. One attempt used a combination of immunisations with mMCAMecd-Fc and subsequent boosts with the cleaved mMCAMecd. Another attempt used only mMCAMecd cleaved throughout the immunisation protocol (protocols described in materials and methods section 2.8.1.2). Both failed to generate mouse anti-mouse MCAM hybridomas.

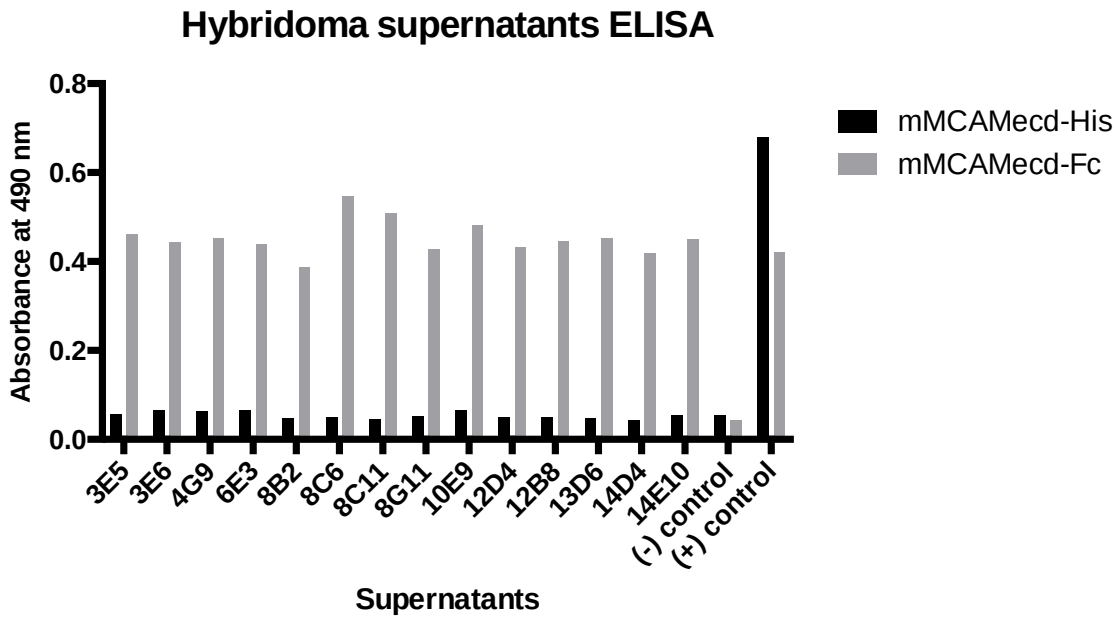

Figure 3.7 Screening hybridoma supernatants by ELISA. 500 ng per well of mMCAMecd-His and mMCAMecd-Fc was used to coat the ELISA plate; undiluted mouse hybridoma supernatants were used to probe the ELISA overnight and the absorbance was recorded at 490 nm. Secondary antibody only was used as a negative control, and 1 µg/ml of anti-His (MAB050, R&D) and anti-Fc (A0170, Sigma) antibodies were used as positive controls.

3.5 Generation of monoclonal antibodies that recognise mMCAMecd in rats

Repeated failure to break tolerance in mice to mouse MCAM prompted us to immunise rats with mouse MCAM. To confirm that there are amino acid sequence differences between the mouse and rat protein, the sequences of extracellular domains were compared using online Blastp program (protein-protein BLAST, NCBI), which showed 90% identity between these sequences. Praline (http://www.ibi.vu.nl/programs/pralinewww/) [139] online tool was used to map the conserved and non-conserved amino acid residue types to investigate if the differences between amino acid sequences are sufficient to promote an immune response in rat (Figure 3.8). There are several epitopes with poorly conserved amino acids, which led us to believe the immunisation of rats with mouse protein would yield an immune response.

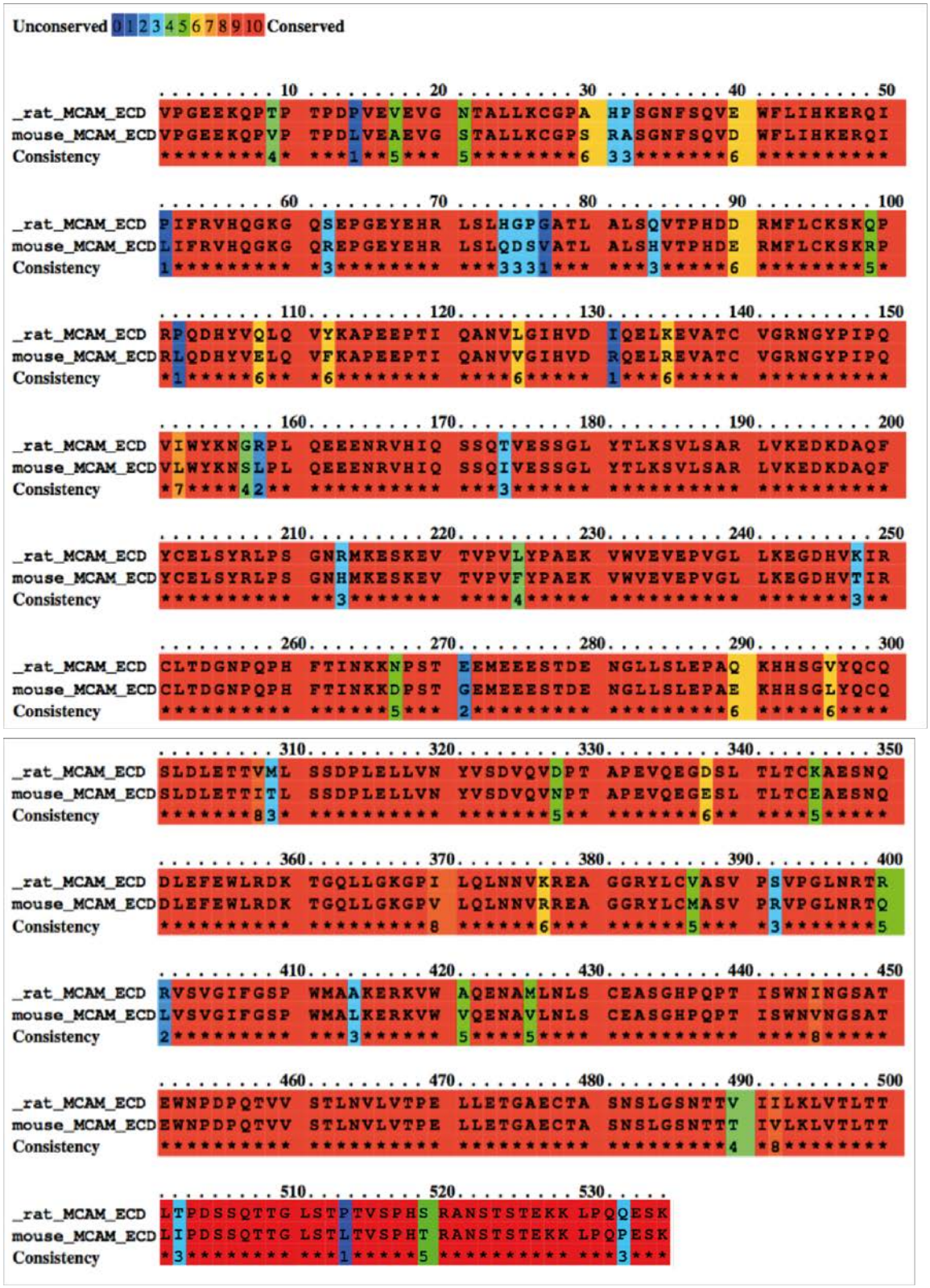

Figure 3.8 Comparison of amino acid sequence of mouse and rat MCAM extracellular domain using Praline online software.

Biogenes GmbH was sub-contracted to immunise rats with mMCAM recombinant proteins. A standard immunisation protocol was used, where rats were immunised at one-week intervals according to the schedule in Table 3.2. In the first and the second immunisation, rats were immunised with 50 µg of mMCAMecd-Fc, while the rest of the boosts were carried out with 50 µg of the cleaved mMCAMecd (Table 3.2).

Table 3.2 Rat immunisation protocol - Biogenes GmbH

Day	Date	Protocol
0	04/10/16	Preimmune bleed Injection with 50 µg mMCAMecd-Fc/ Freund's complete adjuvant
7	11/10/16	Injection with 50 µg mMCAMecd-Fc/ Freund's incomplete adjuvant
14	18/10/16	Injection with 50 µg mMCAMecd/ Freund's incomplete adjuvant
21	25/10/16	Test bleed
34	07/11/16	Final boost (rat 1, 3) 50 µg mMCAMecd/ Freund's incomplete adjuvant
38	11/11/16	Fusions (rat 1, 3)
131	13/02/17	Final boost (rat 2) 50 µg mMCAMecd/ Freund's incomplete adjuvant
135	17/02/17	Fusions (rat 2)

3.5.1. Screening of the immune response in rat serum by ELISA

Pre-bleeds were taken from the rats as a negative control. Bleeds were taken one week after the 3rd immunisation and examined for serum antibodies to mMCAMecd-His and hMCAMecd-His. ELISA plates were coated with 500 ng of protein and probed overnight with serial dilutions of rat serum in PBS. All three rats showed a strong response to the mouse protein and a weak response to the human protein (Figure 3.9). Serum from unimmunised mice was used as a negative control.

A)

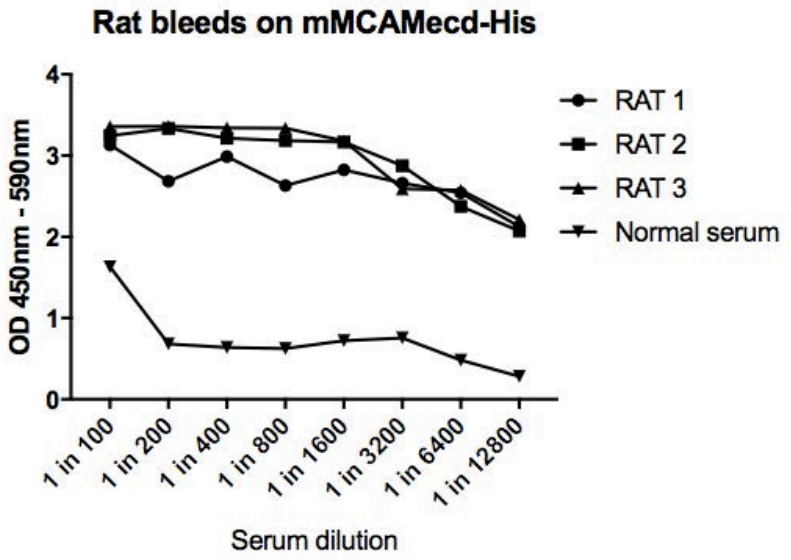

B)

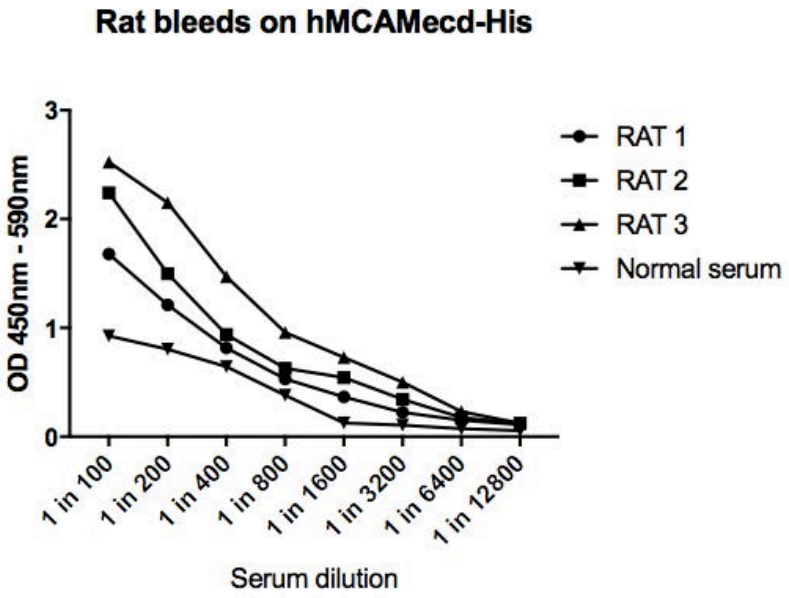

Figure 3.9 Screening of the immune response in rat bleeds by ELISA. 500 ng of **A)** mMCAMecd-His and **B)** hMCAMecd-His was used to coat the ELISA plate. Serial dilutions of rat bleeds were used to probe the ELISA. Unimmunised serum (normal serum) was used as a negative control. The absorbance was recorded at 450 nm, and the background 590 nm absorbance was deducted.

3.5.2. Screening of mMCAM positive hybridoma clones by ELISA

Two rats (rat 1 and 3) were boosted with the final immunisation and culled for fusion three days later. Splenocytes were isolated and fused to mouse myeloma Sp2/0-Ag14 cells. These myeloma cells do not secrete immunoglobulin, are resistant to 8-azaguanine at 20 µg/ml, lack hypoxanthine-guanine phosphoribosyltransferase (HGPRT) activity and are HAT sensitive (final concentration: hypoxanthine at 100 µM, aminopterin at 400 nM and thymidine at 16 µM). The supernatants of hybridoma cells from 2 culled rats were tested on mMCAMecd-His ELISA at Biogenes. However, this fusion failed to generate stable antibody producing hybridomas.

A third rat was left for a period of >3 months before another immunisation was performed again with Fc cleaved mMCAMecd. The rat was culled for splenocyte fusion with mouse myeloma cells 3 days later. Individual hybridoma clones were cultured in separate wells and the supernatants examined by ELISA on mMCAMecd-His protein at Biogenes (data not shown). A single sample for each individual hybridoma was tested by ELISA (due to supernatants' volume restrictions) and a signal higher than the negative control was considered as reactive to MCAM. The plates were coated with 500 ng of mMCAMecd-His and hMCAMecd-His and probed with undiluted hybridoma supernatants, the positive control (anti-m/hMCAM at 1 µg/ml) or the negative control (myeloma cell supernatant). The response to mMCAMecd-His was variable with most of the supernatants strongly positive, but there was no response to the human MCAM protein (Figure 3.10).

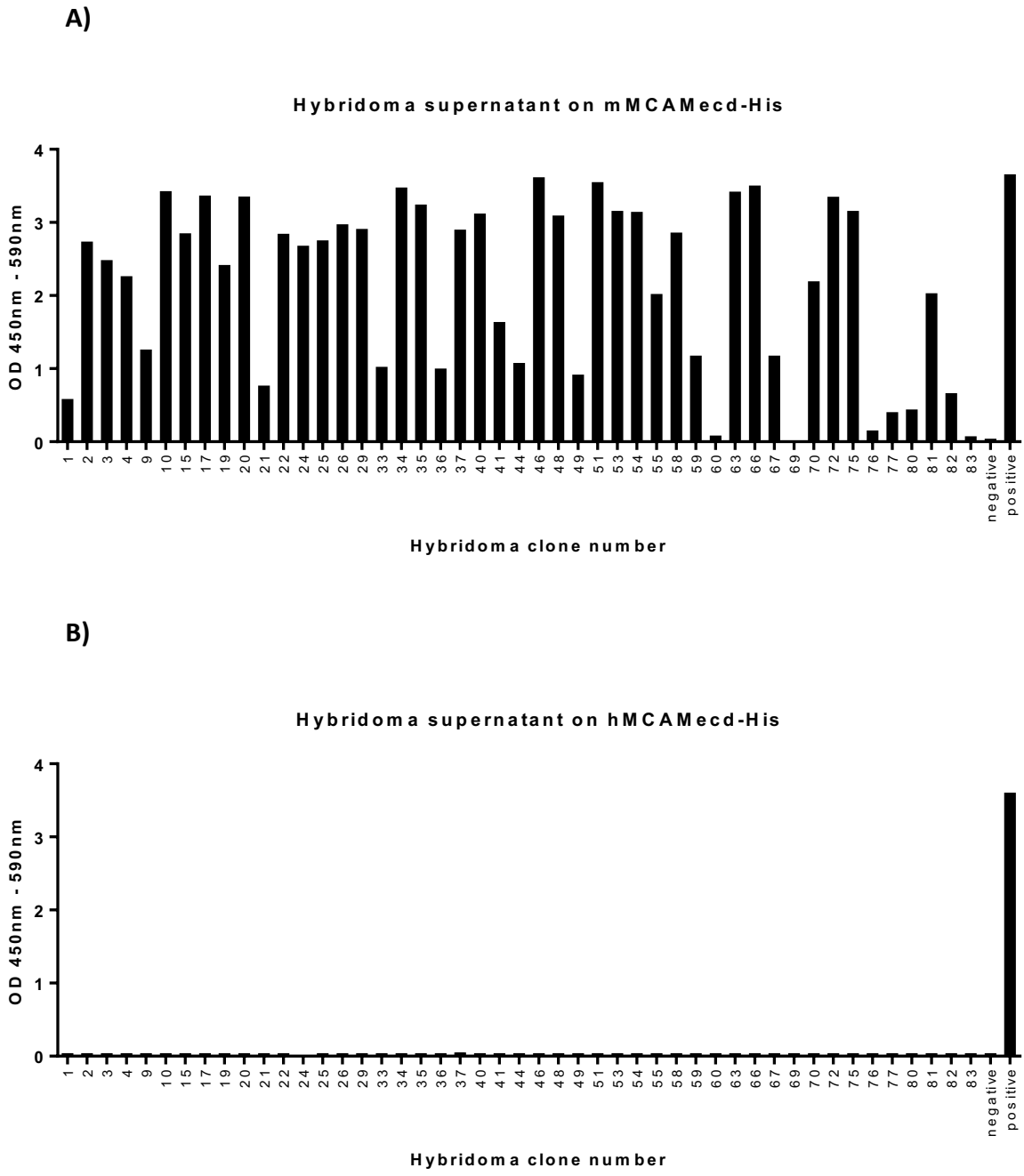

Figure 3.10 Screening supernatants of rat hybridoma cells on A) mMCAMecd-His and **B)** hMCAMecd-His ELISA. 500 ng of protein was used to coat the ELISA plate; undiluted hybridoma supernatants were used to probe the ELISA. The OD was measured at 450 nm – 590 nm to remove the background signal. Positive control 1 µg/ml anti-mMCAM (AF6106), anti-hMCAM (HPA008848), and negative control myeloma cell supernatant.

3.5.3. Screening of strongly positive mMCAM hybridoma clones by Western blot

Thirty strongly positive hybridoma clones were selected for Western blot analysis. MCAM protein has five di-sulphide bonds within the extracellular domain, which are broken under reducing conditions. Individual supernatants were examined by Western blot to see if the antibodies recognise the protein in its reduced or non-reduced state. This showed whether antibodies recognise a linear epitope on mMCAM protein or the folded protein, which is dependent on the disulphide bonds. Mouse MCAMecd-His protein was loaded onto an SDS-polyacrylamide gel in reducing and non-reducing protein loading buffer. The protein was transferred to the PVDF membrane and the membrane cut into small pieces. Each piece of membrane was probed with an individual supernatant. The antibodies in supernatants appear to have different reactivity towards MCAM protein (Figure 3.11). Several antibodies recognise only the non-reduced form (4, 9, 26, 29, 35, 37, 40, 48, 53, 54, 55, 58, 63, 66, 70). The immunisations and screenings by ELISA were performed using non-reduced form of MCAM so it is expected that the antibodies detect either the non-reduced, or both reduced and non-reduced form of MCAM on Western blot. However, some antibodies give a high background staining such as antibody 2 and 3, while some do not recognise or only slightly recognise MCAM by Western blot (4, 9, 17, 58, 63 and 70). Antibodies 10, 15, 17, 20, 22, 24, 34, 41, 46,51, 72, 75 and 81 recognise both the reduced and non-reduced MCAM, indicating they recognise the linear epitope. However, some have a stronger and some weaker binding to the reduced form.

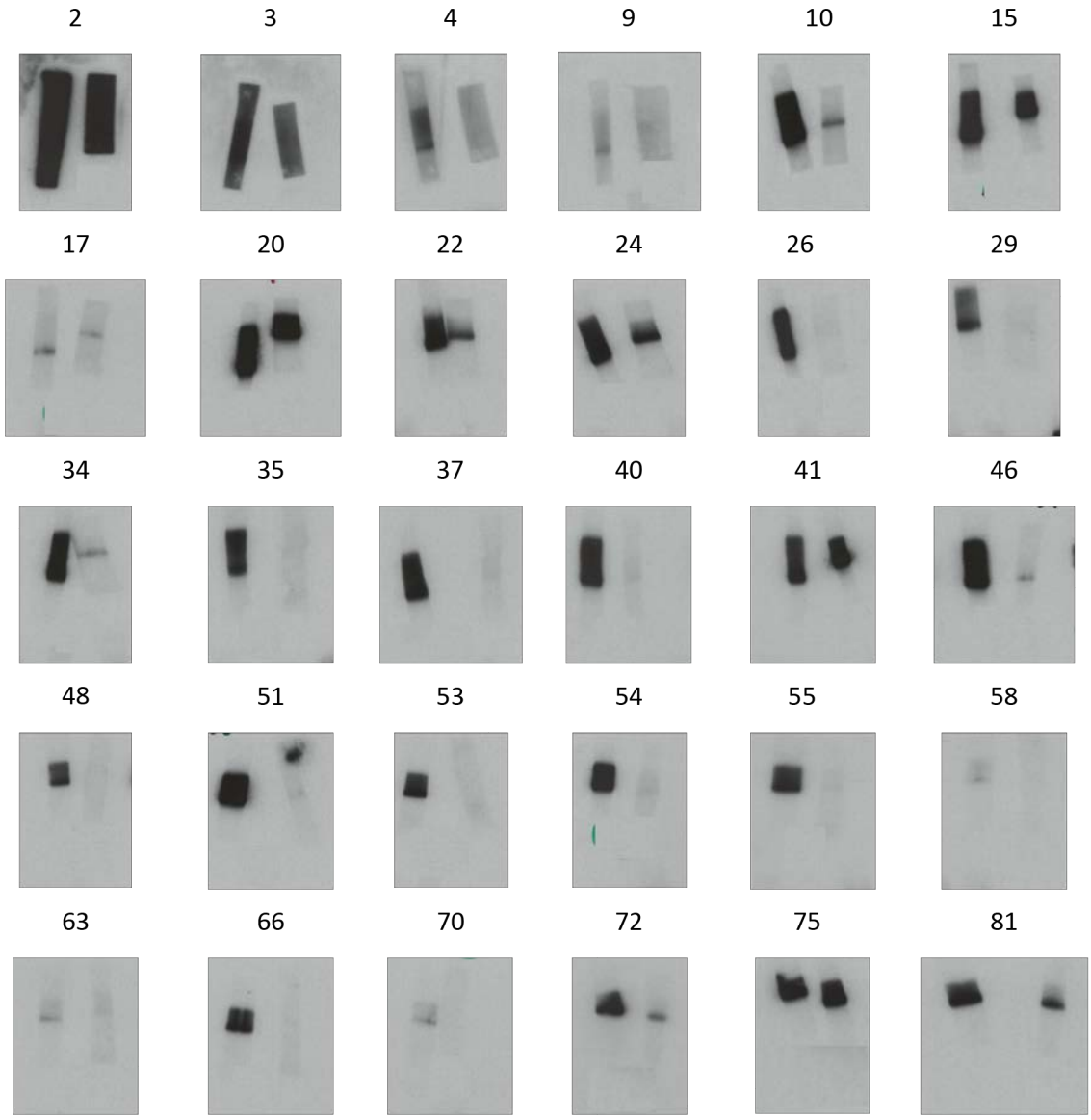

Figure 3.11 Western blot with individual hybridoma supernatants on non-reducing (left) and reducing (right) mMCAMecd-His protein. The proteins were loaded on an SDS-polyacrylamide gel and transferred to the PVDF membrane; the membrane was cut in small strips at the site of the protein and incubated with undiluted hybridoma supernatants.

3.6 Sub-cloning of selected hybridoma clones

Based on the Western blot and ELISA analysis, ten hybridoma clones were selected for further sub-cloning, namely 3, 9, 17, 20, 46, 48, 53, 54, 72 and 75. BioGenes additionally selected primary cultures number 10, 26, 35, 41 and 66 for sub-cloning. Each of these colonies were diluted to form single cells seeded in the wells by limiting dilution. Only wells with single-cell colonies were tested further for mMCAM recognition. Supernatants were tested on ELISA plates coated with mMCAMecd-His protein. The final bleed dilution was used as a positive control (antiserum) and myeloma cell supernatant as a negative control. After the first sub-cloning, clone numbers 10-2, 46-16 and 66-11 continued to secrete antibodies with the expected reactivity profile (Table 3.3). All other primary cultures stopped generating antibodies during the first sub-cloning.

All primary hybridomas were, however, frozen before the first sub-cloning and so in principle the variable regions can be recovered from their mRNA by retro-transcription and PCR with specific primers after cell recovery.

Table 3.3 ELISA results after 1st sub-cloning. The ELISA plates coated with mMCAMecd-His were probed with the supernatants of positive clones 10-2, 46-16 and 66-11, final bleed dilution (Antisera) and myeloma cell supernatant (Negative control). The optical density was recorded at 405 nm.

Clone number	ELISA reaction absorbance at 405 nm
10-2	3.822
46-16	0.445
66-11	3.659
Antiserum (1:100)	3.834
Negative control	0.004

3.7 Generation of stable hybridoma cell lines producing monoclonal antibodies to mMCAM

After the second sub-cloning, clones 10-2-1 and 66-11-5 continued to stably produce antibodies against mMCAMecd-His (Table 3.4). Clone 46-16 lost antibody production during the second cloning procedure. These cells were passaged several times to identify the best clones with regard to cell growth and ELISA signal. Finally, hybridoma cell lines with the stable production of monoclonal antibodies that recognised mMCAMecd were generated and used for antibody production and characterisation described in chapter 4 of this thesis. Both hybridomas were confirmed to be mycoplasma-free by Greiner Bio-One GmbH, Frickenhausen, Germany, and were cryopreserved.

Table 3.4 ELISA results after 2nd sub-cloning. The ELISA reaction was carried out on plates coated with mMCAMecd-His protein; the supernatants of positive clones 10-2-1, and 66-11-5 were compared with final bleed dilution as a positive control (antisera) and myeloma cell supernatant (negative control). The optical density was recorded at 405 nm.

Clone number	ELISA reaction absorbance at 405 nm
10-2-1	1.277
66-11-5	0.766
Antiserum (1:100)	1.293
Negative control	0.004

3.8 Discussion:

To explore the therapeutic potential of MCAM in a renal cancer mouse model, we aimed to generate monoclonal antibodies that recognise the extracellular domain of mouse MCAM protein. Targeting the extracellular domain of endothelial proteins has clear advantages over targeting tumour cells because they are accessible by agents circulating in the blood and since they are part of the stromal compartment they should not develop resistance to therapy. Monoclonal antibody generated in mice would have little risk of mounting a subsequent immune reaction and would thus be optimal for tumour targeting experiments in mice. Previous work showed that fusing a self-antigen to a foreign protein such as human Fc and using a strong adjuvant (such as Freund's complete adjuvant) increased recognition of T-cell helper lymphocytes and generated a stronger B cell response [137,140]. However, several attempts to raise an immune response to MCAM self-protein in mice failed to generate positive hybridoma cells. Tolerance to this self-antigen was much stronger than previously encountered by our group with other proteins [136,135]. In agreement with this, other groups showed that antibodies against human MCAM developed in mice could recognise the human protein but not the mouse one, even though the similarity between the two is 75%, showing a strong tolerance to mouse antigen [58]. One group described six novel anti-hMCAM antibodies generated in mice with none of them being able to recognise the mouse protein [141]. High levels of MCAM during embryonic development could explain the tolerance to this self-protein. MCAM is found highly expressed on embryonic tissue of spleen, thymus and bone marrow [67,142], tissues of maturation and deletion of self-recognising immune cells. However other possibilities that involve self-tolerance such as regulatory T-cells cannot be excluded.

Protein sequence similarity between the mouse and rat MCAM extracellular domain is 90%, indicating that a non-self response to certain parts of protein should be possible. Thus, rat immunisation resulted in around 50 positive primary hybridoma cells. All of these were frozen immediately after confirmation of positivity in order to be able to sequence the variable regions of the heavy and light immunoglobulin chains. Ten hybridomas were chosen for further sub-cloning, but in the process, all lost recognition of mouse MCAM. However, two other clones, selected by Biogenes were sub-cloned and created stable hybridomas. Fusion with rat myeloma cells would possibly have generated a larger number of hybridoma clones, however fusion with mouse myeloma cells was an established protocol within Biogenes and was thus, performed in this study.

The primary aim was to generate antibodies with reactivity towards mouse and human protein. This would enable investigation of antibodies function in mouse models and further validation of antibodies on human tissue. Rat serum antibodies showed a slight response to the human protein, however, none of the generated hybridoma antibodies could recognise the human protein. Potentially, boosting rats with hMCAMecd-Fc recombinant protein would increase the amount of dual reactivity antibodies, and this strategy could be used in future immunisation. Additionally, many new strategies involving synthetic antibody libraries, such as phage and yeast display libraries could be utilised to generate antibodies towards shared epitopes in human and mouse protein.

Despite the fact that the antibodies were generated in rats, the antibody variable regions can be grafted onto a mouse main frame, enabling their use in mouse models of cancer. Thus, further molecular engineering is necessary in order to develop mouse anti-mouse antibodies.

Finally, the hybridoma clones were tested for antibody reactivity by Western blot in reduced and non-reduced conditions. MCAM protein contains 5 disulphide bonds and thus, antibodies that recognise epitopes dependent on these bonds would not be able to recognise the reduced form of MCAM by Western blot. Different patterns were observed with hybridoma supernatants indicating various binding properties of the generated antibodies. Sequencing variable regions would discover the differences between each individual clone. The primary hybridoma clone 10 recognised both reduced and non-reduced form of MCAM, although the band on Western blot for reduced protein was much fainter than on the non-reduced sample. However, primary hybridoma clone 66 did not recognise the reduced form of MCAM but only non-reduced.

These hybridoma cells were sub-cloned to generate stable cell lines producing reactive MCAM antibody and in the next chapter further characterisation of these antibodies will be performed and their specificity and biology investigated in greater depth.

4 BIOCHEMICAL CHARACTERISATION OF RAT MONOCLONAL ANTIBODIES TO MCAM

4.1 Introduction

Monoclonal antibodies are a valuable and widely used tool in scientific research and medicine. For example, monoclonal antibodies targeting EGFR, HER2 and VEGF are routinely used in cancer treatment and have significantly improved patient prognosis when compared to traditional therapies. Nonetheless, the correct use of various antibodies in research and clinical setting is dependent on thorough validation of their properties.

The rat immunisation with the mouse MCAM extracellular domain recombinant protein generated two stable hybridoma clones producing monoclonal antibodies that recognise mMCAMecd (chapter 3 of this thesis). These clones were renamed mMCAM10 and mMCAM66, for clones 10-2-1 and 66-11-5 respectively.

Monoclonal antibodies mMCAM10 and 66 were evaluated for their use in a variety of immunostaining techniques using cells expressing recombinant full-length mouse MCAM and endogenous mouse MCAM expressed on the cell surface. Testing the antibodies by Western blotting, flow cytometry, immunofluorescence and immunohistochemistry indicated their utility in a diverse range of *in vitro* techniques. Epitope mapping and epitope competition assays showed to which part of the MCAM protein the antibodies bind, and whether the binding epitopes are distinct between these two antibodies. Antibodies were injected into the tumour bearing mice to examine the antibody binding properties *in vivo.* The knowledge of the distribution of antibodies in mouse healthy tissue and tumour is important for the therapeutic development of MCAM targeted cancer therapies. Finally, the variable region of the mMCAM10 was sequenced and cloned into the TOPO vector in order to be able to use it for engineering different forms of antibodies or other forms of targeted therapies such as CAR-T cells.

4.2 Generation of cells with stable expression of mMCAMfl-FLAG

In order to characterise monoclonal antibodies for their use in techniques such as cell immunostaining or flow cytometry, a cell line expressing membrane mouse MCAM was generated. Lentiviral vector pWPI (containing an EMCV IRES sequence between a transgene cloning site and a GFP marker) was used to clone in the full-length mMCAM with a C-terminal FLAG tag (mMCAMfl-FLAG). The construct contained a signal peptide to permit cell surface expression. The GFP marker in the vector made it easier to visualise transduced cells.

HEK293T cells were then transduced with pWPI (empty vector) or mMCAMfl-FLAG. The expression of mMCAMfl-FLAG was examined by Western blotting. Cells were lysed, and total protein separated in an SDS-polyacrylamide gel and transferred to a PVDF membrane. Proteins were blotted with commercial rat anti-mouse MCAM antibody (MAB7718, R&D) and anti-FLAG antibody (ab49763, Abcam). mMCAMfl-FLAG was successfully expressed by transduced HEK293T cells (Figure 4.1 A).

The expression of mMCAM on the surface of these cells was then examined by flow cytometry using anti-mouse MCAM antibody (MAB7718) (10 μg/ml) and Alexa Fluor® 546 anti-rat IgG secondary antibody (1:100). The green fluorescence (FITC) gate was set using untransduced HEK293T cells (GFP negative population). Control rat IgG (R&D) and secondary was used to set the gate for red fluorescence (PE) negative population on pWPI cells. The red and green fluorescence channels were compensated using Summit software. Transduced HEK293T cells were first gated for GFP positive cells (FITC+ cells), and then examined for MCAM expression (PE+ cells). GFP-positive mMCAMfl-FLAG cells were over 99% positive for MCAM expression; while pWPI cells were all negative as expected (Figure 4.1 B).

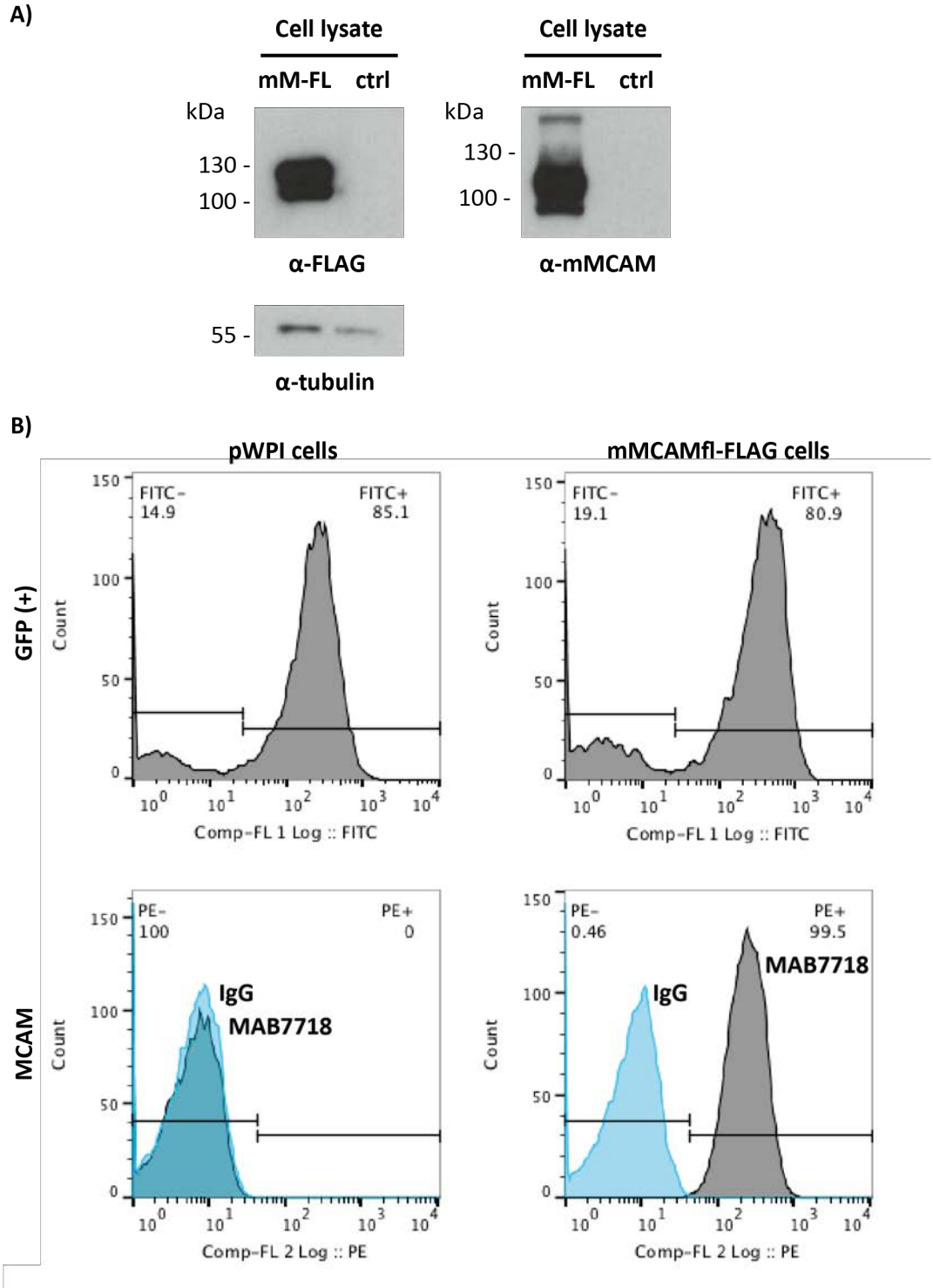

Figure 4.1 Expression of MCAM by mMCAMfl-FLAG (mM-FL) and pWPI (ctrl) transduced HEK293T cells. (A) Western blot of cell lysates from the HEK293T cells transfected with empty pWPI vector (ctrl) and mMCAMfl-FLAG (mM-FL) blotted with anti-mouse MCAM (α-mMCAM), anti-FLAG (α-FLAG) and anti-tubulin antibody (α-tubulin) **(B)** Flow cytometry of pWPI and mMCAMfl-FLAG cells incubated with anti-mMCAM antibody (MAB7718 in grey) or control rat IgG (IgG in blue). Gates were set for GFP positive cells GFP(+), and the mouse MCAM expression was detected via red fluorescence PE(+), IgG/MAB7718. Numbers in the flow cytometry histograms represent percentage of cells.

4.3 Expression of endogenous mouse MCAM in mouse endothelial cell lines and the RENCA carcinoma cell line

Mouse cell lines expressing endogenous mouse MCAM protein are of great use for characterisation of novel monoclonal antibodies. Two different mouse endothelial cell lines were tested for the expression of mMCAM: bENDs (murine brain derived transformed endothelial cells) and sENDs (murine skin derived transformed endothelial cells). Mouse RENCA tumour cell line is a murine model of renal cell carcinoma used to induce tumours *in vivo*. This cell line was tested for MCAM expression in order to confirm that MCAM is not expressed on the tumour cells.

Cells of all three cell lines were lysed and total protein run on an SDS-polyacrylamide gel and transferred to a PVDF membrane. Western blot with anti-mMCAM (MAB7718) antibody showed high expression of mMCAM on bENDs, a lower expression on sENDs, and no expression on RENCA cells (Figure 4.2 A). Due to the higher expression of mouse MCAM on bENDs these cells were used in further validations of monoclonal antibodies described in this chapter.

Flow cytometry with MAB7718 on bENDs further confirmed the expression of mouse MCAM (Figure 4.2 B). Cells were gated for a single cell population, and a PE negative population using unstained bENDs. Rat IgG control was used as a negative control. Over 90% of bENDs immunostained with the MAB7718 antibody showed positive signal for mouse MCAM.

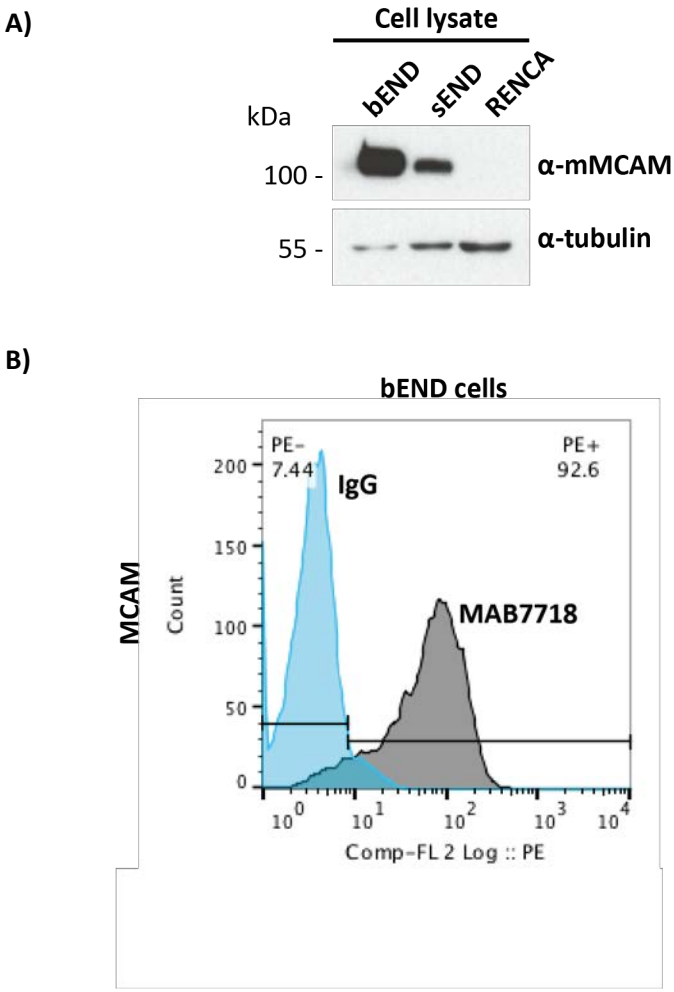

Figure 4.2 Expression of MCAM by mouse endothelial cell lines bENDs and sENDs, and RENCA mouse tumour cell line. A) Western blot of cell lysates from bEND, sEND and RENCA cells with anti-mouse MCAM (α-mMCAM) and anti-tubulin (α-tubulin). **B)** Flow cytometry of bEND cells incubated for 1 h with anti-mouse MCAM antibody (MAB7718 in grey) or control rat IgG (IgG in blue). MCAM expression was detected by red fluorescence PE(+). Numbers in the flow cytometry histograms represent the percentage of cells.

4.4 Analysis of mMCAM10 and 66 by flow cytometry

Chapter 3 described the generation of two stable hybridoma cell clones generated by fusion of rat splenocytes and mouse myeloma cell line: mMCAM10 and mMCAM66. Supernatants from the stable hybridoma cells were used in early stages of validation of these antibodies after being provided by Biogenes. bENDs and HEK293T cells transduced with mMCAMfl-FLAG and pWPI plasmid were used to validate the new monoclonal antibodies by flow cytometry. Cells were incubated with undiluted supernatants from hybridoma clones mMCAM10 and 66 or with the rat IgG control (at 10 µg/ml) for 1 h at 4 °C. The cells were washed and incubated with the anti-rat secondary antibody conjugated to Alexa Fluor® 546 (1:100) and analysed by flow cytometry. Monoclonal antibodies mMCAM10 and 66 were able to immunostain endogenous mouse MCAM on bEND cells (>93% of positive cells, for both) and recombinant mMCAMfl-FLAG protein expressed by HEK293T cells (>99% of positive cells, for both), but did not stain the HEK293T cells transduced with empty pWPI vector (Figure 4.3).

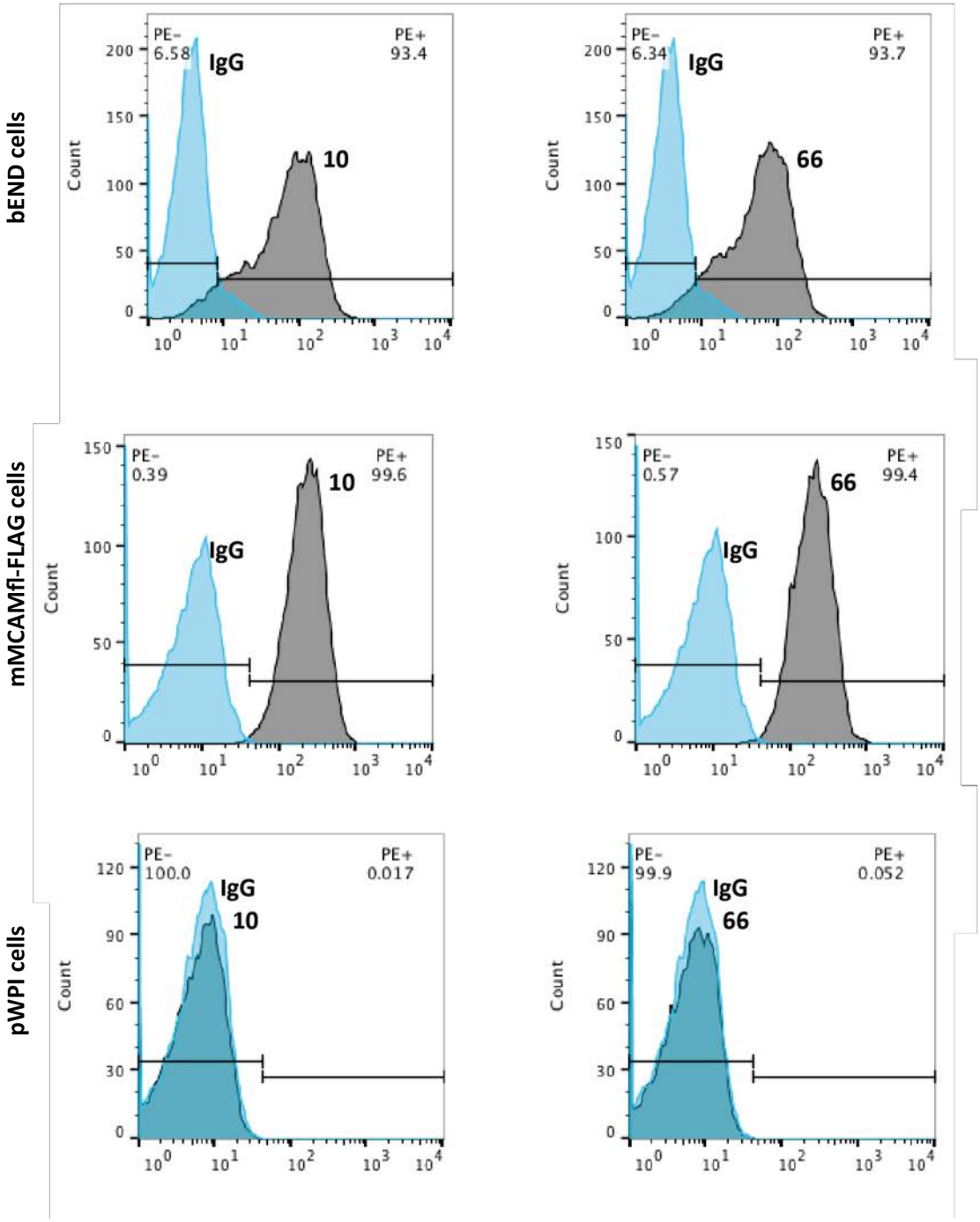

Figure 4.3 Analysis of monoclonal antibodies mMCAM10 and 66 by flow cytometry. bEND and HEK293T cells expressing mMCAMfl-FLAG or pWPI were used to test the antibodies reactivity in flow cytometry. The cells were detached from plates and incubated with hybridoma supernatants from clones mMCAM10 and 66 (10 and 66, in grey) or control rat IgG (IgG in blue). Transduced HEK293T cells were first gated for GFP expression. MCAM recognition was analysed by red fluorescence PE(+). Numbers in the flow cytometry histograms represent the percentage of cells stained for MCAM by the mMCAM10/66.

4.5 Immunoprecipitation of mouse MCAM protein using mMCAM10 and 66

To determine if the antibodies mMCAM10 and 66 can bind and extract native mMCAM protein from cell lysates, an immunoprecipitation experiment was performed. bEND cells were lysed using 1% NP-40 lysis buffer, and the lysates incubated with washed protein G beads and 1 µg/ml of rat IgG isotype control to prevent non-specific binding of proteins. Beads were removed by centrifugation and the lysates incubated overnight at 4 °C with purified monoclonal antibodies (mMCAM10, mMCAM66, MAB7718: commercial anti-mMCAM) or rat IgG control at a concentration of 2 µg/ml. Protein G beads were added to the lysates and incubated for 1 h at 4 °C. The beads were spun down, the supernatants collected, and beads washed 4 times. The lysate sampled before incubation with beads (bEND before beads), supernatants after incubation with beads (bEND lysates after beads) and protein G beads after IP (bEND lysate IP Protein G beads) were boiled in reducing protein loading buffer and run on an SDS-polyacrylamide gel. Purified monoclonal antibodies mMCAM10 and 66 were both able to immunoprecipitate mMCAM protein from the bEND cell lysates, although not in a great extent. Pull-down of the mMCAM protein was confirmed by Western blotting with polyclonal anti-mouse MCAM (AF6106, R&D) (Figure 4.4). Commercial monoclonal antibody MAB7718 (MAB) bound mMCAM to a lesser extent than antibodies mMCAM10 and 66, and there was no pull down with the control rat IgG. However, despite high concentrations of antibodies protein signal in the lysates after beads stayed similar to the signal in the lysates before incubation with beads.

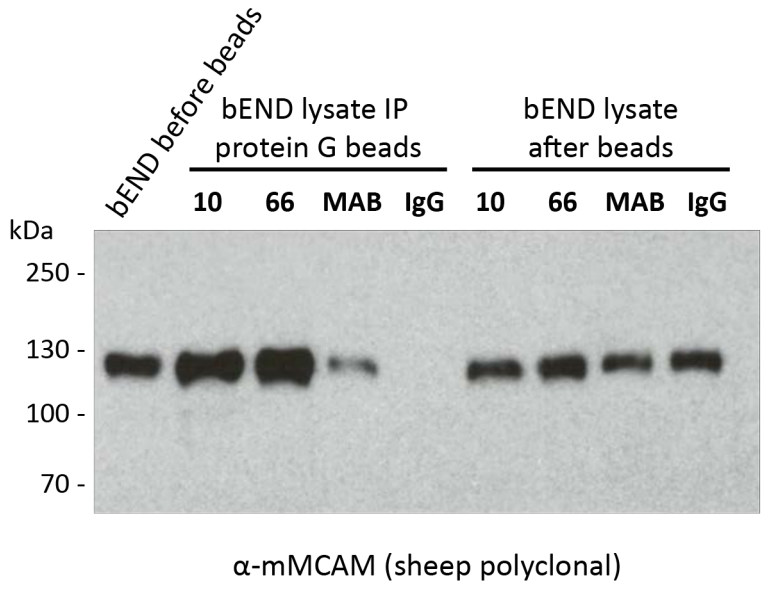

Figure 4.4 Immunoprecipitation of mouse MCAM with mMCAM10 and 66. Monoclonal antibodies mMCAM10, mMCAM66, MAB7718 (MAB) and rat IgG control (IgG) were used to immunoprecipitate mouse MCAM from bEND cell lysate (bEND before beads). Lysates were pre-cleared with rat IgG and protein G beads to remove unspecific binding. The lysates were then incubated with individual antibodies (2 µg/ml) over night and then for 1 h with Protein G beads. The beads (bEND lysate IP protein G beads) and the supernatants after the beads (bEND lysate after beads) were loaded on the gel and blotted with anti-mouse MCAM (α-mMCAM).

4.6 Analysis of mMCAM10 and 66 by immunofluorescence staining of PFA fixed cells

Immunofluorescence staining was used to determine if antibodies mMCAM10 and 66 stain paraformaldehyde (PFA) fixed cells on coverslips. bENDs and HEK293T cells transduced with mMCAMfl-FLAG or pWPI vector were seeded onto glass coverslips and cultured for 2 days. The cells were fixed on coverslips with 4% (w/v) PFA and incubated for 1 h at room temperature with undiluted supernatants of individual hybridoma clones mMCAM10 and mMCAM66, or with the rat IgG control (10 µg/ml). After washing with PBS, cells were incubated for 1 h in the dark with secondary anti-rat antibody conjugated to Alexa Fluor® 546 (1:200). The cells on coverslips were then washed and mounted onto DAPI-containing mounting media on glass slides and imaged. Immunofluorescence staining with supernatants from clones mMCAM10 and mMCAM66 showed MCAM expression on the cell surface and in the cytoplasm of both bENDs and HEK293T with mMCAMfl-FLAG (Figure 4.5 A and B). The same staining pattern was observed with the commercial anti-mMCAM antibody (MAB7718) (data not shown).

Antibodies did not stain pWPI transduced HEK293T cells (Figure 4.5 B), and no staining on any of the cells was observed with the rat IgG control.

A)

bEND cells expressing endogenous mMCAM

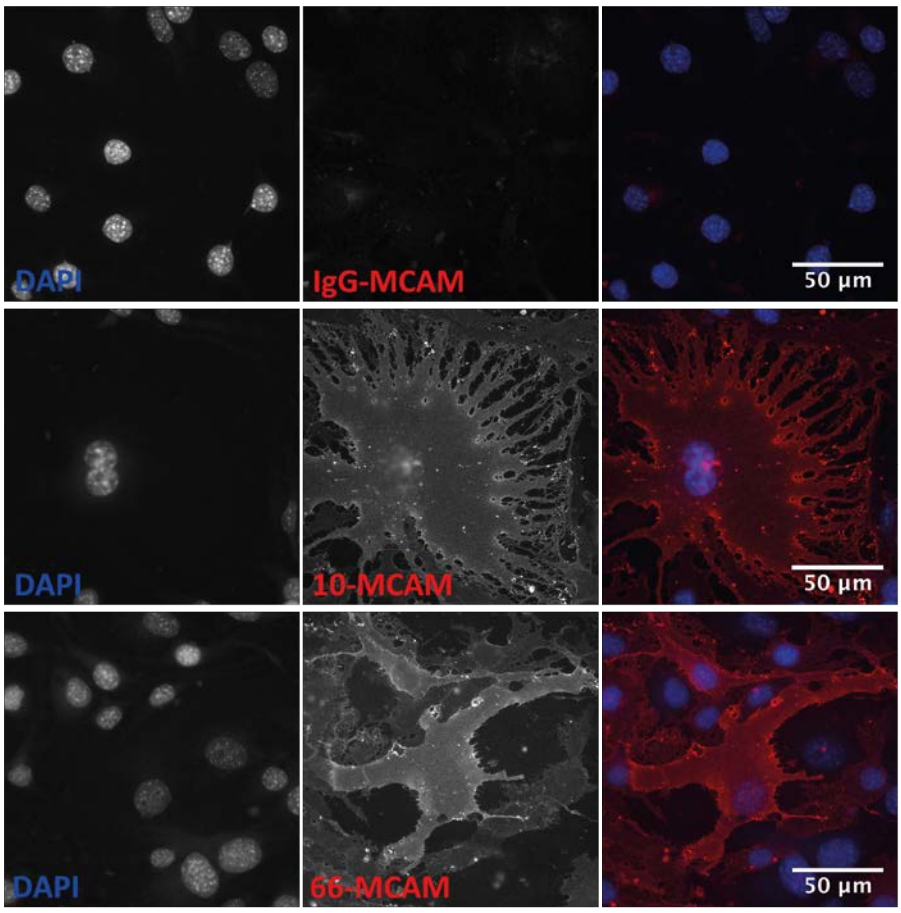

B)

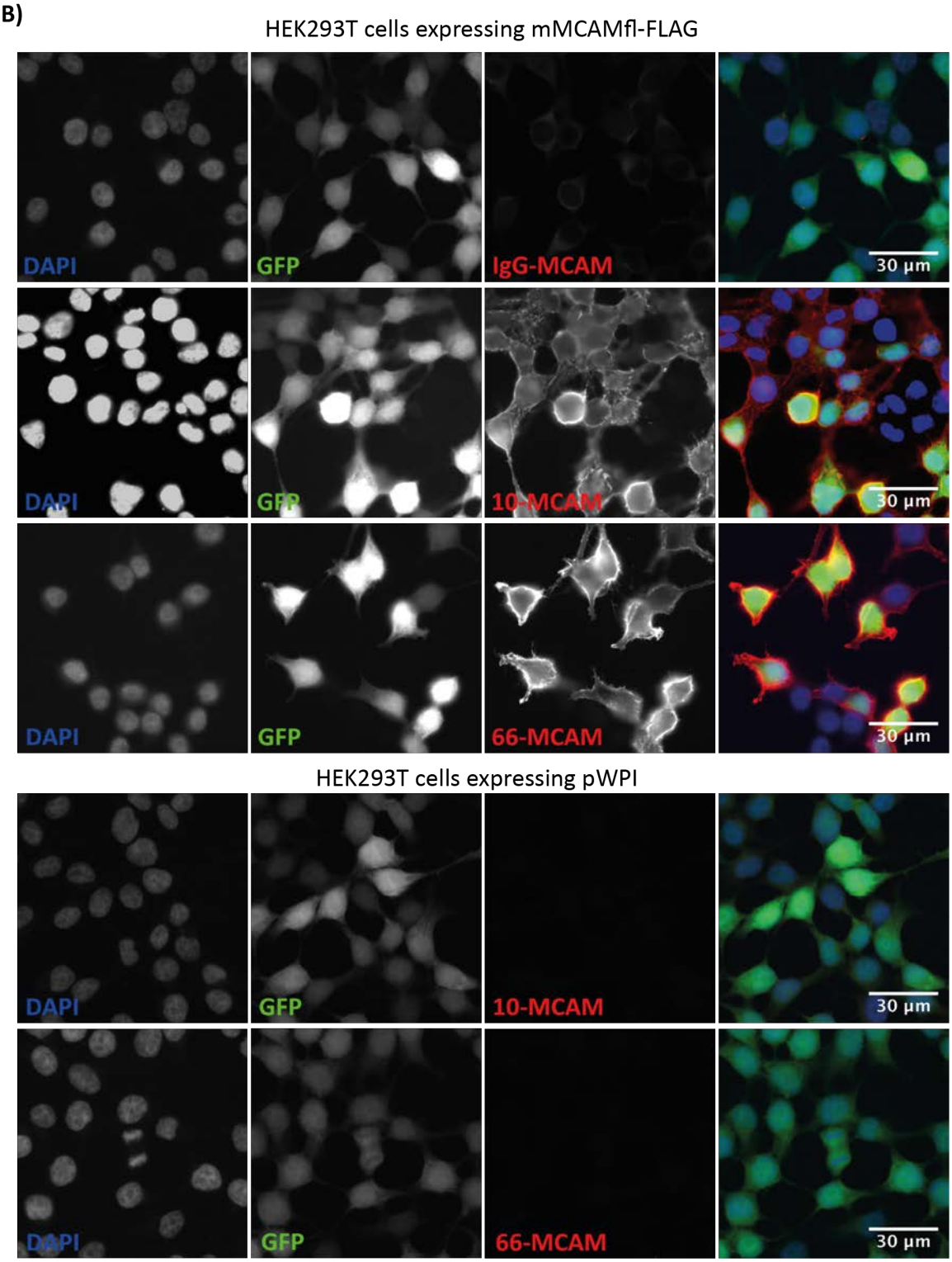

Figure 4.5 Immunofluorescence staining of PFA-fixed cells using mMCAM10 and 66. A) Mouse endothelial cell line bEND and **B)** mMCAMfl-FLAG or pWPI transduced HEK293T cells (expressing GFP) were fixed on coverslips using 4% PFA and stained with the monoclonal antibodies mMCAM10 (10-MCAM) and mMCAM66 (66-MCAM), or with the rat IgG negative control (IgG-MCAM). Nucleus was stained with DAPI (DAPI). The last image in a row is a merge between DAPI (blue), MCAM (red) and GFP (green) staining.

4.7 Analysis of mMCAM10 and 66 by immunofluorescence staining of frozen cell sections

To investigate if antibodies mMCAM10 and 66 stain frozen sections, agarose embedded frozen cell blocks were prepared. HEK293T cells transduced with mMCAMfl-FLAG and pWPI were embedded in low melting agarose blocks and snap frozen in OCT freezing media. Cell-blocks were processed and sectioned. Slides were thawed before the experiment and fixed in acetone at -20 °C. Slides were then incubated with undiluted supernatants of individual hybridoma clones mMCAM10 and 66, or rat IgG control (10 μg/ml) for 1h at room temperature. The slides were washed with PBS and incubated for 1 h in the dark with secondary anti-rat antibody conjugated to Alexa Fluor® 647 (1:200) and mounted in DAPI-containing medium for imaging.

Both monoclonal antibodies mMCAM10 and 66 were able to stain the frozen embedded HEK293T cells expressing mouse MCAM but did not stain the pWPI transduced HEK293T cells. The control rat IgG did not stain the cells (Figure 4.6). The staining pattern was seen in the cell membrane and lightly in the cytoplasm of cells, corresponding to the staining seen with the commercial MAB7718 (data not shown).

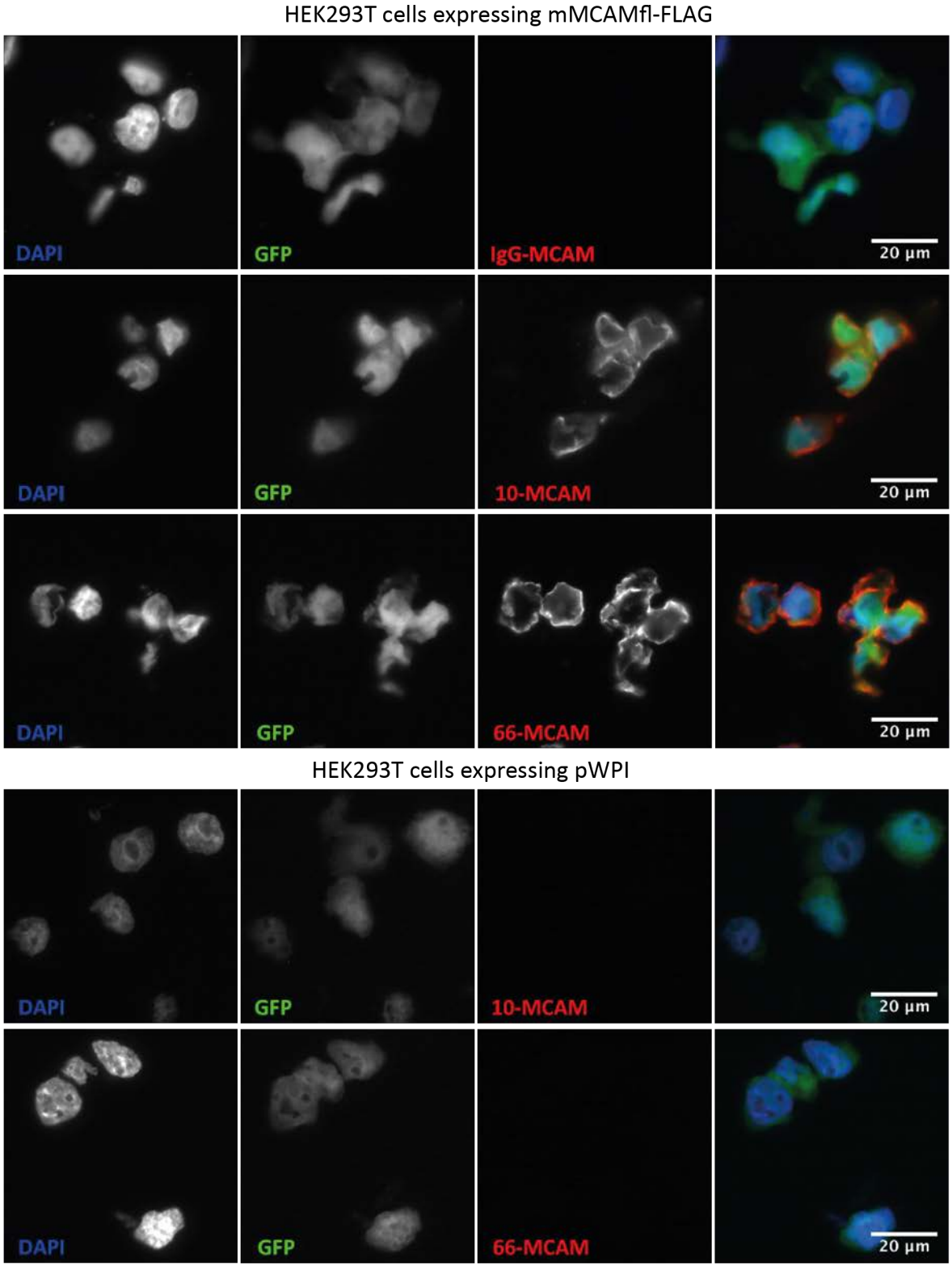

Figure 4.6 Frozen cells sections immunofluorescence staining with mMCAM10 and 66. mMCAMfl-FLAG or pWPI transduced HEK293T cells (expressing GFP) were embedded in low melting agarose, snap frozen and sectioned for immunostaining with undiluted hybridoma supernatants mMCAM10 (10-MCAM) and 66 (66-MCAM), or with the rat IgG control at 10 µg/ml (IgG-MCAM). The nucleus was stained with DAPI (DAPI). The fourth image in a row is a merge between DAPI (blue), GFP (green) and MCAM (red) staining.

4.8 Analysis of mMCAM10 and 66 by immunocytochemical staining of formalin fixed paraffin embedded cells

To examine whether the antibodies mMCAM10 and 66 can stain formalin fixed paraffin embedded tissue sections, paraffin embedded agarose cell blocks were used. HEK293T cells transduced with mMCAMfl-FLAG or pWPI were embedded in low melting agarose blocks and fixed with formalin. Fixed agarose cell blocks were then embedded in paraffin and sectioned. Slides were subjected to two types of antigen retrieval: (i) the pH 6 sodium citrate based and (ii) pH 9 Tris based antigen retrieval. Slides were then incubated with undiluted supernatants from mMCAM10 and 66, or rat IgG control at 10 μg/ml concentration for 1h at room temperature. The slides were washed with PBS and incubated for 1 h with secondary anti-rat antibody conjugated to HRP (1:100).

Monoclonal antibodies mMCAM10 and 66 both stained formalin fixed paraffin embedded HEK293T cells expressing mouse MCAM but did not stain pWPI transduced HEK293T cells (Figure 4.7). The negative control rat IgG did not stain the cells. Both antigen retrievals (citrate buffer pH 6 and with Tris buffer pH 9) were compatible for staining with antibodies mMCAM10 and 66; however, the pH 6 antigen retrieval gave a stronger signal.

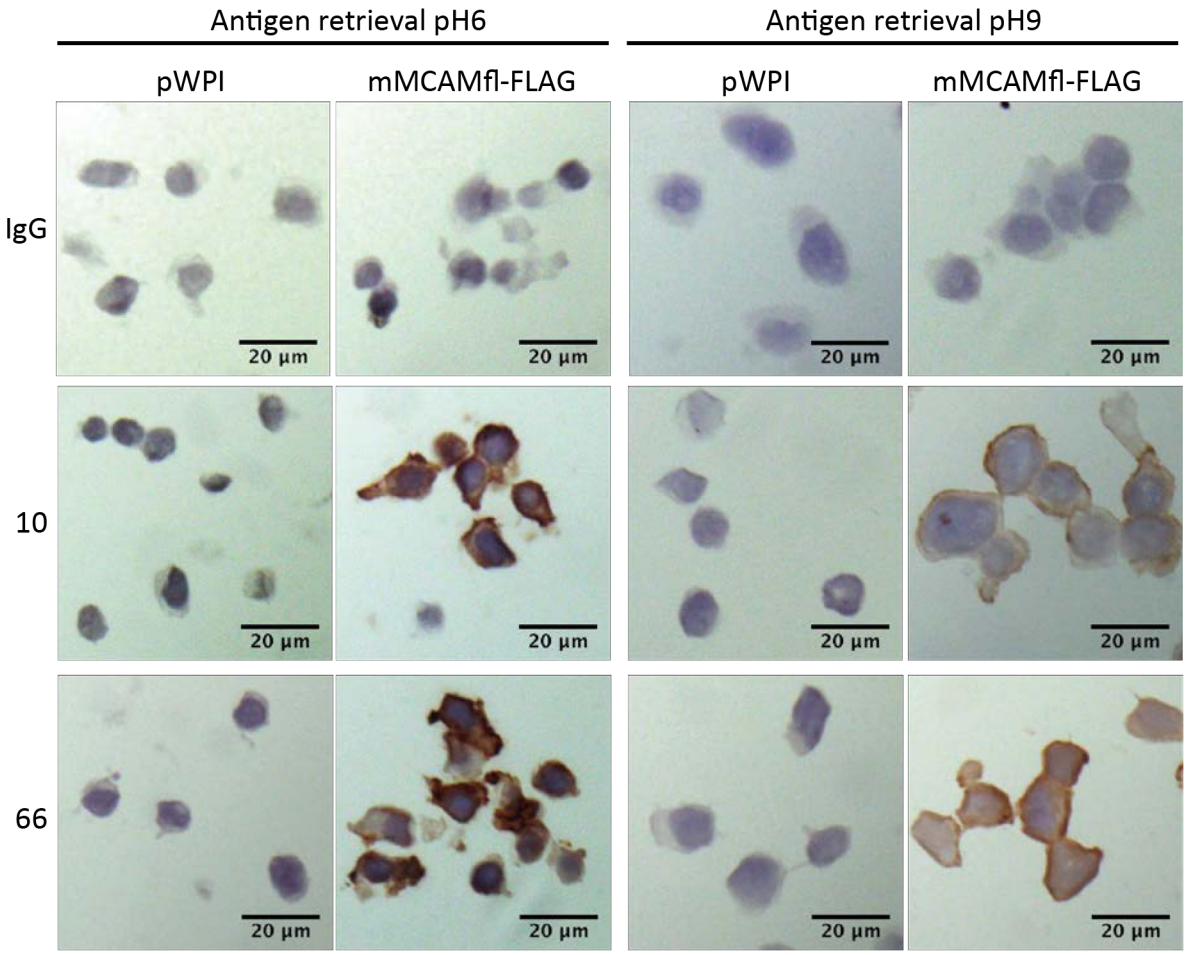

Figure 4.7 Immunocytochemical staining of formalin fixed paraffin embedded sections with mMCAM10 and 66. HEK293T cells expressing mMCAMfl-FLAG and pWPI were embedded in the low melting agarose blocks, fixed in formalin, embedded in paraffin and sectioned. Antigen retrieval was done in two different ways, using sodium citrate pH 6, and Tris based pH 9 with boiling in microwave for 15 min both. Immunocytochemistry staining was performed on slides with undiluted hybridoma supernatants mMCAM10 and 66, or with the rat IgG control (IgG) at 10 µg/ml.

4.9 Generation of deletion constructs of the mouse MCAM extracellular domain

The identification of the binding epitope is useful for monoclonal antibody targeted therapies. To determine which extracellular domain of antibodies mMCAM10 and 66 bind, deletion constructs of the extracellular domain of mMCAM were generated. The deletion PCR inserts were cloned into the pIg vector at EcoRI and NotI restriction sites using T4 DNA ligase (as described in materials and methods). DNA inserts were designed in such way that selected domains of the extracellular part of MCAM were deleted. The first deletion construct (D1) had domain C2'' deleted, the second construct (D2) had C2'' and C2' domains deleted and finally, the third construct (D3) had the C2'', C2' and C2 domains deleted. This is schematically shown in Figure 4.8 A. All constructs were designed to contain a signal peptide for secretion and a human Fc tag on the C-terminal end for detection and affinity purification.

HEK293T cells were transfected with the deletion constructs. Cell supernatants were collected 2 days later, and cells lysed. Supernatants and lysates were run on the gel under reducing and non-reducing conditions. Proteins were transferred to a PVDF membrane and blotted with anti-Fc antibody (Sigma). Cells all expressed proteins (as shown in the cell lysate Western blot), however the D2 construct was not secreted into the cell medium (Figure 4.8 B). This was possibly due to inefficient folding of the protein. For that reason, cell lysates were used to investigate binding of monoclonal antibodies mMCAM10 and 66 by Western blot.

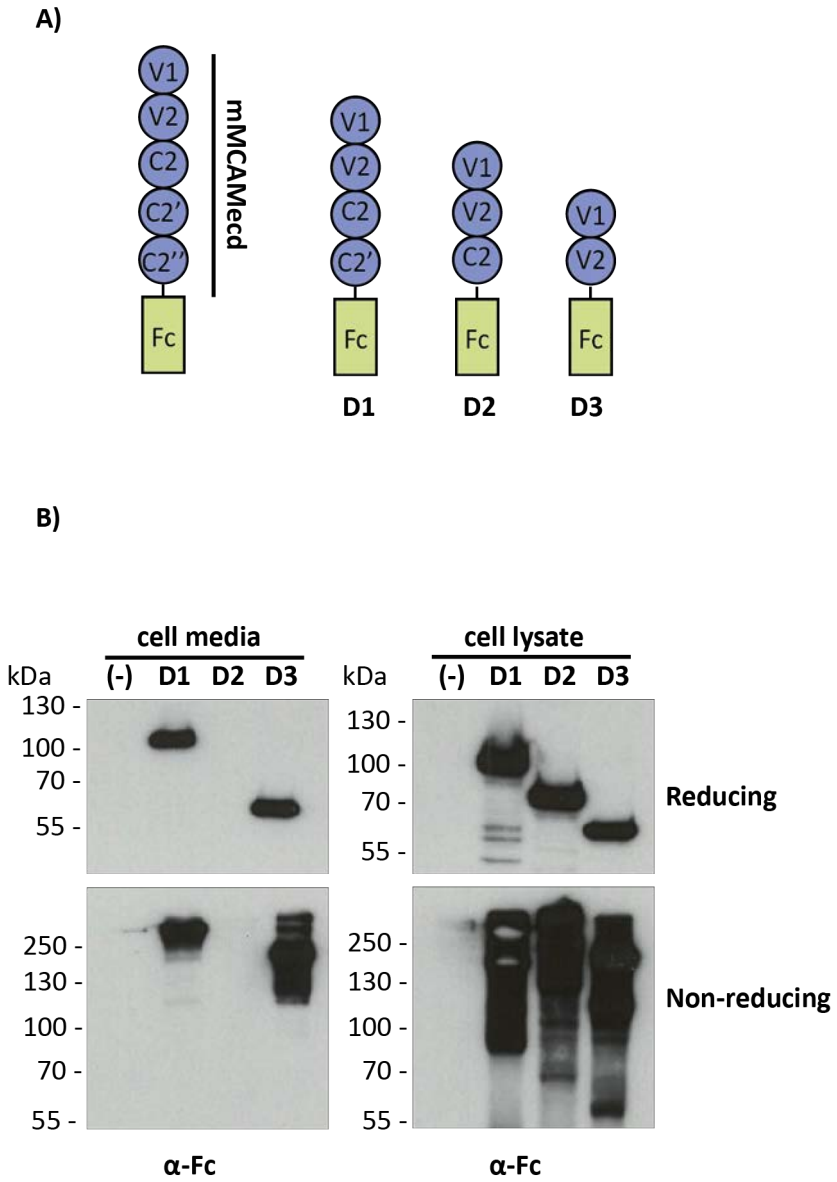

Figure 4.8 Design and expression of mouse MCAM extracellular domain deletion constructs. A) Schematic image of deletion constructs with native mouse MCAM on the left and mMCAMecd-Fc and deletion constructs D1, D2 and D3 on the right; the V1, V2, C2, C2' and C2'' are the domains of the mouse MCAM extracellular domain. **B)** Western blot of cell lysates and conditioned cell media of HEK293T cells producing the deletion constructs D1, D2 and D3; pIg-transfected HEK293T cell were used as a negative control (-). Proteins were loaded under reducing and non-reducing conditions to the gel and blotted with anti-human Fc antibody (α-Fc).

4.10 Epitope mapping of antibodies mMCAM10 and 66

HEK293T cells transfected with the deletion constructs were lysed and total protein loaded on an SDS-polyacrylamide gel under reducing and non-reducing conditions. Proteins were transferred to a PVDF membrane and blotted with anti-Fc antibody (Sigma), mMCAM10 and 66 hybridoma supernatants and commercial MAB7718 anti-mMCAM monoclonal antibody.

Both mMCAM10 and 66 recognised the full-length extracellular domain and the deletion construct D1 without the C2'' domain in the non-reducing conditions. However, they did not recognise the D2 and D3 (Figure 4.9).

Both antibodies mMCAM10 and 66 recognised all the constructs in the reducing conditions showing that the epitope is present in all these forms of the protein, and that the antibodies can recognise the linearized epitope. The commercial MAB7718 failed to recognise any of the deletion constructs in the reduced form. This is further addressed in the discussion (section 4.15).

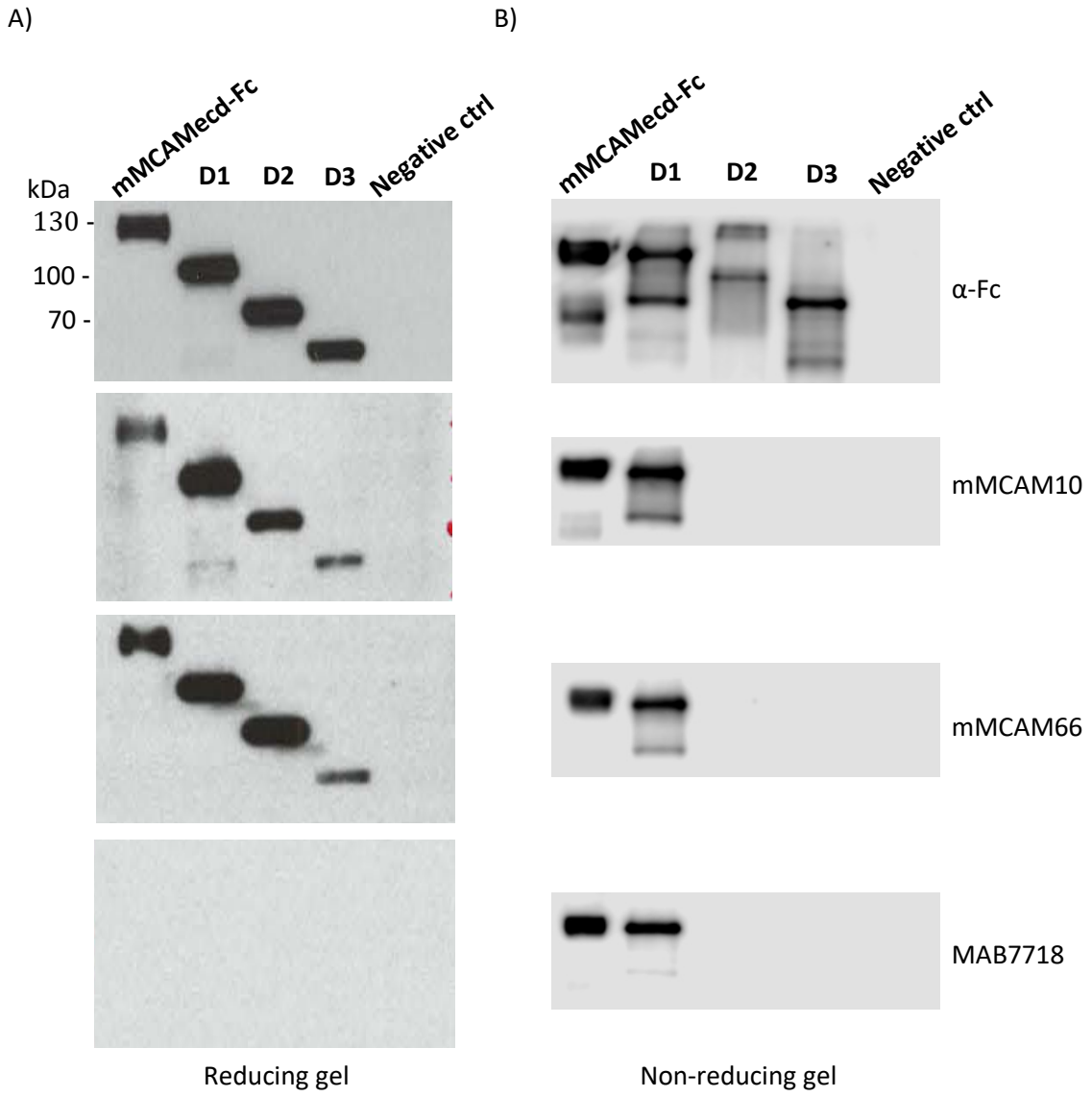

Figure 4.9 Epitope mapping of monoclonal antibodies mMCAM10 and 66 on deletion constructs of mMCAMecd. Cell lysates from deletion constructs D1, D2, D3, control pIg cells and recombinant mMCAMecd-Fc were loaded on the gel in **A)** reducing conditions and **B)** non-reducing conditions and the proteins blotted with anti-human Fc antibody (α-Fc), hybridoma supernatants mMCAM10 and 66 and with commercial anti-mouse MCAM monoclonal antibody MAB7718.

4.11 Competition binding of mMCAM10 and 66 studied by flow cytometry

A flow cytometry competition assay was used to examine if the binding epitopes of monoclonal antibodies mMCAM10 and 66 are overlapping or distinct. Monoclonal antibody mMCAM10 was conjugated with fluorescent label Alexa Fluor™ 488. bENDs were detached from plates, washed and spun down. Cells were first incubated with blocking antibody at 100 µg/ml (monoclonal antibodies mMCAM10 and 66, or control rat IgG) for 2 h at 4 °C to block the epitope on the extracellular domain of mouse MCAM. Following this, the cells were washed 2 times with flow cytometry buffer and incubated with Alexa Fluor™ 488-conjugated mMCAM10 antibody (10-488) at a concentration of 100 µg/ml for 1 h. Flow cytometry buffer was added, and cells were tested for green fluorescent labelling by flow cytometry.

The gates were set for single cells and FITC negative cells using unblocked and unlabelled bENDs. Cells incubated only with antibody 10-Alexa Fluor™ 488 were around 49.6% FITC+. The cells blocked with control rat IgG and then labelled with 10-488 were 47.6% positive for FITC staining. The cells blocked with antibody 10 and 66 had a reduced FITC labelling with 9.87% and 14.5% of cells positive, respectively Figure 4.10. This showed that the antibodies mMCAM10 and 66 both blocked binding of the labelled antibody 10-Alexa Fluor™ 488 in a similar manner. This cross-blocking revealed that the epitopes are either the same or in close proximity.

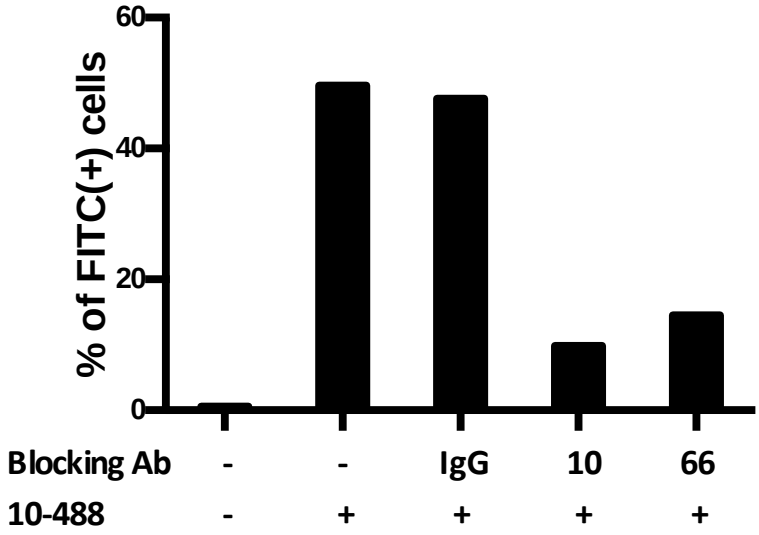

Figure 4.10 Epitope binding competition assay of mMCAM10 and 66. bENDs were blocked with either rat IgG control (IgG), mMCAM10 (10) or mMCAM66 (66) monoclonal antibody and then immunostained with Alexa Fluor™ 488-conjugated mMCAM10 antibody (10-488). The percentage of green cells (FITC+) was checked by flow cytometry. The cells were compared between each other and to negative control bEND cells that were not blocked or stained with any antibody, and to positive control cells stained only with the 488 conjugated mMCAM10.

4.12 Study of mMCAM10 and 66 in IHC staining of formalin fixed paraffin embedded mouse tissue

To investigate whether antibodies mMCAM10 and 66 can stain mouse MCAM expressed in the native form in the mouse tissue, paraffin embedded sections of mouse RENCA tumour were examined. RENCA cells do not express MCAM (as shown in Figure 4.2), however, MCAM is expressed on the blood vessels of mouse RENCA tumour model. The sections were prepared as described in section 4.8. Sections were then subjected to antigen retrieval with sodium citrate pH 6, as this worked better on immunocytochemistry (section 4.8). The slides were blocked and probed with purified monoclonal antibodies mMCAM10, 66 and negative control rat IgG at a concentration of 15 µg/ml and incubated for 1 h at room temperature. The slides were washed with PBS and probed with HRP conjugated anti-rat antibody (1:100) for 45 min at room temperature. The reaction was developed for 5 min and slides stained with haematoxylin.

Staining of blood vessels in RENCA sections was seen only with the monoclonal antibody mMCAM10 and not with 66, or control IgG. Three representative images for each antibody are shown in Figure 4.10.

The antibody mMCAM10 was then tested for staining of blood vessels of healthy mouse organs: brain, heart, kidney, liver and lung. No staining of blood vessels was obtained, showing that antibody mMCAM10 recognises the tumour blood vessels but not the vasculature in healthy tissues (Figure 4.11).

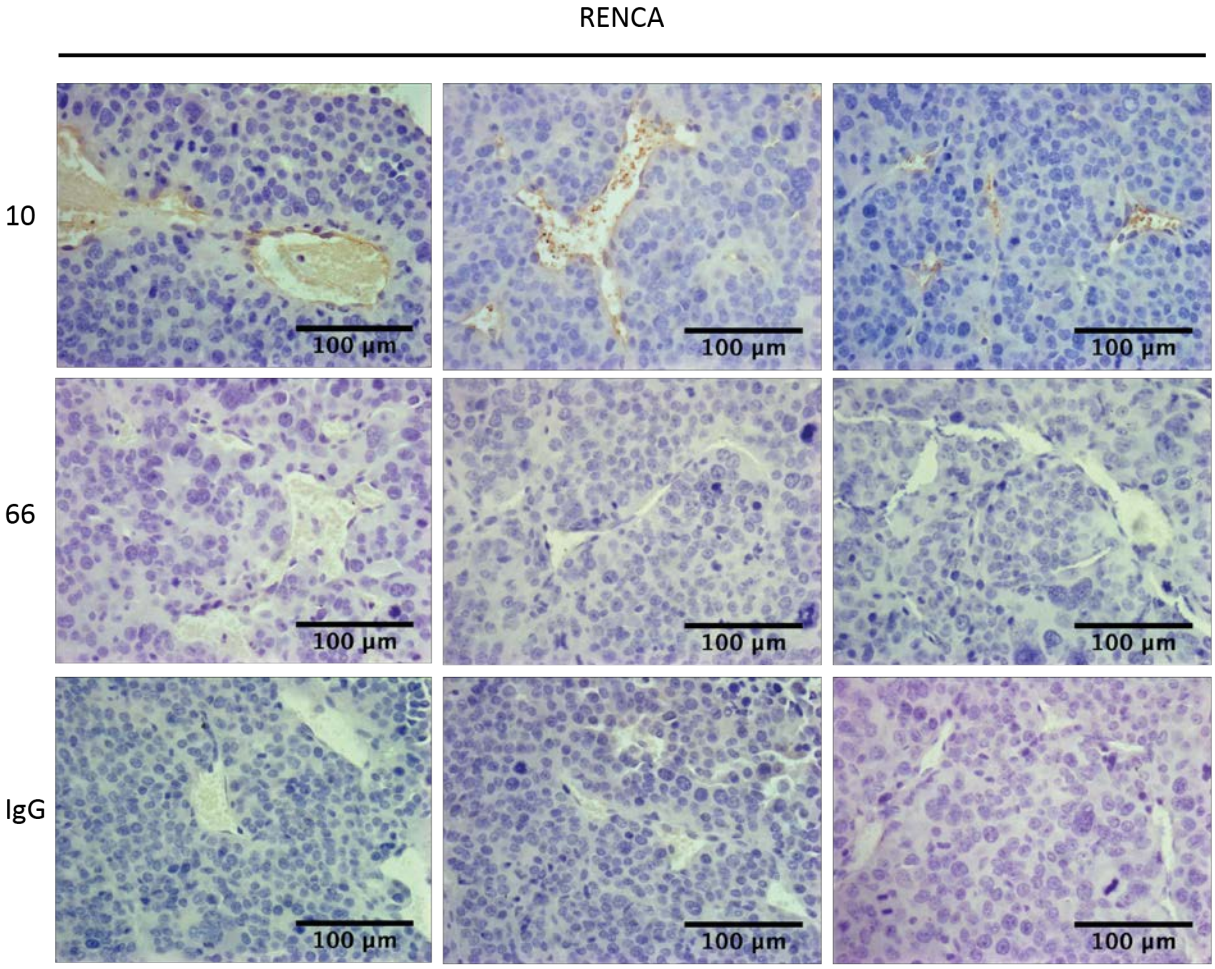

Figure 4.10 Immunohistochemical staining of formalin fixed and paraffin embedded RENCA tumour sections with monoclonal antibodies mMCAM10 (10), mMCAM66 (66) and control rat IgG (IgG). RENCA tumours were taken from tumour bearing mice, fixed in formalin and embedded in paraffin. Sections were stained with 10 µg/ml of each antibody.

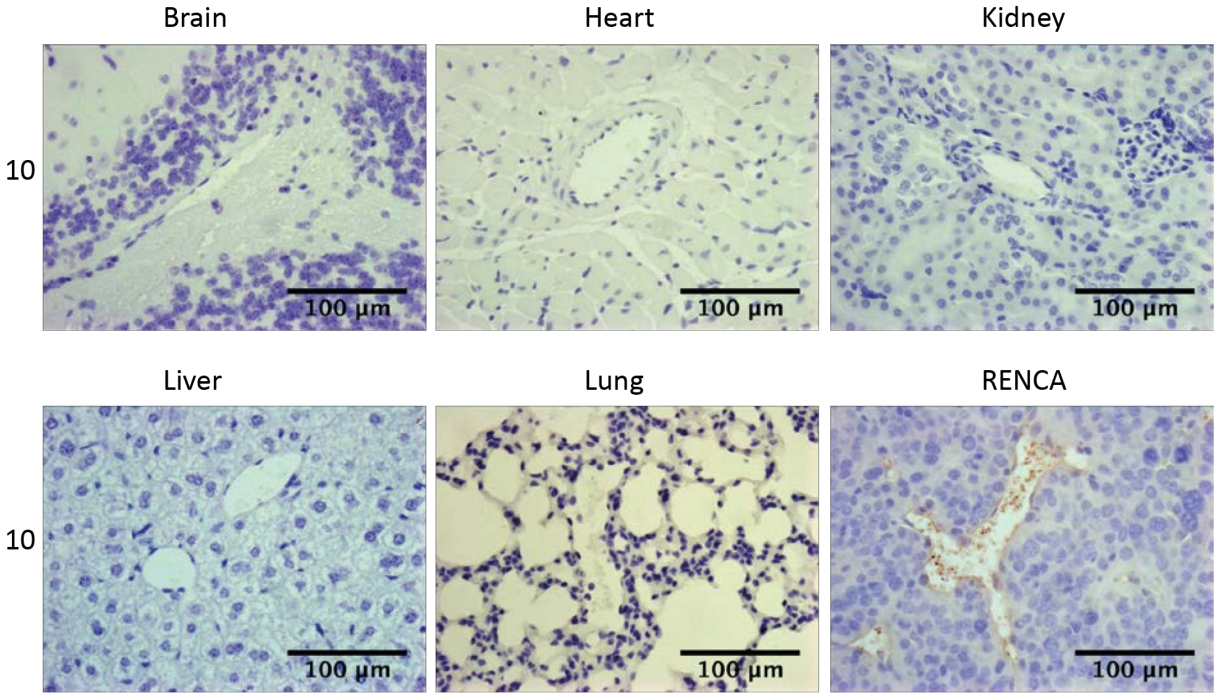

Figure 4.11 Immunohistochemical staining of paraffin embedded mouse healthy organs and RENCA sections with monoclonal antibody mMCAM10. Brain, heart, kidney, liver, lung and RENCA tumour were taken from tumour bearing mice, fixed in formalin and embedded in paraffin. Sections were probed with 10 µg/ml of antibody.

4.13 *In vivo* localisation of mMCAM10 in tissue of tumour bearing mice

Knowledge of distribution of monoclonal antibodies mMCAM10 and 66 after delivery to mice would provide information crucial for the future development of targeted therapies using these antibodies. In order to investigate whether these antibodies specifically localise to the tumour blood vessels a RENCA mouse tumour model was used.

Cultured RENCA cells were harvested and implanted subcutaneously in mice. Tumours were monitored until they reached 1 cm^3. The purified monoclonal antibodies mMCAM10 and 66 were dialysed against PBS and filter sterilised. 20 µg of each antibody was injected into the tail vein. Mice were monitored for 1 h and then culled. The organs were taken, snap-frozen in OCT freezing medium, and sectioned.

The frozen sections were thawed at room temperature and fixed in acetone at -20 °C. Slides were blocked with 100 µl of 2.5% (v/v) horse serum and incubated with the AlexaFluor® 488 conjugated anti-rat IgG (1:200) secondary antibody for 1 h at room temperature in the dark. The antibody localisation into the different organs and the tumour vessels was analysed by green fluorescence staining of the tissues. Antibody mMCAM66 failed to localise in any tissue. mMCAM10 localised in tumour vasculature, but not in vessels of healthy tissue (Figure 4.12).

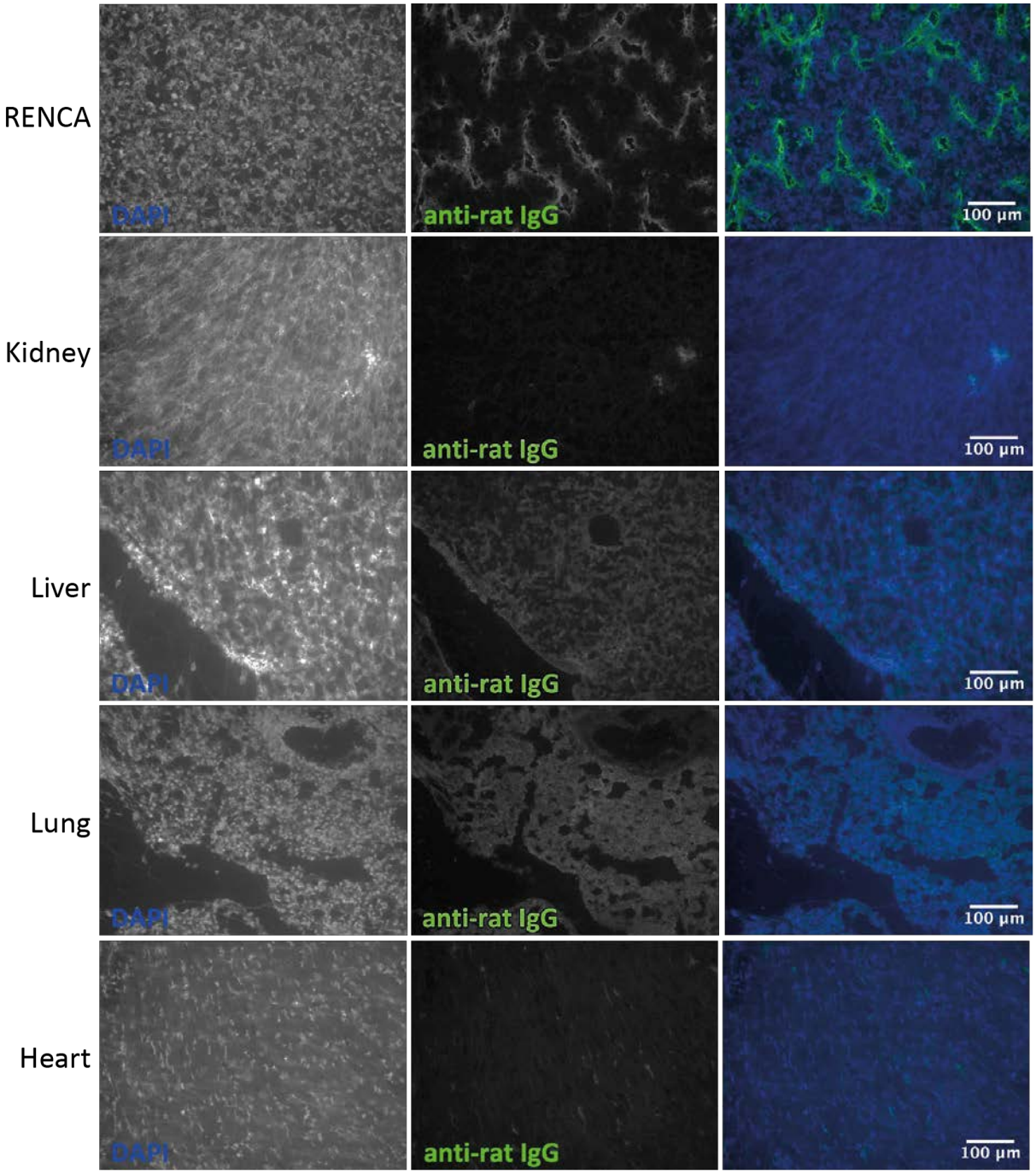

Figure 4.12 Localisation of the antibody mMCAM10 to the tumour blood vessels in mice. Tumour bearing mice were injected with 20 µg of monoclonal antibody intravenously. The mice were culled 1 h later and the organs and tumour snap frozen in OCT medium. The tissue sections were probed with secondary anti-rat antibody conjugated to Alexa Fluor® 488 to determine the localisation of injected antibody in the tissue (anti-rat IgG) and mounted in DAPI mounting media for nuclei staining (DAPI). Third image in a row is a merge of DAPI (blue) and anti-rat IgG staining (green).

4.14 Sequencing of the variable regions of mMCAM10 and 66

To characterise the variable regions of the antibodies mMCAM10 and 66, cloning and sequencing was carried out. Sequences of variable regions can be used in protein engineering, such as switching of a constant region to different isotype or a different species immunoglobulin backbone, or engineering CAR-T cell receptors.

Sequencing variable regions of heavy and light chains of the mMCAM10 and 66 requires the knowledge of the isotype in order to design correct primers for the RACE PCR reaction (Figure 4.13). The Ig Isotyping Rat Uncoated ELISA Kit (Invitrogen) was used to define the isotype of antibodies mMCAM10 and 66. ELISA plate provided in the kit was coated with capture antibodies specific for individual rat heavy and light chains (IgG1, IgG2a, IgG2b and IgG2c heavy chains; and kappa and lambda light chains). The plate was treated with blocking buffer and probed with hybridoma supernatants from clone mMCAM10 and 66. The ELISA showed that both antibodies have an IgG1 heavy chain and kappa light chain (Figure 4.14).

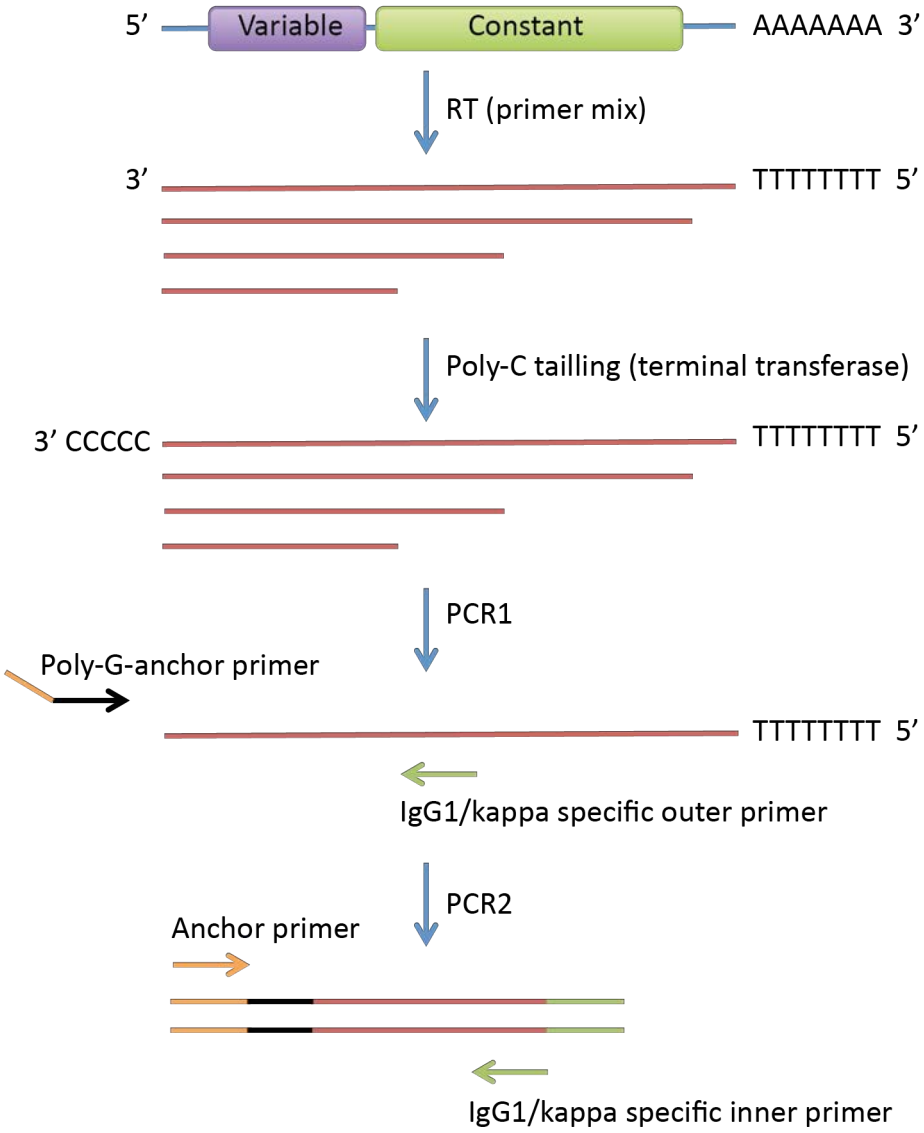

Figure 4.13 A schematic image of the RACE PCR reaction used to amplify the heavy and light chain variable regions of antibodies. The procedure consists of mRNA extraction from the hybridoma cells, reverse transcription and generation of cDNA (RT), addition of the poly-C tail to the cDNA (Poly-C tailing) and 2 PCR reactions (PCR1 and PCR2) using specific primers for the poly-C end (Poly-G-anchor and Anchor primer) and for the constant regions of the heavy and light chains (IgG1/kappa specific outer primer and IgG1/kappa specific inner primer).

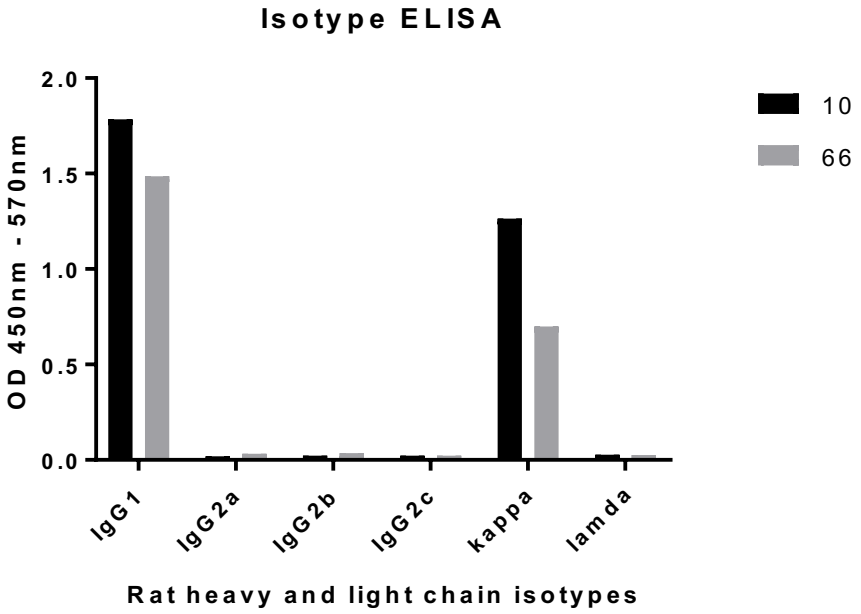

Figure 4.14 Monoclonal antibody isotype determination by ELISA. The ELISA plate was coated with antibodies to different IgG heavy chains (IgG1, IgG2a, IgG2b, IgG2c) and light chains (kappa, lambda) of rat antibodies. This was probed with supernatants of hybridoma mMCAM10 and 66. The absorbance was recorded at 450 nm and 570 nm (450 nm – 570 nm) (570 nm is background absorbance).

To determine variable region sequences, hybridoma cells were lysed and mRNA extracted. The cDNA was then transcribed from the mRNA. Poly-C tail was added to the cDNA 3' end using terminal transferase, and the buffer exchanged to nuclease free H_2O. The DNA was then used in the first PCR using a primer for the poly-C tail (Poly-G-anchor) and IgG1/kappa constant region specific outer primer. The PCR product from this reaction was then used as a template for the second PCR reaction using Anchor primer and IgG1/kappa constant region specific inner primer (as shown in the schematic image Figure 4.13).

The final PCR product was then cloned into the TOPO vector and transformed into bacterial cells. The plasmids from single colonies were screened for the presence of the PCR insert using colony PCR (with Anchor primer and IgG1/kappa specific inner primer) and restriction digest.

The sequence of the heavy and light chain of antibody mMCAM10 was confirmed as a variable region of a rat monoclonal antibody using the online program IMGT/V-QUEST [143] (Table 4.1 and Table 4.2). However, sequencing of antibody 66 variable region failed at the step of TOPO cloning. No colonies were screened as positive for the PCR of the insert in the TOPO vector, or restriction digest.

The program identified these regions as CDR regions of the antibody:

V-D-J-REGION amino acid sequence of the heavy chain of monoclonal antibody mMCAM10:

EVQLVESGG.GLVQPGRSLKLSCTASGFTF.....SYYSFYWIRQAPTKGLEWVASISPS..GDTTYYRDSVK.GRFTISRDN
AKSTLYLQMDSLRSEDTATY.YCTTDRNYSAYFDSWGQGVVVTVSS
CDR1: GFTFSYYS
CDR2: ISPSGDTT
CDR3: TTDRNYSAYFDS

V-J-REGION amino acid sequence of the light chain of monoclonal antibody mMCAM10:

DVMMTQTPVSLSVSLGGQVSISCRSSQTFVHS.DGNTYLNWYLQKPGQSPQLLICKV.....FNRLSGVP.DRFSGSG.
.SGTDFTLKISRVENDDLGVYYCGQAAKIPPTFGGGTKLELK
CDR1: QTFVHSDGNTY

CDR2: KVF
CDR3: GQAAKIPPT

Table 4.1 Comparison of the mMCAM10 heavy chain variable sequence to the online rat immunoglobulin database.

Result summary:	Productive IGH rearranged sequence: (no stop codon and in-frame junction)		
V-GENE and allele	Ratnor IGHV5-19*01 F	score = 1309	identity = 95.14% (274/288 nt)
J-GENE and allele	Ratnor IGHJ2*01 F	score = 205	identity = 90.00% (45/50 nt)
D-GENE and allele by IMGT/JunctionAnalysis	Ratnor IGHD1-1*01 F	D-REGION is in reading frame 3	
FR-IMGT lengths, CDR-IMGT lengths and AA JUNCTION	[25.17.38.11]	[8.8.12]	CTTDRNYSAYFDSW

Table 4.2 Comparison of the mMCAM10 light chain variable sequence to the online rat immunoglobulin database.

Result summary:	Productive IGK rearranged sequence: (no stop codon and in-frame junction)		
V-GENE and allele	Ratnor IGKV1S27*01 F	score = 1402	identity = 97.62% (287/294 nt)
J-GENE and allele	Ratnor IGKJ1*01 F	score = 175	identity = 100.00% (35/35 nt)
FR-IMGT lengths, CDR-IMGT lengths and AA JUNCTION	[26.17.36.10]	[11.3.9]	CGQAAKIPPTF

4.15 Discussion

This chapter describes the generation of two stable hybridoma cell clones, mMCAM10 and mMCAM66, and their biochemically characterisation. Screening of positive hybridoma clones was performed by ELISA on recombinant full length mMCAM extracellular domain in order to identify antibodies to the native protein. mMCAM10 and 66, could detect mMCAM on cells via flow cytometry and by staining PFA fixed cells on coverslips. These techniques are useful in cell biology when monitoring expression of protein in various conditions, such as protein knock down, or detecting expression changes in response to treatment. Thus, siRNA silencing of mouse MCAM gene would be a useful indicator of sensitivity of these antibodies and is yet to be done. Furthermore, both antibodies immunprecipitated native mMCAM protein. Using this technique can further investigate MCAM binding partners by protein pull down and performing mass spectrometry analysis. The mMCAM10 and 66 detected mMCAM by immunocytochemistry and immunofluorescence staining of agarose embedded cells overexpressing mMCAM. It would be useful to establish the lowest antibody concentration that can be used in this technique in order to titrate down the use of the antibodies.

MCAM extracellular domain deletion constructs D1, D2 and D3 were used in order to investigate the binding domain of mMCAM10 and 66. Western blot analysis showed the recognition of a linear epitope present in reduced conditions in all three deletion constructs. However, the D2 and D3 deletion constructs were not recognised in the non-reduced form, possibly due to conformational changes. It is possible that the important domain for stabilization of the epitope is missing from these two constructs and the protein is folding in such a way that the epitope is hidden. Thus, the results show that the possible binding site of antibodies mMCAM10 and 66 is within domains V1 or V2, that the epitope is linear and

recognisable in both non-reducing and reducing conditions. Commercial rat monoclonal antibody to mouse MCAM recognised only the non-reduced form of deletion construct D1, but not D2 or D3, and did not recognise any of the recombinant mMCAM on the reducing gel.

Competition flow cytometry assay showed that the two antibodies compete for the same or a similar epitope. Given the results observed in mice we assumed that the antibodies do not recognise the rat MCAM and so, the possible binding site of the antibodies could be the amino acids that are different between the rat and mouse sequence in the V1 or V2 domain (The sequence difference can be seen in Figure 3.8). Inserting point mutations would help determine the exact place to which the antibodies are binding. Furthermore, in this study the competition assay was performed in one way, by blocking with antibody mMCAM66 and then detecting with antibody mMCAM10, and so the other way around would possibly better show the binding differences between these two antibodies.

Monoclonal antibody ME-9F1 was previously shown to recognize mouse MCAM that seemed to be present on all vessels in mouse tissue [144]. In contrast, the mMCAM10 antibody detects only RENCA tumour vessels, but not vessels in healthy tissues when studied by immunohistochemistry. Similarly, antibodies towards human MCAM show a different spectrum of tissue recognition depending on the antibody. Several papers showed that the carbohydrates, which constitute 35% of the MCAM molecular weight, vary between different cell types and tissues [60,93]. Furthermore, MCAM forms dimers and binds different proteins in different environments. Thus, epitopes exposed on MCAM in one tissue may be hidden in another.

In order to use a specific antibody for therapeutic purposes it is essential to determine its distribution in mice after administration. Antibody mMCAM10 showed preferential

localisation to the tumour vasculature of RENCA tumours within 1 h post injection, while only faint or no staining was observed in the examined healthy tissue. In contrast ME-9F1 localises to the healthy tissue when injected intravenously [144]. Furthermore, MCAM on healthy tissue had to be pre-blocked by un-labelled antibody in order for the radionuclide labelled ME-9F1 antibody to localise to tumour blood vessels only.

This study is a starting point for further investigation of mMCAM10 as a therapeutic agent. In order to be able to use this antibody in mice with a fully functional immune system, which is important to generate similar conditions to clinical tumours, the variable regions need to be cloned into the mouse immunoglobulin backbone. Several plasmids are available commercially and used routinely for this purpose. Furthermore, these sequences can be used to generate other types of immunotherapies such as modified CAR-T cells, engineered antibodies with bound cytotoxic drug or modified Fc portion. All of these are rapidly entering clinical trials and will form part of the future of antibody-based immunotherapies.

In conclusion, work performed in this study resulted in characterisation of novel monoclonal antibodies against mouse MCAM and will enable the future use of these tools in research and assessment of MCAM potential as a target on tumour vasculature.

5 EFFECTS OF THE HUMAN MCAM EXTRACELLULAR DOMAIN ON ANGIOGENESIS

5.1 Introduction

MCAM is expressed on blood vessels of 90 % of RCC and its expression correlates with cancer stage [56]. The importance of MCAM expression on tumour vasculature is however, poorly understood. RCC is a highly vascular tumour where angiogenesis aids progression and metastatic spread, and because of this targeting tumour angiogenesis has been a paradigm treatment approach for this cancer in the recent years [145]. However, targeting VEGF pathway either by using receptor tyrosine kinase inhibitors or Bevacizumab still has not achieved complete response in metastatic disease [146]. Soluble extracellular domains of cell surface proteins can act as scavengers or antagonists of pro-angiogenic factors and in this way block angiogenesis such as in the case of the soluble VEGFR-2 (flk-1) receptor trap [147]. MCAM has a number of ligands which induce angiogenesis and associated signalling, including Netrin-1, VEGF and LAMA4 [111,113]. Thus, studying the effects of extracellular domain of human MCAM protein in angiogenesis assays could provide more information on the role of MCAM as well as create a base for new treatment opportunities for advanced and metastatic RCC.

In order to investigate soluble MCAM in angiogenesis assays, the soluble extracellular domain of human MCAM was produced and purified with a human Fc fusion tag. The recombinant soluble protein was investigated in *in vitro* angiogenesis assays using HUVECs. Soluble MCAM showed blocking activity in three different endothelial cell network formation assays, cell migration and cell transmigration through a semipermeable membrane. The effects of the soluble recombinant MCAM were also examined in cell proliferation and cell cycle.

5.2 Production and purification of hMCAMecd-Fc recombinant protein

To investigate whether the extracellular domain of MCAM has an effect on HUVECs in angiogenesis associated behaviour, such as migration, proliferation and tube formation, human MCAM extracellular domain was cloned with human Fc tag at the C-terminal end (Figure 5.1 A). Vector construction was performed as described in materials and methods: A PCR insert (hMCAMecd) was cloned into the pcDNA-Fc (pIg) vector using EcoRI and NotI restriction enzymes and T4 DNA ligase (hMCAMecd-Fc).

HEK293T cells were transfected with hMCAMecd-Fc or with the empty pIg vector and cultured to confluence in complete DMEM, and then placed in Opti-MEM. The protein was successfully expressed by cells and secreted into the cell culture medium, as confirmed by Western blotting using anti-human Fc (Sigma) and anti-hMCAM antibodies (Sigma) (Figure 5.1 B).

The protein was next pulled-down from the conditioned Opti-MEM (collected 48h after addition to transfected cells) with protein A beads. The beads were run on an SDS-polyacrylamide gel and protein stained with Coomassie blue. The hMCAMecd-Fc protein efficiently bound to the beads and was not degraded (Figure 5.1 C).

Purification on a large scale was carried out from one litre of conditioned Opti-MEM obtained from ten 15 cm cell culture dishes. Opti-MEM was collected every third day over two weeks and then run through a Protein A column. The eluted protein was run on an SDS-polyacrylamide gel and stained with Coomassie blue (Figure 5.1 D). The protein yield was >15 mg/litre of media. The elution fractions were pooled and dialysed to exchange the elution buffer with PBS.

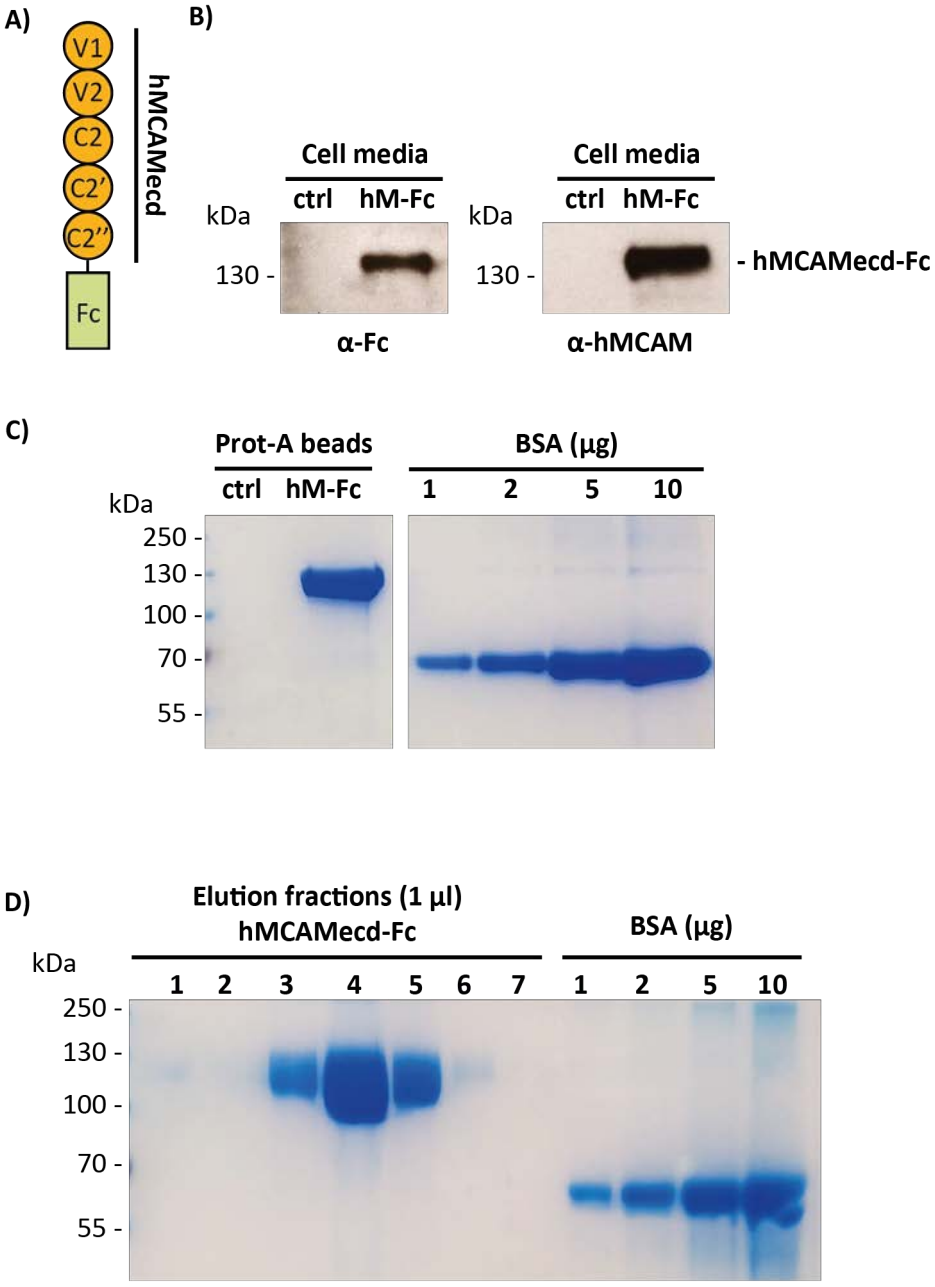

Figure 5.1 Production and purification of hMCAMecd-Fc recombinant protein. A) Schematic image of the extracellular domain of hMCAM fused to the human Fc tag; **B)** Western blot of supernatants from the HEK293T cells transfected with empty pIg vector (ctrl) and hMCAMecd-Fc (hM-Fc) blotted with anti-human Fc antibody (α-Fc) and anti-hMCAM antibody (α-hMCAM); **C)** Coomassie blue staining of small scale protein pull down with Protein A beads from the hMCAMecd-Fc and pIg transfected HEK293T cell media (1 ml), 20 µl of beads were loaded on the gel, BSA standard in µg; **D)** Coomassie blue staining of large scale purification of hMCAMecd-Fc on a Protein A column, 1 µl of elution fractions with the highest amount of protein was loaded on the gel, BSA standard in µg.

5.3 Effects of hMCAMecd-Fc on endothelial cell tube formation in the fibroblast co-culture 3D assay

Tube or network formation assays are one of the preferred assays to investigate effects of materials on angiogenesis. There exist different models of network formation assays in which cells are tested in a monoculture or co-culture with other cells involved in angiogenesis. Cells are usually seeded in different extracellular matrices either on top (2D) or inside the matrix (3D) [148]. To examine if the recombinant hMCAMecd-Fc has an effect on network formation of endothelial cells, the 3D fibrin matrix co-culture with human dermal fibroblasts (HDFs) was carried out. This experiment was initially carried out by Aleksandra Korzystka using commercially obtained HUVECs (mixed cells from different donors) at a range of MCAM concentrations; and later confirmed by the author using HUVECs prepared form individual cords by our group at a concentration of MCAM at 200 µg/ml (1.54 µM). The experiment was repeated three times with three technical replicates for each condition and analysed using ImageJ angiogenesis plugin software.

HUVECs were lentiviraly transduced with GFP prior to the assay in order to distinguish them from HDFs. HUVECs and HDFs were mixed in a ratio of 2:1 in the fibrin matrix. Cells were cultured for 10 days in complete EBM-2 medium containing the recombinant hMCAMecd-Fc or control Fc protein at different concentrations. Cells were monitored every day and medium changed every second day.

The recombinant hMCAMecd-Fc protein at a concentration of 200 µg/ml (1.54 µM) had a significant effect on the cell tube formation as shown by decreasing total network length, number of meshes, nodes, and junctions when compared to the human Fc control (Figure 5.2, Figure 5.3).

Fc

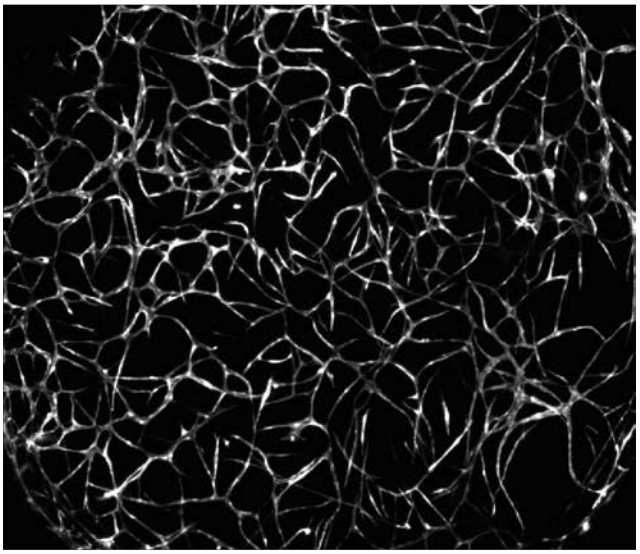

hMCAMecd-Fc

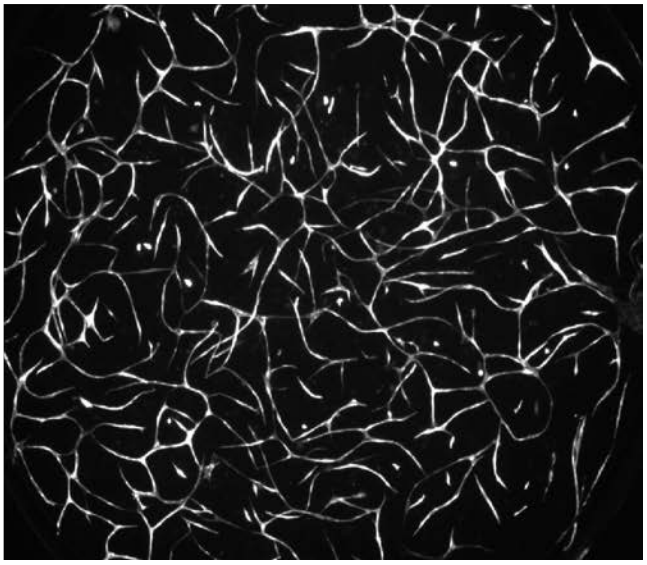

Figure 5.2 Representative images of 3D co-culture tube formation assay. HUVECs (fluorescently labelled) and human dermal fibroblast cells were embedded in fibrin matrix and cultured in medium containing either control Fc protein or hMCAMecd-Fc at a concentration of 200 μg/ml. Images were taken at day 10.

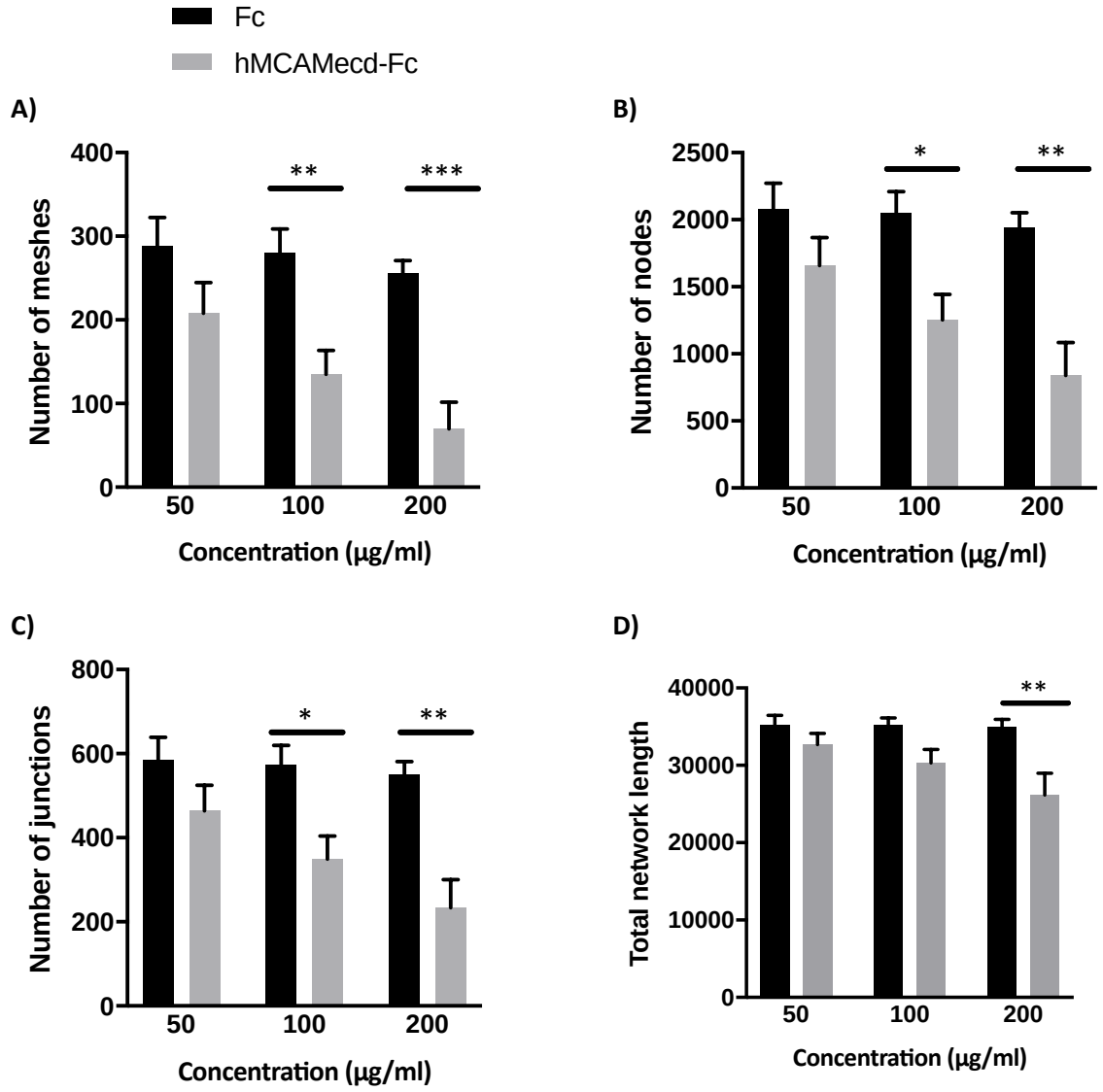

Figure 5.3 hMCAMecd-Fc inhibits HUVECs tube formation in 3D fibrin matrix co-culture. HUVECs and HDFs were assayed in 3D fibrin matrix co-culture tube formation assay; cells were seeded in the matrix and cultured for 10 days in medium containing either control Fc protein or hMCAMecd-Fc at the concentrations of 50, 100 and 200 µg/ml, after which cells were fixed and several aspects of tube formation analysed by ImageJ angiogenesis plugin (**A, B, C, D).** Three separate experiments with triplicates were taken into analysis. Error bars represent SEM. (Statistical test used: Two-way ANOVA, * $p<0.05$; ** $p<0.01$; *** $p<0.001$)

5.4 Effects of hMCAMecd-Fc on endothelial cell tube formation in the 2D matrigel assay

In order to confirm the effects found in the 3D co-culture assay (section 5.3), a second tube formation assay was used. Matrigel is a 2D monoculture angiogenesis tube formation assay. The effects of recombinant hMCAMecd-Fc on the co-culture could be because of the effects on human dermal fibroblast cells, thus monoculture assay was performed to eliminate that possibility. Cells were seeded on top of the matrigel matrix in 12 well plates and cultured in complete M199 with addition of recombinant protein hMCAMecd-Fc or control Fc (at 1.54 μM). Cells were cultured for 24 h and live images taken every 6 h. Three experiments using HUVECs from distinct umbilical cords were analysed with 9 fields of view for each well. The ImageJ angiogenesis plugin software was used to calculate the parameters of endothelial cell network formation in each field of view. A paired t test showed significant reduction in number of meshes, nodes, junctions and total network length for hMCAMecd-Fc protein treated cells compared to human Fc treated ones (Figure 5.4 and Figure 5.5). The tube formation assay showed that hMCAMecd-Fc reduced the ability of HUVECs to form capillary like structures and networks when seeded on matrigel extracellular matrix components already at 6h post seeding for all the parameters. This confirmed results from fibrin matrix 3D fibroblast co-culture in the previous section.

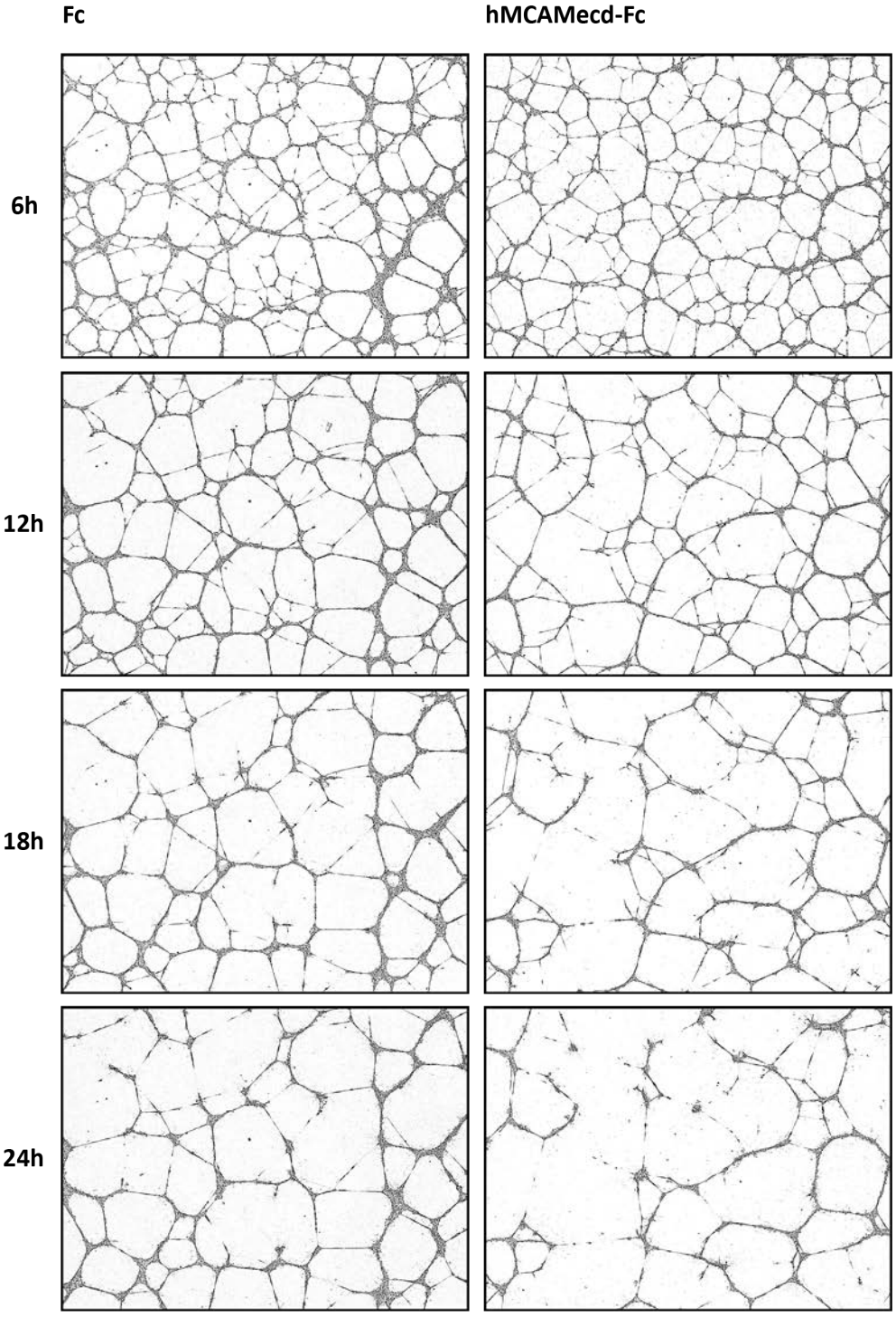

Figure 5.4 Representative images of 2D matrigel tube formation assay. HUVECs were seeded onto matrigel and cultured for 24 h in medium containing either control Fc protein or hMCAMecd-Fc at a concentration of 1.54 µM. Images were taken live at time-points 6, 12, 18 and 24 h after seeding.

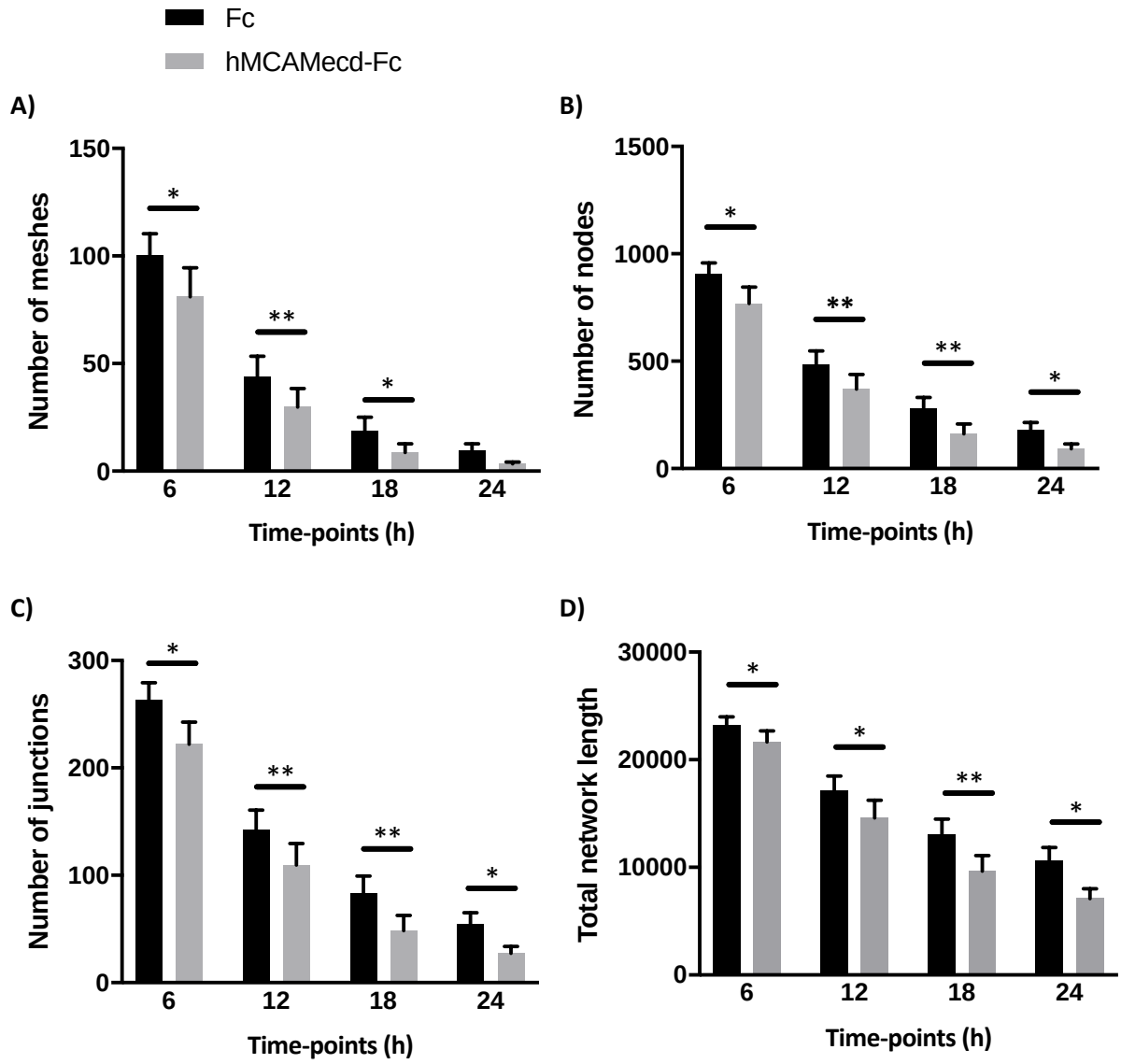

Figure 5.5 hMCAMecd-Fc inhibit HUVECs tube formation in 2D matrigel mono-culture. HUVECs were seeded onto matrigel and cultured for 24 h in medium containing either control Fc protein or hMCAMecd-Fc at a concentration of 1.54 µM. Images were taken live at time-points 6, 12, 18 and 24 h after seeding and several aspects of the tube formation analysed by ImageJ angiogenesis plugin. Nine fields of view per experiment were averaged and 3 experiments analysed. Error bars represent SEM. (Statistical test used: Paired t test, * $p<0.05$; ** $p<0.01$)

5.5 Effects of hMCAMecd-Fc on EC tube formation in the fibroblast co-culture 2D assay

In order to further confirm an effect on angiogenesis, another tube formation co-culture was performed. The 3D co-culture used premade fibrin matrix in which the cells were immersed, while the 2D co-culture took advantage of the fibroblast-secreted matrix. Here, HDFs were seeded and cultured for 5 days in order to form a monolayer on the bottom of the well and to secrete matrix proteins. HUVECs were seeded onto the fibroblast monolayer and cultured for 6 days, after which cells were fixed and immunostained with anti-human CD31 (in order to visualise only the endothelial cells). The experiment was repeated with HUVECs from five distinct umbilical cords and whole wells analysed using ImageJ angiogenesis plugin. The recombinant hMCAMecd-Fc protein again significantly but modestly reduced the number of meshes, nodes, junctions and total network length when compared to human Fc control (Figure 5.6). The fact that recombinant hMCAMecd-Fc consistently reduced tube formation in three different assays indicated its role in blocking *in vitro* tube formation.

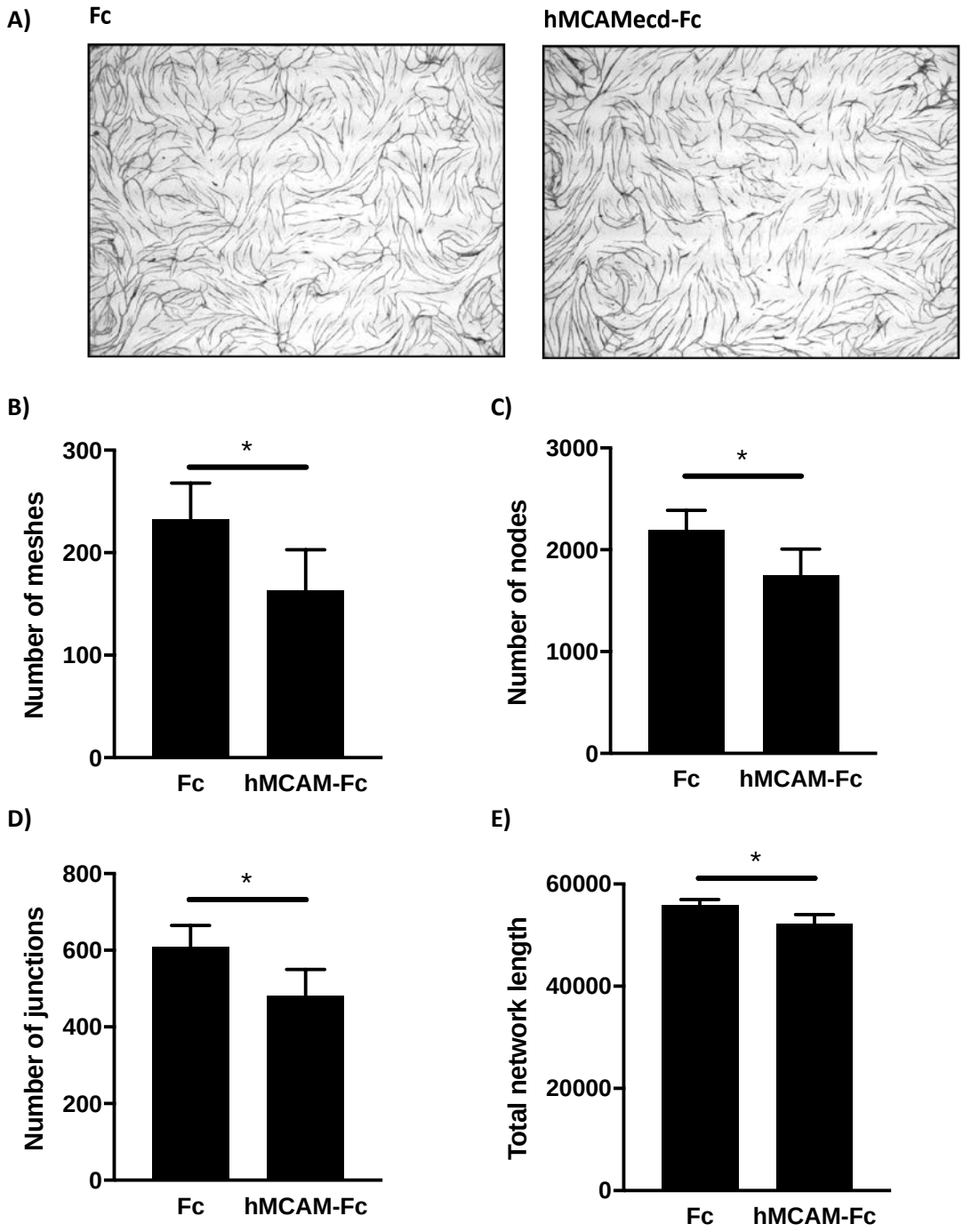

Figure 5.6 hMCAMecd-Fc protein inhibits tube formation of HUVECs in 2D fibroblast co-culture. HUVECs were seeded on the layer of confluent human dermal fibroblast cells and cultured for 6 days in the presence of control Fc protein and hMCAMecd-Fc protein at a concentration of 1.54 µM. Cells were fixed and stained with anti- human CD31 antibody for HUVEC visualisation. **A)** Representative images of endothelial cell network at day 6; **B, C, D, E)** Whole wells of five experiments with HUVECs from distinct cords were analysed using ImageJ angiogenesis plugin. Error bars represent SEM. (Statistical test used: Paired t test, * $p<0.05$)

5.6 Effects of hMCAMecd-Fc on HUVEC proliferation and cell cycle

Proliferation of endothelial cells is an important component of angiogenesis. Tip cells migrate through the extracellular matrix attracted by pro-angiogenic signals from the environment while stalk cells proliferate to elongate the newly formed micro-vessels [149]. In order to investigate the effect of recombinant MCAM extracellular domain on proliferation of HUVECs the CellTiter 96® Non-Radioactive Cell Proliferation Assay was used. HUVECs were seeded in 96 well plates and cultured in complete M199 medium (cM199), cM199 with addition of hMCAMecd-Fc, or cM199 with human Fc control protein (at a concentration of 1.54 µM). Proliferation was measured at time-points of 24, 48 and 72 h using a commercial kit (materials and methods). HUVECs from three distinct umbilical cords were analysed, with three technical replicates for each time-point. Recombinant hMCAMecd-Fc protein did not affect the proliferation of HUVECs over the period of three days (Figure 5.7 A).

The disruption of cell cycle can also affect angiogenesis processes. The cell cycle consists of G1 (Gap1), S (synthesis) and G2/M (gap2/mitosis) and was distinguished by the amount of DNA in cells stained by propidium iodide. HUVECs were cultured for 24 h in cM199 medium, cM199 with hMCAMecd-Fc, or cM199 with human Fc control protein (at 1.54 µM), fixed and stained with propidium iodide. HUVECs from three distinct umbilical cords were analysed using flow cytometry. The percentages of cells in G1, S and G2 phases were unchanged in the presence of hMCAMecd-Fc or Fc control, when compared to untreated HUVECs (Figure 5.7 B).

A)

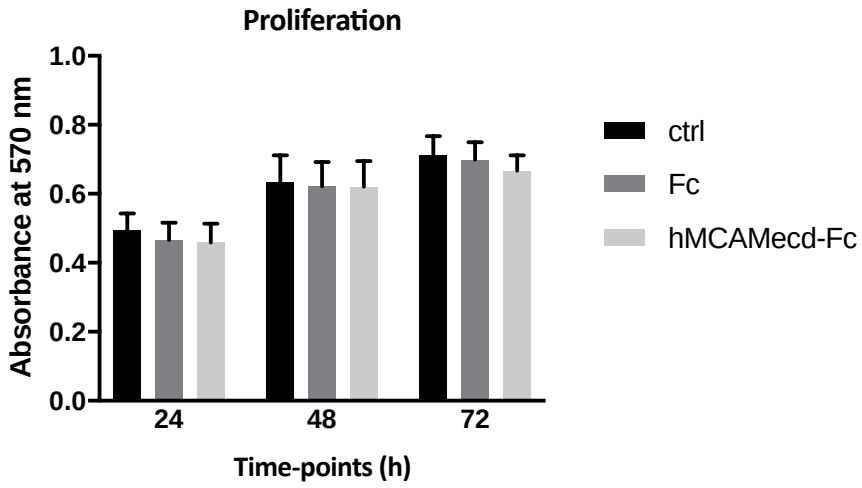

B)

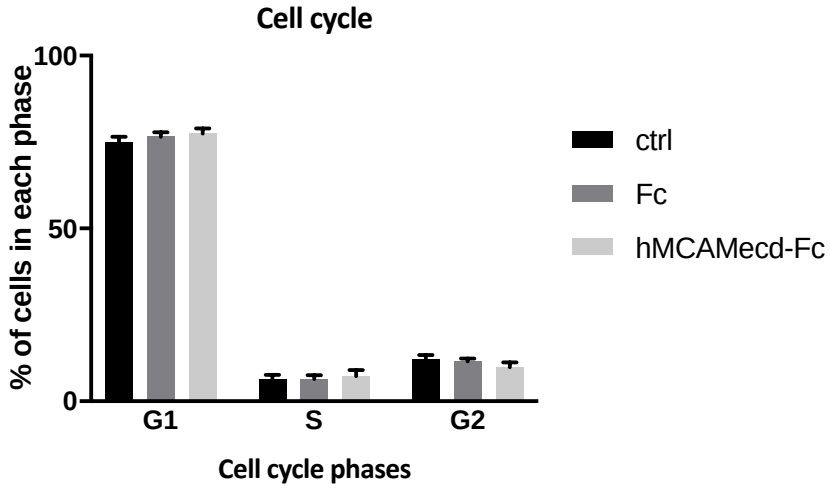

Figure 5.7 hMCAMecd-Fc does not have an effect on HUVECs proliferation and cell cycle. A) HUVECs were seeded in 96 well plates with addition of complete medium (ctrl), hMCAMecd-Fc or human Fc, at 1.54 µM. Cell proliferation was analysed at 24, 48 and 72 h after seeding using CellTiter 96® Non-Radioactive Cell Proliferation Assay. Absorbance was measured at 570 nm. **B)** HUVECs were cultured for 24h in complete medium or with addition of hMCAMecd-Fc or human Fc at 1.54 µM. The fixed cells were stained with propidium iodide and analysed by flow cytometry. Percentage of cells in each phase was calculated for HUVECs from three distinct umbilical cords. For both figures experiments were repeated three times, with error bars representing SEM. (Statistical test used: 2-way ANOVA)

5.7 Effects of hMCAMecd-Fc on endothelial cell migration in the scratch wound assay

The blocking effect of MCAM recombinant protein in network formation assays could be due to an effect on cell migration. Cells need to migrate in order to reach other cells, connect to them and form a functional tube. Knock down of MCAM and some anti-MCAM antibodies have previously shown to impair HUVEC cell motility [102,111,113]. In order to investigate if recombinant hMCAMecd-Fc has an effect on the cell migration the cell culture wound closure assay was used. HUVECs were seeded in a 96 well plate. After the cells reached confluence a wound was created in the cell monolayer and the detached cells removed by washing. The cell culture medium was replaced by the medium containing the recombinant hMCAMecd-Fc protein or the control Fc protein at a concentration of 1.54 μM. Cells were monitored over 24 h and live images taken at 6, 12, 18 and 24 h. Images were analysed for the percentage of wound closure compared to the wound area at time-point 0 h and statistical analysis performed with GraphPad Prism software. Three experiments with HUVECs from distinct umbilical cords were used with three technical replicates for each. No significant difference was observed between the two groups at 18 or 24 h possibly due to some HUVECs being able to close the wound in a faster manner, however migration was slightly but significantly reduced in the first 12 hours (Figure 5.8). hMCAMecd-Fc protein effects migration but not to such a great extent as it effects tube formation.

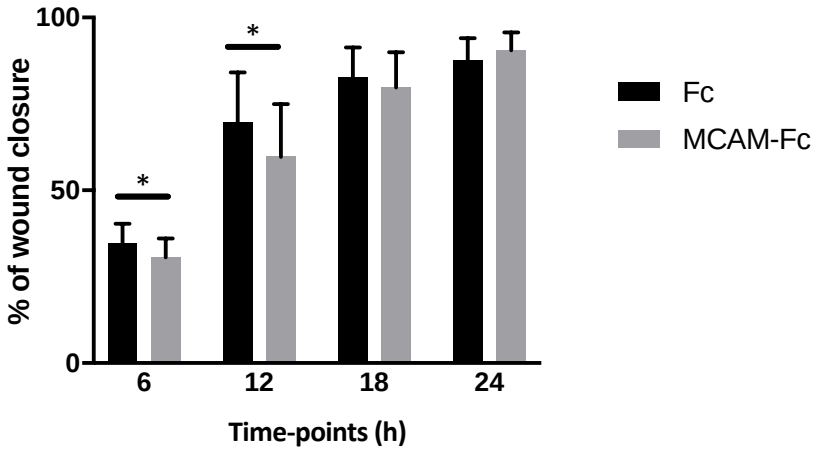

Figure 5.8 hMCAMecd-Fc inhibits endothelial cell migration. HUVECs were cultured to confluence in 96 well plates. Wound in the monolayer was made and cells cultured in the presence of control Fc protein and hMCAMecd-Fc protein at a concentration of 1.54 µM. Cells were monitored over 24 h and images taken live at time-points 0, 6, 12, 18 and 24 h after scratching and percentage of wound closure analysed using ImageJ. Three experiments with three technical replicates were analysed. Error bars represent SEM. (statistic test used: Paired t test, * $p<0.05$)

5.8 Effects of hMCAMecd-Fc on endothelial cell transmigration

MCAM was shown to be involved both in lymphocyte and tumour cell transmigration through the endothelium [99,150]. In order to investigate the effects of recombinant hMCAMecd-Fc protein on cell chemotaxis and transmigration, a HUVEC trans-well cell migration assay was carried out.

HUVECs were ´starved´ in serum free and brain extract free M199 medium for 1 h before seeding to the upper side of the trans-well insert in the same medium. The trans-well insert was then placed in the cell culture 24 well plate containing complete M199 medium. Recombinant hMCAMecd-Fc or control human Fc were added to the upper side of the trans-well together with the cells (at a concentration of 1.54 μM). The cells were left to migrate through the membrane in response to FCS and brain extract for 5 h. After this, cells were fixed, and nuclei of migrated cells stained and counted. Nine fields of view per insert were analysed for HUVECs from three distinct umbilical cords. The counted cells were averaged per field of view for each experiment. hMCAMecd-Fc protein significantly impaired ability of the endothelial cells to migrate through the membrane towards growth factors from the FCS and brain extract used in complete M199, when compared to control Fc protein (Figure 5.9).

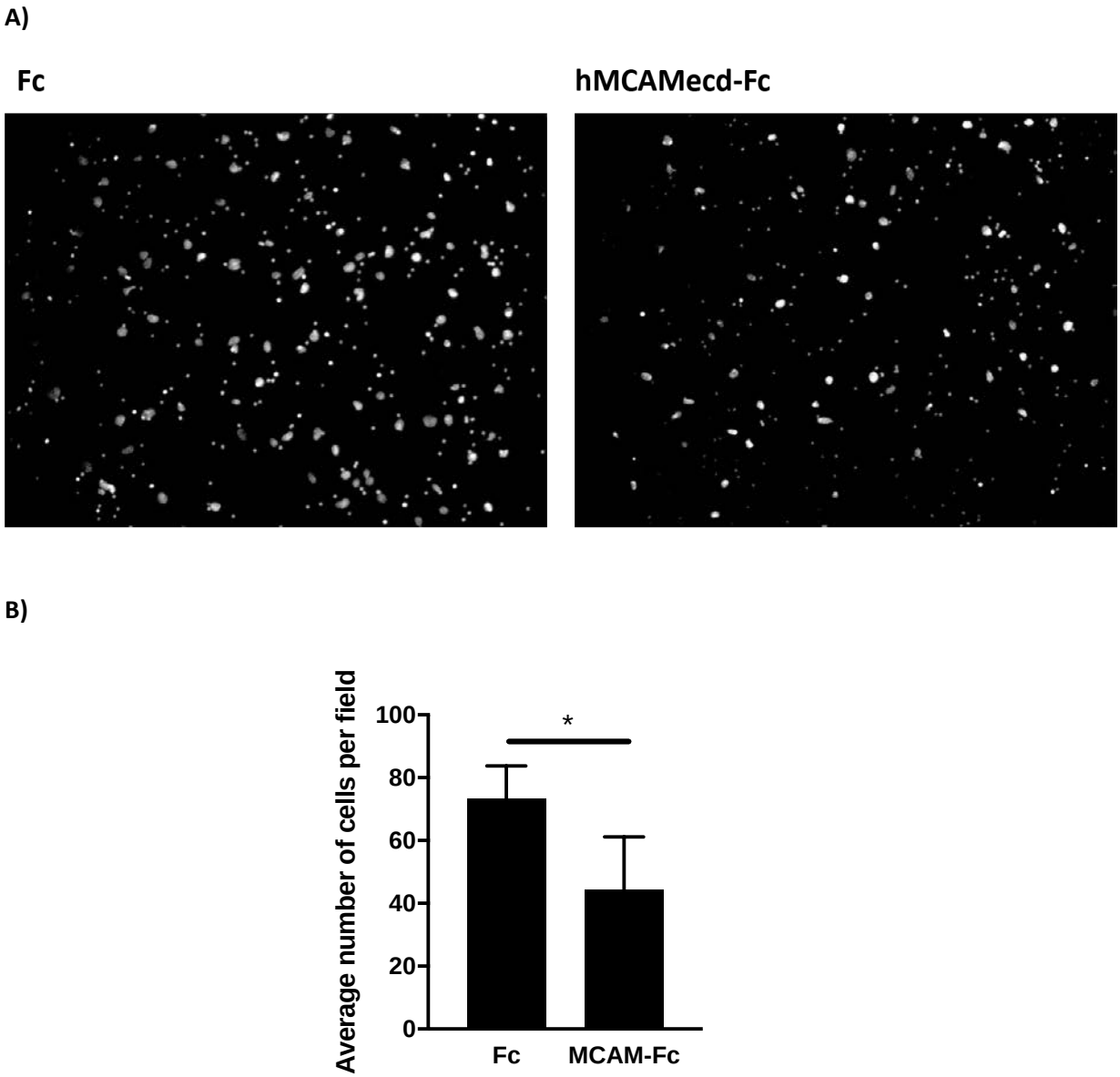

Figure 5.9 hMCAMecd-Fc inhibits HUVEC chemotactic transmigration. HUVECs were starved for 1 h in serum and brain extract free media. HUVECs were then seeded on the upper side of trans-well insert in the same serum free media, and the inserts placed in the wells containing complete media. Recombinant protein hMCAMecd-Fc and control Fc were added to the inserts with cells at 1.54 µM and the cells left to migrate towards the bottom part for 5 h. **A**) representative images of migrated cells after 5h; **B**) Nuclei of migrated cells were stained and counted in 9 fields of view per experiment. Average number of cells per field of view were calculated and paired for each experiment. Error bars represent SEM. (Statistical test: paired t test, * $p<0.05$)

5.9 Discussion

This chapter showed recombinant hMCAMecd-Fc protein significantly impaired HUVECs cell migration, transmigration and tube formation when compared to the Fc treated control at a concentration of 1.54 µM using *in vitro* angiogenesis assays. The recombinant hMCAMecd-Fc protein however, had no effect on HUVEC cell proliferation or cell cycle.

MCAM has previously been reported to play a role in several cell processes that are important for angiogenesis. For example, knock down of MCAM by siRNA had a negative effect on cell proliferation, adhesion, migration and netrin-1 induced tube formation in HUVECs matrigel assay [102,111]. Similarly, endothelial cell sprouting, migration and tube formation as well as tumour angiogenesis are impaired in the endothelial MCAM knock-out mice [151]. Several antibodies to MCAM have also shown anti-angiogenic activity [108,111,152,153]. One antibody to human MCAM (ABX-MA1) reduced HUVECs tube formation after binding MCAM on the cell surface [103] possibly by blocking its interaction with ligands or by altering its signalling. A possible mode of action of the recombinant hMCAMecd-Fc could be binding of MCAM ligands. MCAM was shown to bind laminin411 and laminin421 (components of extracellular matrices), and in this way promote endothelial cell adhesion and migration [109,110]. Recombinant hMCAMecd-Fc could be binding to its extracellular matrix ligands and thus restrict the binding of cell surface MCAM on HUVECs and in this way inhibit the ability of HUVECs to migrate on or through the matrix to form endothelial cell network. However, other possibilities such as hMCAMecd-Fc binding a ligand on HUVECs cannot be excluded. Future experiments investigating recombinant hMCAMecd localisation and binding in these assays need to be performed.

In contrast with our data, recent publication using soluble recombinant MCAM extracellular domain protein showed pro-angiogenic effects on HUVECs and endothelial progenitor cells (EPCs). Stalin et al. (2016) showed that treating HUVECs with 100 ng/ml of soluble MCAMecd-myc had similar effects as 100 ng/ml of VEGF; it induced HUVECs proliferation and tumour vascularization in mice [106]. Furthermore, soluble MCAM promoted expression of Ang-2, IL-8 and MMP-9, as well as increased mRNA expression of VEGF in tumour cells, indicating pro-angiogenic effects [106]. Similarly, Harhouri et al. (2010) showed that 50 ng/ml of soluble MCAM promoted proliferation, migration and tube formation in late endothelial progenitor cells (EPCs) *in vitro* and showed that soluble MCAM recruited EPCs to ischemic mouse tissue and caused increase in vascularization in mouse experimental hind limb ischemia [119]. The difference between these observations and our experiment could be due to different concentrations and recombinant protein tag used. The Fc tag form dimers and it was shown that MCAM function can vary depending on dimeric or monomeric form [154,155]. Dimeric MCAM could sequester binding proteins and thus inhibit their effects on HUVECs [115,156] while soluble monomeric MCAM could have a pro-angiogenic properties by binding Angiomotin p80 on endothelial cells [106]. Furthermore, higher concentrations used could initiate opposite effects as seen with other proteins such as Netrin-1. Netrin-1 at lower concentrations promotes angiogenesis via MCAM binding while it blocks angiogenesis in higher concentrations by binding to the UNC5B membrane protein [111,157]. Further experiments with a range of recombinant MCAM concentrations, as well as recombinant protein with a different tag need to be performed in order to identify the cause of these differences. Repeating the experiments with deletion constructs of soluble MCAM could show which domain of MCAM is important for the effects seen. Experiments exploring the change in signalling pathways that

have been reported for MCAM signalling in angiogenesis have to be performed in order to investigate molecular basis of the effects of soluble MCAM on HUVECs. Furthermore, a pull-down experiment with HUVECs cell lysate and supernatant might shed light to which proteins hMCAMecd-Fc binds, however this could be difficult if the interactions are transient or weak.

Data presented here make a starting point for utilization of soluble MCAM extracellular domain as a receptor trap, which could be used as a novel approach for anti-angiogenic treatment for RCC. Previous attempts to use soluble receptor traps such as extracellular domains of EphB4, Tie2 or TGFβ type III receptor inhibited the effects of pro-angiogenic factors such as VEGF or bFGF and inhibited tumour growth in murine models [158–160]. Soluble EphB4 showed inhibitory effects on tube formation already at a concentration of 14 nM, and reduced angiogenesis and tumour growth in mouse xengraft tumours [160]. Soluble ROBO4 inhibited *in vivo* angiogenesis at a concentration of 1.25 µM [161], while Tie2 receptor trap inhibited angiogenesis at a concentration of 3 µM [158]. Experiments testing soluble MCAM protein in *in vivo* angiogenesis or murine xengraft tumour models would be crucial in order to further investigate the anti-angiogenic potential of a soluble MCAM receptor trap.

6 GENERAL DISCUSSION

6.1 Therapeutic potential for targeting MCAM on tumour vessels

The main goal of this thesis was to explore the possibility of developing strategies to therapeutically target MCAM in renal cell carcinoma. Our group was the first to show that MCAM was highly expressed on the vasculature of renal cell carcinoma, specifically those of clear cell histology [56]. The work described in this thesis confirmed those of Wragg et al. (2016) by developing a novel monoclonal antibody that localises *in vivo* to mouse RENCA tumour blood vessels.

Clear cell renal cell carcinomas are known to be highly vascular and previous targeting of angiogenesis has proven an effective treatment for these tumours [49,55]. Most of these therapies target the VEGF pathway and it is now well documented that such therapies can cause complicating side effects due to VEGF's involvement in the maintenance of healthy blood vessels [162]. Resistance and aggressive recurrence of the cancer are also frequent events due to bypassing of the VEGF pathway by, possibly, expression of additional angiogenic factors [163,164]. Indeed, MCAM itself has been reported to aid development of resistance to anti-angiogenic therapy in RCC. For example, resistance to the widely used anti-angiogenic drug sunitinib has been linked to higher levels of MCAM RNA expression in metastatic RCC and an increase in soluble MCAM in patients' plasma [126]. Thus, targeting MCAM on tumour blood vessels raises the possibility of increased efficacy of established anti-angiogenic therapies.

It is worthy of note that MCAM involvement in resistance to other chemotherapies has been reported in cancers beyond renal cell carcinoma. For example, in breast cancer, high expression of MCAM correlated with increased cell surface expression of ErbB3 and ErbB4 and increased resistance to doxorubicin and docetaxel chemotherapy [165]. In cervical cancer, high expression of MCAM reduced sensitivity to radiotherapy [166]. In this paper it was shown that

targeting MCAM with the AA98 monoclonal antibody abrogated the reduced sensitivity to radiotherapy, showing that targeting MCAM in combination with other therapies could improve cancer treatment. Another study has shown that simultaneous targeting VEGF with Bevacizumab and anti-MCAM antibody AA98 gave rise to slower tumour growth in mouse xenograft models [108]. Having monoclonal antibodies that recognise mouse MCAM will aid further studies in mouse models of cancer. Nevertheless, to determine if the mMCAM10 antibody shows an inhibitory effect on tumour growth, the variable region needs insertion into the mouse immunoglobulin main frame so that the antibody can be used in immuno-competent mice. Although of course it could be studied in human xenografts in SCID mice that will not generate antibodies to the rat monoclonal.

Greater efficacy would probably be seen with an antibody drug conjugate (ADC). ADCs are comprised of an antibody to which a toxic drug is attached [167]. There are several ADCs in clinical development for cancer [168]. The first such therapy for RCC (AMG 172) is currently in phase I clinical trial (NCT01497821). AMG 172 is the anti-CD27L human monoclonal antibody conjugated to the maytansinoid DM1 by a non-cleavable linker. The most important requirement of an ADC is high specificity of the antibody in order to prevent toxicities caused by binding to healthy tissue [169]. The mMCAM10 showed specific tumour vessel, as compared to vessels in healthy tissue, localisation one hour after intra venous injection, making it a promising tool for an ADC approach.

Another therapeutic approach is to use CAR modified T cells. CAR-T cells represent one of the currently most exciting approaches to cancer treatment [170,171]. CAR T cell therapy involves isolation of a patient's T-cells followed by viral introduction of the modified

recombinant T-cell receptor targeting the antigen of interest. The modified T cells are then expanded *in vitro* and infused back into the patient where they destroy the antigen expressing cells [3]. Our collaborators from S. Lee's laboratory cloned the variable region of the mMCAM10 into the chimeric antigen receptor and introduced it into mouse T-cells. They confirmed that the mMCAM10 chimeric antigen receptor conserved specificity to mouse MCAM after cloning. Transfected T-cells were shown to be activated by recombinant mMCAM *in vitro* (S. Lee. personal communication). Further work is funded and in progress.

In humans an anti-MCAM antibody, PRX003, has been used in clinical trials for the treatment of psoriasis patients. The rationale for clinical trial of an anti MCAM antibody in psoriasis is the expression of MCAM on Th17 T-cells. This subset of T-cells are defined by their expression of IL17, and are involved in several autoimmune diseases such as psoriasis and multiple sclerosis [172]. The expression of MCAM on these cells has been shown to increase their ability to bind LAMA4 and cross the endothelium into the inflamed tissue. PRX003 blocks MCAM binding to LAMA4, as well as reduces expression of MCAM on treated cells, causing inhibition of T-cell transmigration in several animal autoimmune disease models [173]. This antibody showed no off-target toxicities but reduced psoriasis symptoms by 40-60% when used in animals [174]. The fact that PRX003 had a desired effect in patients and had no severe toxicities, poses a possible proof of concept that anti-MCAM targeted therapy could be a promising approach in treatment of cancer [175]. Furthermore, combination with immune checkpoint inhibitors may possibly benefit MCAM targeting, as these therapies often cause autoimmune conditions. Anti-MCAM antibody could thus have a dual purpose: the targeting of blood vessels and inhibiting T-cells involved in autoimmune processes. It has already been

shown that targeting immune checkpoint molecules in RCC treatment gave improved patient survival when combined with anti-angiogenics [176].

Soluble MCAM as a receptor trap to block angiogenesis

Blocking angiogenesis by targeting the specificity of receptor-ligand interactions using soluble receptor traps such as the VEGF receptor trap (aflibercept) has proven an effective therapeutic strategy for cancer and other pathologies [177,178]. MCAM is implicated in tumour angiogenesis and thought to react with several soluble or membrane bound angiogenic factors [66,111]. Furthermore, it has been shown that galectin-3, a protein that promotes cancer progression and metastasis, binds MCAM and initiates its dimerization, which leads to activation of ACT kinase [179]. This thesis has shown that the MCAM extracellular domain Fc fusion protein inhibited the *in vitro* pro-angiogenic properties of HUVECs. Soluble extracellular MCAM shed from endothelium has also been shown to promote angiogenesis and shown to be elevated in the plasma of patients with pathologies in which there is increased vascularisation [68,69]. In contrast to these reports, other groups have shown that the MCAM extracellular domain fused to a myc tag and used in lower concentrations had an opposite effect on HUVECs and endothelial progenitor cells (EPCs) [106,119]. It is possible that the Fc tag, which mediates dimerization, could be an explanation for these different observations.

Recombinant receptor traps have entered the clinic mostly for the treatment of immunological diseases. An exception is the VEGF receptor trap Aflibercept (Eylea®, Zaltrap®). Aflibercept is comprised of one VEGFR1 domain and one VEGFR2 domain fused to an Fc tag. Aflibercept blocks angiogenesis by sequestering VEGF-A, VEGF-B and placental growth factor [180] and has been FDA approved for the treatment of metastatic colorectal cancer in combination with chemotherapy. Interestingly, when compared to other anti-VEGF blocking

agents the VEGF trap presents the best efficacy, especially in terms of pharmacologic properties. The utilisation of the Fc tag has also proven beneficial in such chimeric biological drug therapies over un-tagged proteins due to its ability to increase the serum half-life of the protein [181]. Additionally, the Fc provides several other advantages such as ease of production and purification, good solubility and stability and Fc immune effector functions, which could be manipulated in order to create more efficient and longer-lasting therapies [182]. However, due to the immune system engagement with the Fc receptors it is important to closely monitor the patients' responses. Furthermore, even though the receptor and the Fc are presumably not immunogenic, the region where the protein and Fc tag are fused could elicit immune responses to the novel antigen part [183,184]. Future preclinical studies in mouse models of cancer will provide insight into the efficacy of hMCAMecd-Fc receptor trap as a therapy.

7 REFERENCES

7.1 A list of references

1. Roncador, G. *et al.* The European antibody network's practical guide to finding and validating suitable antibodies for research. *MAbs* **8,** 27–36 (2016).
2. Weiner, L. M., Surana, R. & Wang, S. Monoclonal antibodies: versatile platforms for cancer immunotherapy. *Nat. Rev. Immunol.* **10,** 317–327 (2010).
3. Smyth, M. J., Ngiow, S. F., Ribas, A. & Teng, M. W. L. Combination cancer immunotherapies tailored to the tumour microenvironment. *Nat. Rev. Clin. Oncol.* **13,** 143–158 (2016).
4. Bayer, V. *et al.* Cancer Immunotherapy: An Evidence-Based Overview and Implications for Practice. *Clin. J. Oncol. Nurs.* **21,** 13–21 (2017).
5. Ramsdell, F. & Fowlkes, B. J. Clonal deletion versus clonal anergy: the role of the thymus in inducing self tolerance. *Science* **248,** 1342–8 (1990).
6. Nossal, G. J. Negative selection of lymphocytes. *Cell* **76,** 229–39 (1994).
7. Sliwkowski, M. X. & Mellman, I. Antibody Therapeutics in Cancer. *Science (80-.).* **341,** 1192–1198 (2013).
8. Scott, A. M., Wolchok, J. D. & Old, L. J. Antibody therapy of cancer. *Nature Reviews Cancer* (2012). doi:10.1038/nrc3236
9. Bobisse, S., Foukas, P. G., Coukos, G. & Harari, A. Neoantigen-based cancer immunotherapy. *Ann. Transl. Med.* **4,** 262–262 (2016).
10. Restifo, N. P., Smyth, M. J. & Snyder, A. Acquired resistance to immunotherapy and future challenges. *Nat. Rev. Cancer* **16,** 121–126 (2016).
11. Köhler, G. & Milstein, C. Continuous cultures of fused cells secreting antibody of predefined specificity. *Nature* **256,** 495–7 (1975).

12. Jones, P. T., Dear, P. H., Foote, J., Neuberger, M. S. & Winter, G. Replacing the complementarity-determining regions in a human antibody with those from a mouse. *Nature* **321,** 522–5 (1986).

13. Tiwari, S. R. *et al.* Retrospective study of the efficacy and safety of neoadjuvant docetaxel, carboplatin, trastuzumab/pertuzumab (TCH-P) in nonmetastatic HER2-positive breast cancer. *Breast Cancer Res. Treat.* **158,** 189–93 (2016).

14. Bzowska, M. *et al.* Antibody-based antiangiogenic and antilymphangiogenic therapies to prevent tumor growth and progression. *Acta Biochim. Pol.* **60,** 263–75 (2013).

15. Decker, W. K. *et al.* Cancer Immunotherapy: Historical Perspective of a Clinical Revolution and Emerging Preclinical Animal Models. *Front. Immunol.* **8,** 829 (2017).

16. Lee, S. *et al.* Autocrine VEGF Signaling Is Required for Vascular Homeostasis. *Cell* **130,** 691–703 (2007).

17. Casanovas, O., Hicklin, D. J., Bergers, G. & Hanahan, D. Drug resistance by evasion of antiangiogenic targeting of VEGF signaling in late-stage pancreatic islet tumors. *Cancer Cell* **8,** 299–309 (2005).

18. Ceran, C. *et al.* Novel anti-HER2 monoclonal antibodies: synergy and antagonism with tumor necrosis factor-α. *BMC Cancer* **12,** 450 (2012).

19. Baeriswyl, V. & Christofori, G. The angiogenic switch in carcinogenesis. *Semin. Cancer Biol.* **19,** 329–337 (2009).

20. Sherwood, L. M., Parris, E. E. & Folkman, J. Tumor Angiogenesis: Therapeutic Implications. *N. Engl. J. Med.* **285,** 1182–1186 (1971).

21. Pugh, C. W. & Ratcliffe, P. J. Regulation of angiogenesis by hypoxia: role of the HIF system. *Nat. Med.* **9,** 677–684 (2003).

22. Giaccia, A. J., Simon, M. C. & Johnson, R. The biology of hypoxia: the role of oxygen sensing in development, normal function, and disease. *Genes Dev.* **18,** 2183–2194 (2004).

23. Wang, G. L., Jiang, B. H., Rue, E. A. & Semenza, G. L. Hypoxia-inducible factor 1 is a basic-helix-loop-helix-PAS heterodimer regulated by cellular O2 tension. *Proc. Natl. Acad. Sci. U. S. A.* **92,** 5510–4 (1995).

24. Wan, J., Ma, J., Mei, J. & Shan, G. The effects of HIF-1alpha on gene expression profiles of NCI-H446 human small cell lung cancer cells. *J. Exp. Clin. Cancer Res.* **28,** 150 (2009).

25. Schödel, J. *et al.* High-resolution genome-wide mapping of HIF-binding sites by ChIP-seq. *Blood* **117,** e207-17 (2011).

26. Mole, D. R. *et al.* Genome-wide association of hypoxia-inducible factor (HIF)-1alpha and HIF-2alpha DNA binding with expression profiling of hypoxia-inducible transcripts. *J. Biol. Chem.* **284,** 16767–75 (2009).

27. Gerhardt, H. *et al.* VEGF guides angiogenic sprouting utilizing endothelial tip cell filopodia. *J. Cell Biol.* **161,** 1163–77 (2003).

28. Nagy, J., Chang, S.-H., Shih, S.-C., Dvorak, A. & Dvorak, H. Heterogeneity of the Tumor Vasculature. *Semin. Thromb. Hemost.* **36,** 321–331 (2010).

29. Ferlay, J. *et al.* Cancer incidence and mortality worldwide: Sources, methods and major patterns in GLOBOCAN 2012. *Int. J. Cancer* **136,** E359–E386 (2015).

30. Lipworth, L., Tarone, R. E. & McLaughlin, J. K. The Epidemiology of Renal Cell Carcinoma. *J. Urol.* **176,** 2353–2358 (2006).

31. Jemal, A. *et al.* Cancer statistics, 2003. *CA. Cancer J. Clin.* **53,** 5–26 (2003).

32. Mathew, A., Devesa, S. S., Fraumeni, J. F. & Chow, W.-H. Global increases in kidney

cancer incidence, 1973-1992. *Eur. J. Cancer Prev.* **11,** 171–8 (2002).

33. Cancer Research UK. *http://www.cancerresearchuk.org/health-professional/cancer-statistics/statistics-by-cancer-type/kidney-cancer/incidence#ref-2*

34. Comprehensive molecular characterization of clear cell renal cell carcinoma. *Nature* **499,** 43–49 (2013).

35. Baldewijns, M. M. L. *et al.* Genetics and epigenetics of renal cell cancer. *Biochim. Biophys. Acta - Rev. Cancer* **1785,** 133–155 (2008).

36. Kaelin, W. G. The von Hippel-Lindau Tumor Suppressor Protein and Clear Cell Renal Carcinoma. *Clin. Cancer Res.* **13,** 680s–684s (2007).

37. Latif, F. *et al.* Identification of the von Hippel-Lindau disease tumor suppressor gene. *Science* **260,** 1317–20 (1993).

38. Linehan, W. M., Lerman, M. I. & Zbar, B. Identification of the von Hippel-Lindau (VHL) gene. Its role in renal cancer. *JAMA* **273,** 564–70 (1995).

39. Choueiri, T. K. & Motzer, R. J. Systemic Therapy for Metastatic Renal-Cell Carcinoma. *N. Engl. J. Med.* **376,** 354–366 (2017).

40. Janzen, N. K., Kim, H. L., Figlin, R. A. & Belldegrun, A. S. Surveillance after radical or partial nephrectomy for localized renal cell carcinoma and management of recurrent disease. *Urol. Clin. North Am.* **30,** 843–52 (2003).

41. Motzer, R. J. *et al.* Overall Survival and Updated Results for Sunitinib Compared With Interferon Alfa in Patients With Metastatic Renal Cell Carcinoma. *J. Clin. Oncol.* **27,** 3584–3590 (2009).

42. Ball, M. W., Singer, E. A. & Srinivasan, R. Renal cell carcinoma. *Curr. Opin. Oncol.* **29,** 201–209 (2017).

43. Edwards, M. J., Anderson, J. A., Angel, J. R. & Harty, J. I. Spontaneous regression of primary and metastatic renal cell carcinoma. *J. Urol.* **155,** 1385 (1996).

44. Atzpodien, J. *et al.* Interleukin-2- and interferon alfa-2a-based immunochemotherapy in advanced renal cell carcinoma: a Prospectively Randomized Trial of the German Cooperative Renal Carcinoma Chemoimmunotherapy Group (DGCIN). *J. Clin. Oncol.* **22,** 1188–94 (2004).

45. Atzpodien, J. *et al.* Adjuvant treatment with interleukin-2- and interferon-alpha2a-based chemoimmunotherapy in renal cell carcinoma post tumour nephrectomy: results of a prospectively randomised trial of the German Cooperative Renal Carcinoma Chemoimmunotherapy Group (DGCIN). *Br. J. Cancer* **92,** 843–6 (2005).

46. Yang, J. C. *et al.* Randomized Study of High-Dose and Low-Dose Interleukin-2 in Patients With Metastatic Renal Cancer. *J. Clin. Oncol.* **21,** 3127–3132 (2003).

47. Fyfe, G. *et al.* Results of treatment of 255 patients with metastatic renal cell carcinoma who received high-dose recombinant interleukin-2 therapy. *J. Clin. Oncol.* **13,** 688–96 (1995).

48. Fisher, R. I., Rosenberg, S. A. & Fyfe, G. Long-term survival update for high-dose recombinant interleukin-2 in patients with renal cell carcinoma. *Cancer J. Sci. Am.* **6 Suppl 1,** S55-7 (2000).

49. Gill, D. M., Agarwal, N. & Vaishampayan, U. Evolving Treatment Paradigm in Metastatic Renal Cell Carcinoma. *Am. Soc. Clin. Oncol. Educ. B.* **37,** 319–329 (2017).

50. Motzer, R. J. *et al.* Sunitinib versus Interferon Alfa in Metastatic Renal-Cell Carcinoma. *N. Engl. J. Med.* **356,** 115–124 (2007).

51. Sternberg, C. N. *et al.* Pazopanib in Locally Advanced or Metastatic Renal Cell

Carcinoma: Results of a Randomized Phase III Trial. *J. Clin. Oncol.* **28,** 1061–1068 (2010).

52. Escudier, B. *et al.* Bevacizumab plus interferon alfa-2a for treatment of metastatic renal cell carcinoma: a randomised, double-blind phase III trial. *Lancet* **370,** 2103–2111 (2007).

53. Choueiri, T. K. *et al.* Cabozantinib Versus Sunitinib As Initial Targeted Therapy for Patients With Metastatic Renal Cell Carcinoma of Poor or Intermediate Risk: The Alliance A031203 CABOSUN Trial. *J. Clin. Oncol.* **35,** 591–597 (2017).

54. Motzer, R. J. *et al.* Lenvatinib, everolimus, and the combination in patients with metastatic renal cell carcinoma: a randomised, phase 2, open-label, multicentre trial. *Lancet. Oncol.* **16,** 1473–1482 (2015).

55. Hutson, T. E., Thoreson, G. R., Figlin, R. A. & Rini, B. I. The Evolution of Systemic Therapy in Metastatic Renal Cell Carcinoma. *Am. Soc. Clin. Oncol. Educ. B.* **36,** 113–117 (2016).

56. Wragg, J. W. *et al.* MCAM and LAMA4 Are Highly Enriched in Tumor Blood Vessels of Renal Cell Carcinoma and Predict Patient Outcome. *Cancer Res.* **76,** 2314–2326 (2016).

57. Lehmann, J. M., Riethmüller, G. & Johnson, J. P. MUC18, a marker of tumor progression in human melanoma, shows sequence similarity to the neural cell adhesion molecules of the immunoglobulin superfamily. *Proc. Natl. Acad. Sci. U. S. A.* **86,** 9891–5 (1989).

58. Johnson, J. P., Rothbächer, U. & Sers, C. The progression associated antigen MUC18: a unique member of the immunoglobulin supergene family. *Melanoma Res.* **3,** 337–40 (1993).

59. Sers, C., Kirsch, K., Rothbächer, U., Riethmüller, G. & Johnson, J. P. Genomic organization of the melanoma-associated glycoprotein MUC18: implications for the evolution of the immunoglobulin domains. *Proc. Natl. Acad. Sci. U. S. A.* **90,** 8514–8

(1993).

60. Shih, I. M., Elder, D. E., Speicher, D., Johnson, J. P. & Herlyn, M. Isolation and functional characterization of the A32 melanoma-associated antigen. *Cancer Res.* **54,** 2514–20 (1994).

61. Kohama, K. *et al.* Molecular cloning and analysis of the mouse gicerin gene. *Neurochem. Int.* **46,** 465–470 (2005).

62. Taira, E., Takaha, N., Taniura, H., Kim, C. H. & Miki, N. Molecular cloning and functional expression of gicerin, a novel cell adhesion molecule that binds to neurite outgrowth factor. *Neuron* **12,** 861–72 (1994).

63. Tsukamoto, Y. *et al.* Expression of gicerin, a cell adhesion molecule, in the abnormal retina in silver plumage color mutation of Japanese quail (Coturnix japonica). *Neurosci. Lett.* **266,** 53–6 (1999).

64. Chan, B., Sinha, S., Cho, D., Ramchandran, R. & Sukhatme, V. P. Critical roles of CD146 in zebrafish vascular development. *Dev. Dyn.* **232,** 232–44 (2005).

65. Lehmann, J. M. *et al.* Discrimination between Benign and Malignant Cells of Melanocytic Lineage by Two Novel Antigens , a Glycoprotein with a Molecular Weight of 113 , 000 and a Protein with a Molecular Weight of 76 , 000. *Cancer Res.* **47,** 841–5 (1987).

66. Wang, Z. & Yan, X. CD146, a multi-functional molecule beyond adhesion. *Cancer Lett.* **330,** 150–162 (2013).

67. Vainio, O. *et al.* HEMCAM, an adhesion molecule expressed by c-kit+ hemopoietic progenitors. *J. Cell Biol.* **135,** 1655–68 (1996).

68. Bardin, N., Francès, V., Combes, V., Sampol, J. & Dignat-George, F. CD146: biosynthesis

and production of a soluble form in human cultured endothelial cells. *FEBS Lett.* **421,** 12–4 (1998).

69. Boneberg, E.-M., Illges, H., Legler, D. F. & Fürstenberger, G. Soluble CD146 is generated by ectodomain shedding of membrane CD146 in a calcium-induced, matrix metalloprotease-dependent process. *Microvasc. Res.* **78,** 325–31 (2009).

70. Taira, E., Kohama, K., Tsukamoto, Y., Okumura, S. & Miki, N. Gicerin/CD146 is involved in neurite extension of NGF-treated PC12 cells. *J. Cell. Physiol.* **204,** 632–7 (2005).

71. Takaha, N. *et al.* Expression of gicerin in development, oncogenesis and regeneration of the chick kidney. *Differentiation.* **58,** 313–20 (1995).

72. Sers, C., Riethmüller, G. & Johnson, J. P. MUC18, a melanoma-progression associated molecule, and its potential role in tumor vascularization and hematogenous spread. *Cancer Res.* **54,** 5689–94 (1994).

73. Bardin, N. *et al.* Identification of the S-Endo 1 Endothelial-Associated Antigen. *Biochem. Biophys. Res. Commun.* **218,** 210–216 (1996).

74. Tormin, A. *et al.* CD146 expression on primary nonhematopoietic bone marrow stem cells is correlated with in situ localization. *Blood* **117,** 5067–77 (2011).

75. Maijenburg, M. W. *et al.* The composition of the mesenchymal stromal cell compartment in human bone marrow changes during development and aging. *Haematologica* **97,** 179–83 (2012).

76. Elshal, M. F. *et al.* A unique population of effector memory lymphocytes identified by CD146 having a distinct immunophenotypic and genomic profile. *BMC Immunol.* **8,** 29 (2007).

77. Dagur, P. K. *et al.* MCAM-expressing CD4(+) T cells in peripheral blood secrete IL-17A

and are significantly elevated in inflammatory autoimmune diseases. *J. Autoimmun.* **37,** 319–27 (2011).

78. Huber, M. *et al.* A Th17-like developmental process leads to CD8(+) Tc17 cells with reduced cytotoxic activity. *Eur. J. Immunol.* **39,** 1716–25 (2009).

79. Shih, I. M. & Kurman, R. J. Expression of melanoma cell adhesion molecule in intermediate trophoblast. *Lab. Invest.* **75,** 377–88 (1996).

80. Liu, Q. *et al.* Pre-eclampsia is associated with the failure of melanoma cell adhesion molecule (MCAM/CD146) expression by intermediate trophoblast. *Lab. Investig.* **84,** 221–228 (2004).

81. Schrage, A. *et al.* Murine CD146 is widely expressed on endothelial cells and is recognized by the monoclonal antibody ME-9F1. *Histochem. Cell Biol.* **129,** 441–51 (2008).

82. Despoix, N. *et al.* Mouse CD146/MCAM is a marker of natural killer cell maturation. *Eur. J. Immunol.* **38,** 2855–64 (2008).

83. Pacifico, M. D. *et al.* Development of a tissue array for primary melanoma with long-term follow-up: discovering melanoma cell adhesion molecule as an important prognostic marker. *Plast. Reconstr. Surg.* **115,** 367–75 (2005).

84. Rapanotti, M. C. *et al.* Melanoma-associated markers expression in blood: MUC-18 is associated with advanced stages in melanoma patients. *Br. J. Dermatol.* **160,** 338–44 (2009).

85. Wu, G. J. *et al.* Isolation and characterization of the major form of human MUC18 cDNA gene and correlation of MUC18 over-expression in prostate cancer cell lines and tissues with malignant progression. *Gene* **279,** 17–31 (2001).

86. Wu, G.-J. *et al.* Ectopical expression of human MUC18 increases metastasis of human prostate cancer cells. *Gene* **327,** 201–13 (2004).

87. Aldovini, D. *et al.* M-CAM expression as marker of poor prognosis in epithelial ovarian cancer. *Int. J. cancer* **119,** 1920–6 (2006).

88. Wu, Z. *et al.* MCAM is a novel metastasis marker and regulates spreading, apoptosis and invasion of ovarian cancer cells. *Tumour Biol.* **33,** 1619–28 (2012).

89. Liu, W.-F. *et al.* CD146 expression correlates with epithelial-mesenchymal transition markers and a poor prognosis in gastric cancer. *Int. J. Mol. Sci.* **13,** 6399–406 (2012).

90. Zabouo, G. *et al.* CD146 expression is associated with a poor prognosis in human breast tumors and with enhanced motility in breast cancer cell lines. *Breast Cancer Res.* **11,** R1 (2009).

91. Zeng, Q. *et al.* CD146, an epithelial-mesenchymal transition inducer, is associated with triple-negative breast cancer. *Proc. Natl. Acad. Sci.* **109,** 1127–1132 (2012).

92. Zhang, X. *et al.* MCAM expression is associated with poor prognosis in non-small cell lung cancer. *Clin. Transl. Oncol.* **16,** 178–83 (2014).

93. Shih, L. M., Hsu, M. Y., Palazzo, J. P. & Herlyn, M. The cell-cell adhesion receptor Mel-CAM acts as a tumor suppressor in breast carcinoma. *Am. J. Pathol.* **151,** 745–51 (1997).

94. Ouhtit, A., Abdraboh, M. E., Hollenbach, A. D., Zayed, H. & Raj, M. H. G. CD146, a novel target of CD44-signaling, suppresses breast tumor cell invasion. *Cell Commun. Signal.* **15,** 45 (2017).

95. Lin, J.-C. *et al.* Significance of expression of human METCAM/MUC18 in nasopharyngeal carcinomas and metastatic lesions. *Asian Pac. J. Cancer Prev.* **15,** 245–52 (2014).

96. Li, Q., Yu, Y., Bischoff, J., Mulliken, J. B. & Olsen, B. R. Differential expression of CD146

in tissues and endothelial cells derived from infantile haemangioma and normal human skin. *J. Pathol.* **201,** 296–302 (2003).

97. Filshie, R. J. *et al.* MUC18, a member of the immunoglobulin superfamily, is expressed on bone marrow fibroblasts and a subset of hematological malignancies. *Leukemia* **12,** 414–21 (1998).

98. Liu, J.-W. *et al.* Hypermethylation of MCAM gene is associated with advanced tumor stage in prostate cancer. *Prostate* **68,** 418–26 (2008).

99. Bardin, N. *et al.* CD146 and its soluble form regulate monocyte transendothelial migration. *Arterioscler. Thromb. Vasc. Biol.* **29,** 746–53 (2009).

100. Jouve, N. *et al.* CD146 mediates VEGF-induced melanoma cell extravasation through FAK activation. *Int. J. Cancer* (2015). doi:10.1002/ijc.29370

101. Yan, X. *et al.* A novel anti-CD146 monoclonal antibody, AA98, inhibits angiogenesis and tumor growth. *Blood* **102,** 184–91 (2003).

102. Kang, Y. *et al.* Knockdown of CD146 reduces the migration and proliferation of human endothelial cells. *Cell Res.* **16,** 313–318 (2006).

103. Mills, L. *et al.* Fully human antibodies to MCAM/MUC18 inhibit tumor growth and metastasis of human melanoma. *Cancer Res.* **62,** 5106–14 (2002).

104. Welti, J., Loges, S., Dimmeler, S. & Carmeliet, P. Recent molecular discoveries in angiogenesis and antiangiogenic therapies in cancer. *J. Clin. Invest.* **123,** 3190–3200 (2013).

105. Solovey, A. N. *et al.* Identification and functional assessment of endothelial P1H12. *J. Lab. Clin. Med.* **138,** 322–31 (2001).

106. Stalin, J. *et al.* Targeting soluble CD146 with a neutralizing antibody inhibits

vascularization, growth and survival of CD146-positive tumors. *Oncogene* **35,** 5489–5500 (2016).

107. Bardin, N. *et al.* Identification of CD146 as a component of the endothelial junction involved in the control of cell-cell cohesion. *Blood* **98,** 3677–84 (2001).

108. Jiang, T. *et al.* CD146 is a coreceptor for VEGFR-2 in tumor angiogenesis. *Blood* **120,** 2330–9 (2012).

109. Flanagan, K. *et al.* Laminin-411 is a vascular ligand for MCAM and facilitates TH17 cell entry into the CNS. *PLoS One* **7,** e40443 (2012).

110. Ishikawa, T. *et al.* Laminins 411 and 421 differentially promote tumor cell migration via ??6??1 integrin and MCAM (CD146). *Matrix Biol.* (2014). doi:10.1016/j.matbio.2014.06.002

111. Tu, T. *et al.* CD146 acts as a novel receptor for netrin-1 in promoting angiogenesis and vascular development. *Nat. Publ. Gr.* **25,** (2015).

112. Luo, Y. *et al.* Recognition of CD146 as an ERM-binding protein offers novel mechanisms for melanoma cell migration. *Oncogene* **31,** 306–21 (2012).

113. Ye, Z. *et al.* Wnt5a uses CD146 as a receptor to regulate cell motility and convergent extension. *Nat. Commun.* **4,** (2013).

114. Witze, E. S., Litman, E. S., Argast, G. M., Moon, R. T. & Ahn, N. G. Wnt5a control of cell polarity and directional movement by polarized redistribution of adhesion receptors. *Science* **320,** 365–9 (2008).

115. Anfosso, F. *et al.* Activation of human endothelial cells via S-endo-1 antigen (CD146) stimulates the tyrosine phosphorylation of focal adhesion kinase p125(FAK). *J. Biol. Chem.* **273,** 26852–6 (1998).

116. Batt, D. B. & Roberts, T. M. Cell density modulates protein-tyrosine phosphorylation. *J. Biol. Chem.* **273,** 3408–14 (1998).

117. Abedi, H. & Zachary, I. Vascular endothelial growth factor stimulates tyrosine phosphorylation and recruitment to new focal adhesions of focal adhesion kinase and paxillin in endothelial cells. *J. Biol. Chem.* **272,** 15442–51 (1997).

118. Duan, H. *et al.* Soluble CD146 in cerebrospinal fluid of active multiple sclerosis. *Neuroscience* (2013). doi:10.1016/j.neuroscience.2013.01.020

119. Harhouri, K. *et al.* Soluble CD146 displays angiogenic properties and promotes neovascularization in experimental hind-limb ischemia. *Blood* **115,** 3843–51 (2010).

120. Bardin, N. *et al.* Soluble CD146, a novel endothelial marker, is increased in physiopathological settings linked to endothelial junctional alteration. *Thromb. Haemost.* **90,** 915–20 (2003).

121. Pasquier, E. *et al.* The first assessment of soluble CD146 in women with unexplained pregnancy loss. A new insight? *Thromb. Haemost.* **94,** 1280–4 (2005).

122. Chung, A. S. *et al.* An interleukin-17-mediated paracrine network promotes tumor resistance to anti-angiogenic therapy. *Nat. Med.* **19,** 1114–23 (2013).

123. Ueno, K. *et al.* IGFBP-4 activates the Wnt/beta-catenin signaling pathway and induces M-CAM expression in human renal cell carcinoma. *Int. J. cancer* **129,** 2360–9 (2011).

124. Moon, R. T., Kohn, A. D., Ferrari, G. V. De & Kaykas, A. WNT and β-catenin signalling: diseases and therapies. *Nat. Rev. Genet.* **5,** 691–701 (2004).

125. Feng, G. *et al.* CD146 gene expression in clear cell renal cell carcinoma: a potential marker for prediction of early recurrence after nephrectomy. *Int. Urol. Nephrol.* **44,** 1663–9 (2012).

126. Dufies, M. *et al.* Soluble CD146 is a predictive marker of pejorative evolution and of sunitinib efficacy in clear cell renal cell carcinoma. *Theranostics* **8,** 2447–2458 (2018).

127. Pickl, W. F. *et al.* MUC18/MCAM (CD146), an activation antigen of human T lymphocytes. *J. Immunol.* **158,** 2107–15 (1997).

128. Nollet, M. *et al.* A novel anti-CD146 antibody specifically targets cancer cells by internalizing the molecule. *Oncotarget* **8,** 112283–112296 (2017).

129. Shih, I. M., Schnaar, R. L., Gearhart, J. D. & Kurman, R. J. Distribution of cells bearing the HNK-1 epitope in the human placenta. *Placenta* **18,** 667–74 (1997).

130. McGary, E. C. *et al.* A fully human antimelanoma cellular adhesion molecule/MUC18 antibody inhibits spontaneous pulmonary metastasis of osteosarcoma cells *in vivo*. *Clin. Cancer Res.* **9,** 6560–6 (2003).

131. Bu, P. *et al.* Anti-CD146 monoclonal antibody AA98 inhibits angiogenesis via suppression of nuclear factor-kappaB activation. *Mol. Cancer Ther.* **5,** 2872–8 (2006).

132. Maciag, T., Cerundolo, J., Ilsley, S., Kelley, P. R. & Forand, R. An endothelial cell growth factor from bovine hypothalamus: identification and partial characterization. *Proc. Natl. Acad. Sci. U. S. A.* **76,** 5674–8 (1979).

133. George, D. J. & Kaelin, W. G. The von Hippel–Lindau Protein, Vascular Endothelial Growth Factor, and Kidney Cancer. *N. Engl. J. Med.* **349,** 419–421 (2003).

134. Sosman, J. A., Puzanov, I. & Atkins, M. B. Opportunities and obstacles to combination targeted therapy in renal cell cancer. *Clin. Cancer Res.* **13,** 764s–769s (2007).

135. Noy, P. J. *et al.* Blocking CLEC14A-MMRN2 binding inhibits sprouting angiogenesis and tumour growth. *Oncogene* **34,** 5821–5831 (2015).

136. Zhuang, X. *et al.* Robo4 vaccines induce antibodies that retard tumor growth.

Angiogenesis **18,** 83–95 (2015).

137. Huijbers, E. J. M. *et al.* Vaccination against the extra domain-B of fibronectin as a novel tumor therapy. *FASEB J.* **24,** 4535–44 (2010).

138. Fawcett, J. Molecular aspects of angiogenesis and metastasis. (University of Oxford, 1994).

139. Heringa, J. Local weighting schemes for protein multiple sequence alignment. *Comput. Chem.* **26,** 459–77 (2002).

140. Saupe, F. *et al.* Vaccines targeting self-antigens: mechanisms and efficacy-determining parameters. *FASEB J.* **29,** 3253–62 (2015).

141. Zhang, Y. *et al.* Generation and characterization of a panel of monoclonal antibodies against distinct epitopes of human CD146. *Hybridoma (Larchmt).* **27,** 345–52 (2008).

142. Seftalioğlu, A. & Karakoç, L. Expression of CD146 adhesion molecules (MUC18 or MCAM) in the thymic microenvironment. *Acta Histochem.* **102,** 69–83 (2000).

143. Brochet, X., Lefranc, M.-P. & Giudicelli, V. IMGT/V-QUEST: the highly customized and integrated system for IG and TR standardized V-J and V-D-J sequence analysis. *Nucleic Acids Res.* **36,** W503–W508 (2008).

144. Thomann, S. *et al.* Selective targeting of liver cancer with the endothelial marker CD146. *Oncotarget* **5,** 8614–8624 (2014).

145. Barata, P. C. & Rini, B. I. Treatment of renal cell carcinoma: Current status and future directions. *CA. Cancer J. Clin.* **67,** 507–524 (2017).

146. Sabanathan, D. *et al.* Cure in Advanced Renal Cell Cancer: Is It an Achievable Goal? *Oncologist* theoncologist.2017-0159 (2017). doi:10.1634/theoncologist.2017-0159

147. Lin, P. *et al.* Inhibition of tumor growth by targeting tumor endothelium using a soluble

vascular endothelial growth factor receptor. *Cell Growth Differ.* **9,** 49–58 (1998).

148. Brown, R. M., Meah, C. J., Heath, V. L., Styles, I. B. & Bicknell, R. in *Methods in molecular biology (Clifton, N.J.)* **1430,** 149–157 (2016).

149. Kume, T. Novel insights into the differential functions of Notch ligands in vascular formation. *J. Angiogenes. Res.* **1,** 8 (2009).

150. Larochelle, C. *et al.* Melanoma cell adhesion molecule identifies encephalitogenic T lymphocytes and promotes their recruitment to the central nervous system. *Brain* **135,** 2906–24 (2012).

151. Zeng, Q. *et al.* Impaired tumor angiogenesis and VEGF-induced pathway in endothelial CD146 knockout mice. *Protein Cell* **5,** 445–56 (2014).

152. Stalin, J., Nollet, M., Dignat-George, F., Bardin, N. & Blot-Chabaud, M. Therapeutic and Diagnostic Antibodies to CD146: Thirty Years of Research on Its Potential for Detection and Treatment of Tumors. *Antibodies* **6,** 17 (2017).

153. Ruma, I. M. W. *et al.* MCAM, as a novel receptor for S100A8/A9, mediates progression of malignant melanoma through prominent activation of NF-κB and ROS formation upon ligand binding. *Clin. Exp. Metastasis* **33,** 609–27 (2016).

154. Zhuang, J. *et al.* NADPH oxidase 4 mediates reactive oxygen species induction of CD146 dimerization in VEGF signal transduction. *Free Radic. Biol. Med.* **49,** 227–36 (2010).

155. Bu, P. *et al.* Visualization of CD146 dimerization and its regulation in living cells. *Biochim. Biophys. Acta* **1773,** 513–20 (2007).

156. Anfosso, F. *et al.* Outside-in signaling pathway linked to CD146 engagement in human endothelial cells. *J. Biol. Chem.* **276,** 1564–9 (2001).

157. Lu, X. *et al.* The netrin receptor UNC5B mediates guidance events controlling

morphogenesis of the vascular system. *Nature* **432,** 179–86 (2004).

158. Lin, P. *et al.* Inhibition of tumor angiogenesis using a soluble receptor establishes a role for Tie2 in pathologic vascular growth. *J. Clin. Invest.* **100,** 2072–8 (1997).

159. Bandyopadhyay, A. *et al.* Extracellular domain of TGFbeta type III receptor inhibits angiogenesis and tumor growth in human cancer cells. *Oncogene* **21,** 3541–51 (2002).

160. Kertesz, N. *et al.* The soluble extracellular domain of EphB4 (sEphB4) antagonizes EphB4-EphrinB2 interaction, modulates angiogenesis, and inhibits tumor growth. *Blood* **107,** 2330–8 (2006).

161. Suchting, S., Heal, P., Tahtis, K., Stewart, L. M. & Bicknell, R. Soluble Robo4 receptor inhibits *in vivo* angiogenesis and endothelial cell migration. *FASEB J.* **19,** 121–3 (2005).

162. Gacche, R. N. & Meshram, R. J. Angiogenic factors as potential drug target: efficacy and limitations of anti-angiogenic therapy. *Biochim. Biophys. Acta* **1846,** 161–79 (2014).

163. Pàez-Ribes, M. *et al.* Antiangiogenic therapy elicits malignant progression of tumors to increased local invasion and distant metastasis. *Cancer Cell* **15,** 220–31 (2009).

164. Ebos, J. M. L. *et al.* Accelerated metastasis after short-term treatment with a potent inhibitor of tumor angiogenesis. *Cancer Cell* **15,** 232–9 (2009).

165. Imbert, A.-M. *et al.* CD146 expression in human breast cancer cell lines induces phenotypic and functional changes observed in Epithelial to Mesenchymal Transition. *PLoS One* **7,** e43752 (2012).

166. Cheng, H. Inhibiting CD146 by its Monoclonal Antibody AA98 Improves Radiosensitivity of Cervical Cancer Cells. *Med. Sci. Monit.* **22,** 3328–33 (2016).

167. Beck, A., Goetsch, L., Dumontet, C. & Corvaïa, N. Strategies and challenges for the next generation of antibody–drug conjugates. *Nat. Rev. Drug Discov.* **16,** 315–337 (2017).

168. Junttila, T. T., Li, G., Parsons, K., Phillips, G. L. & Sliwkowski, M. X. Trastuzumab-DM1 (T-DM1) retains all the mechanisms of action of trastuzumab and efficiently inhibits growth of lapatinib insensitive breast cancer. *Breast Cancer Res. Treat.* **128,** 347–56 (2011).

169. Peters, C. & Brown, S. Antibody-drug conjugates as novel anti-cancer chemotherapeutics. *Biosci. Rep.* **35,** e00225–e00225 (2015).

170. Barrett, D. M., Grupp, S. A. & June, C. H. Chimeric Antigen Receptor- and TCR-Modified T Cells Enter Main Street and Wall Street. *J. Immunol.* **195,** 755–61 (2015).

171. Almåsbak, H., Aarvak, T. & Vemuri, M. C. CAR T Cell Therapy: A Game Changer in Cancer Treatment. *J. Immunol. Res.* **2016,** 5474602 (2016).

172. Hu, Y., Shen, F., Crellin, N. K. & Ouyang, W. The IL-17 pathway as a major therapeutic target in autoimmune diseases. *Ann. N. Y. Acad. Sci.* **1217,** 60–76 (2011).

173. Flanagan, K. *et al.* Anti-Mcam Monoclonal Antibody PRX003 Inhibits the Unique Migratory Potential of Pathogenic IL-17–Producing T Cells. *J. Allergy Clin. Immunol.* **137,** AB190 (2016).

174. Koller, M. *et al.* OP0205 Clinical and Preclinical Assessment of The Anti-MCAM Monoclonal Antibody PRX003, A Potential Novel Treatment for Th17-Mediated Inflammatory Diseases. *Ann. Rheum. Dis.* **75,** 134.2-134 (2016).

175. Kinney, G. G. *et al.* Clinical Assessment of the Monoclonal Anitbody , PRX003 , a Potential Novel Treatment for Th17-Mediated In ammatory Disease. 2–3 (2016).

176. Kuusk, T. *et al.* Antiangiogenic therapy combined with immune checkpoint blockade in renal cancer. *Angiogenesis* **20,** 205–215 (2017).

177. Holash, J. *et al.* VEGF-Trap: A VEGF blocker with potent antitumor effects. *Proc. Natl.*

Acad. Sci. **99,** 11393–11398 (2002).

178. Konner, J. & Dupont, J. Use of soluble recombinant decoy receptor vascular endothelial growth factor trap (VEGF Trap) to inhibit vascular endothelial growth factor activity. *Clin. Colorectal Cancer* **4 Suppl 2,** S81-5 (2004).

179. Colomb, F. *et al.* Galectin-3 interacts with the cell-surface glycoprotein CD146 (MCAM, MUC18) and induces secretion of metastasis-promoting cytokines from vascular endothelial cells. *J. Biol. Chem.* **292,** 8381–8389 (2017).

180. Papadopoulos, N. *et al.* Binding and neutralization of vascular endothelial growth factor (VEGF) and related ligands by VEGF Trap, ranibizumab and bevacizumab. *Angiogenesis* **15,** 171–85 (2012).

181. Huang, C. Receptor-Fc fusion therapeutics, traps, and MIMETIBODY technology. *Curr. Opin. Biotechnol.* **20,** 692–9 (2009).

182. Rath, T. *et al.* Fc-fusion proteins and FcRn: structural insights for longer-lasting and more effective therapeutics. *Crit. Rev. Biotechnol.* **35,** 235–54 (2015).

183. Beck, A. & Reichert, J. M. Therapeutic Fc-fusion proteins and peptides as successful alternatives to antibodies. *MAbs* **3,** 415–416 (2011).

184. Yu, K., Liu, C., Kim, B.-G. & Lee, D.-Y. Synthetic fusion protein design and applications. *Biotechnol. Adv.* **33,** 155–164 (2015).